ISSN 1732-9353 (suspended)
eISSN 2543-7496

Scientific Review

Engineering and Environmental Sciences

Przegląd Naukowy
Inżynieria i Kształtowanie Środowiska

Vol. 34 (4) 2025 Issue 110
Quarterly

SCIENTIFIC REVIEW
ENGINEERING AND ENVIRONMENTAL SCIENCES
Quarterly

EDITORIAL OFFICE ADDRESS
Wydział Budownictwa i Inżynierii Środowiska SGGW, ul. Nowoursynowska 159, 02-776 Warsaw, Poland
tel. (+48 22) 59 35 363, 59 35 210, 59 35 302
e-mail: srees@sggw.edu.pl
https://srees.sggw.edu.pl

Electronic version of the Scientific Review Engineering and Environmental Sciences is primary version

All papers are indexed in the data bases as follows: AGRO(Poznań), BazTech, Biblioteka Nauki, **CrossRef**, **DOAJ**, **Google Scholar**, **Index Copernicus**, INFONA, POL-Index, **SCOPUS**, SIGŻ(CBR)

Scientific Review

Engineering and Environmental Sciences

Przegląd Naukowy

Inżynieria i Kształtowanie Środowiska

Vol. 34 (4) 2025 Issue 110

Contents

Wydawnictwo SGGW, Warsaw 2025

Wydawnictwo SGGW wydawnictwosggw

Editorial work – Anna Dołomisiewicz, Tomasz Ruchniewicz

ISSN 1732-9353 (suspended) eISSN 2543-7496

Scientific Review Engineering and Environmental Sciences (2025), 34 (4), 327–347

Sci. Rev. Eng. Env. Sci. (2025), 34 (4) https://srees.sggw.edu.pl

ISSN 1732-9353 (suspended) eISSN 2543-7496 DOI 10.22630/srees.10568

Received: 09.07.2025
Accepted: 17.10.2025

Rahima HAMIDECHE✉

Samy MEZHOUD

Youcef TOUMI

University Mentouri of Constantine, Department of Civil Engineering, Laboratory of Materials and Construction Durability, Algeria

Study on the mechanical performance of sustainable earth blocks from sandy granite saprolite and marble waste

Keywords: compressed earth block, sandy granite saprolite, cement, compaction, mechanical property

Introduction

In the last 60–70 years, stabilized soils have gained significant attention in the construction of structural components for buildings and infrastructure. Among these materials, stabilized soil blocks, particularly compressed earth blocks (CEBs), have emerged as a sustainable and cost-effective alternative to conventional masonry units (Venkatarama Reddy & Latha, 2014). CEBs are produced by compressing moist soil, often in combination with stabilizers, followed by immediate demolding. These blocks are engineered to meet specific performance criteria, including a minimum dry compressive strength of 2 MPa (Cid-Falceto et al., 2012).

The performance of cement-stabilized earth blocks is strongly influenced by the cement content (Venkatarama Reddy & Latha, 2014). According to Walker

✉rahima.hamideche@doc.umc.edu.dz

(1995), producing cement-stabilized blocks requires less than 10% of the energy needed for fired clay or concrete units. Furthermore, constructing 1 m^2 of CEB masonry can consume up to 15 times less energy than traditional concrete block construction (Poullain et al., 2019). Numerous studies have demonstrated that increasing cement content not only improves the mechanical strength of CEBs but also reduces their water absorption (Kerali, 2001; Venkatarama Reddy & Gupta, 2005; Dao et al., 2018). Additionally, higher compaction pressure has been shown to further enhance these properties by decreasing porosity and improving internal bonding (Kerali, 2001; Taallah, 2014).

However, the environmental and economic sustainability of CEBs can be further enhanced by integrating local and recycled materials, especially in regions where natural resources are abundant but underutilized. In this context, sandy granite saprolite from Chétaïbi, a locally available volcanic material in Algeria, presents favorable properties for use in earth-based construction. Moreover, marble waste, a by-product of the stone industry, offers potential as a partial soil replacement while contributing to industrial waste valorization. Despite these promising prospects, few studies have explored the combined use of sandy granite saprolite from Chétaïbi and marble waste in stabilized CEBs, particularly in relation to variations in cement dosage and compaction effort.

The present study aims to fill this research gap by evaluating the hydromechanical performance of CEBs produced with 85% sandy granite saprolite from Chétaïbi and 15% marble waste, stabilized with different cement contents and compacted under varying pressures. This marble waste content was selected based on findings reported in the literature. Guettala et al. (2006) demonstrated that adding 30% sand improves soil quality for the production of CEBs. Other studies, particularly those by Muhwezi and Achanit (2019), indicated that a 10% sand addition provides optimal strength for the manufacture of cement-stabilized earth blocks. Based on the results obtained, the mixture containing 15% marble waste was selected for the production of CEBs.

Marble waste is characterized by a dense crystalline structure and low porosity, resulting from the compact nature of calcium carbonate (calcite) that forms its composition. This microstructure limits both water penetration and moisture retention within the material. To verify this advantage, Proctor compaction tests were carried out to determine the optimal compaction parameters of the studied mixtures. Two formulations were examined: the first composed solely of tuff, and the second incorporating 15% marble waste as a partial substitution. The results showed that the incorporation of marble waste leads to a reduction in the optimum moisture content compared to the tuff-based mixture. This decrease is attributed

to the low porosity and non-plastic nature of the marble particles, which reduces water retention while promoting more efficient compaction and better material densification.

The novelty of this study lies in the simultaneous valorization of sandy granite saprolite and marble waste for the production of sustainable CEBs, offering an innovative approach to the management of local resources and a material combination that remains scarcely explored in the scientific literature. The experimental program focuses on key performance indicators: density, compressive strength, flexural strength, and total water absorption, with the goal of determining optimal formulation conditions that balance mechanical efficiency, water resistance, and environmental impact. The results are analyzed with reference to established international standards for CEBs.

Materials and experimental program

Materials

The two main materials used in this study are sandy granite saprolite and marble waste. The sandy granite saprolite, collected from the Chétaïbi region (Annaba, Algeria), was selected as the base material due to its local availability and favorable granulometric characteristics for the production of CEBs. The marble waste, obtained from local marble processing plants located in Skikda (Algeria), was incorporated as part of a valorization approach for local and bio-based materials, thereby contributing to the enhancement of the environmental sustainability of the developed products.

Sandy granite saprolite. The material originates from the Koudiat Zoubia quarry, located within the municipality and district (*daïra*) of Chetaïbi, in the Annaba province. The quarry is situated approximately 50 km northwest of the city of Annaba. The grain size distribution of the tuff was determined using two methods: a sieve analysis after washing, in accordance with the French standard NF P 94-056 (Association Française de Normalisation [AFNOR], 1992a) for particles larger than 80 µm, and a sedimentation test following the NF P 94-057 standard (AFNOR, 1992b) for particles smaller than 80 µm. The particle size distribution of the soil, along with its physical characteristics, is presented in Figure 1 and Table 1, respectively.

Hamideche, R., Mezhoud, S., Toumi, Y. (2025). Study on the mechanical performance of sustainable earth blocks from sandy granite saprolite and marble waste. *Sci. Rev. Eng. Env. Sci.*, *34* (4), 327–347. DOI 10.22630/srees.10568

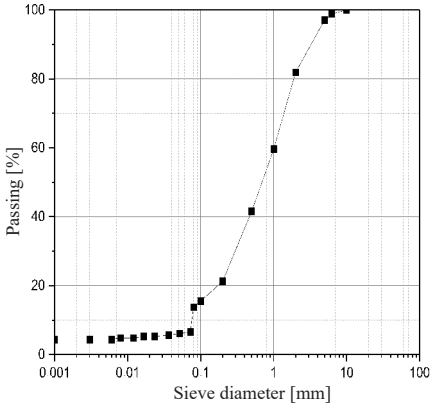

FIGURE 1. Grain size distribution curve of sandy granite saprolite

Source: own work.

TABLE 1. Physical properties of the sandy granite saprolite

Water content[a] [%]	Bulk density[b] [kg·m^{-3}]	Solid particle density[c] [kg·m^{-3}]	Sand equivalent[d] [%]	Proctor test[e]		*VBS*[f] [-]
				ρ [g·cm^{-3}]	W_{opt} [%]	
11.11	1 460.66	2 427.18	80.93	1.75	11.6	0.24

[a]According to NF P 94-050 (AFNOR, 1995); [b]According to NF P 18-554 (AFNOR, 1990); [c]According to NF P 94-054 (AFNOR, 1991), [d]According to EN 933-8 (CEN, 2015); [e]According to NF P 94-093 (AFNOR, 2014); [f]According to NF P 94-068 (AFNOR, 1998).

Source: own work.

Marble waste. The marble sand used in all block mixtures is white marble waste (0.2 mm) sourced from the Fil-fila quarry, located 25 km east of the city of Skikda. The grain size distribution of marble waste was determined in accordance with the European standard EN 933-2 (European Committee for Standardization [CEN], 2020). The physical properties of this marble waste, determined according to European standards, are presented in Table 2. The particle size distribution of the sand is illustrated in Figure 2.

TABLE 2. Physical properties of marble waste

Bulk density [g·cm^{-3}]	Absolute density [g·cm^{-3}]	Grain size distribution [%]			Fineness modulus	Sand equivalent [%]
		< 0.08 mm	0.08–1.25 mm	1.25–5.0 mm		
1.665	2.665	2.3	84.7	12.3	2.48	89.6

Source: own work.

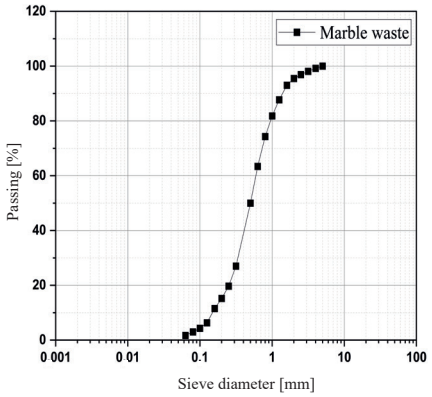

FIGURE 2. Grain size distribution curve of marble waste
Source: own work.

Cement. The cement used is a high-performance portland cement, classified as CEM I 42.5R, in accordance with the Algerian standard NA 442-2013 (Institut Algérien de Normalisation [IANOR], 2013). It is sourced from the Biskra cement plant, located in the Biskra province. The chemical properties, potential clinker composition, and compressive strength are presented in Table 3.

TABLE 3. Properties of the cement

Property	Value
Chemical analysis [%]	
Loss on ignition	2.6–3.7
Sulfate content (SO_3)	2.2–2.8
Magnesium oxide (MgO)	1.7–2.8
Chloride content (Cl)	0.03–0.07
Potential clinker composition [%]	
Tricalcium silicate (C_3S)	56–66
Tricalcium aluminate (C_3A)	5.1–7.2
Compressive strength [MPa]	
For the 2-day-aged sample	20–29
For the 28-day-aged sample	42.5–52.5

Source: own work.

Water. The water used in this study is potable water sourced from the Laboratory of Materials and Construction Durability of the University Mentouri of Constantine. As this is drinking water, its characteristics comply with NF P 18-303 (AFNOR, 1941).

Hamideche, R., Mezhoud, S., Toumi, Y. (2025). Study on the mechanical performance of sustainable earth blocks from sandy granite saprolite and marble waste. *Sci. Rev. Eng. Env. Sci.*, *34* (4), 327–347. DOI 10.22630/srees.10568

Block preparation and testing methods

Prior to block preparation, both the soil and marble waste were sieved through a two-millimeter mesh to eliminate coarse particles. The sieved materials were then oven-dried at 105°C for 24 h to ensure consistent moisture content. For each block, the total dry mass of the mixture was fixed at 2 kg, comprising 85% sandy granite saprolite and 15% marble waste by weight.

This base mixture was then combined with three different cement contents: 6%, 9%, and 12% by weight of the dry mixture. The dry components (sandy granite saprolite, marble waste, and cement) were thoroughly mixed for 3 min using a five-liter concrete mixer. The water corresponding to the Proctor optimum moisture content was subsequently added, and mixing continued for an additional 2 min to ensure uniform hydration, following the method described by Guettala et al. (2006).

The fresh mixture was placed into a steel mold with dimensions of 100 × 100 × 200 mm and compacted using a hydraulic press equipped with a movable lower plate and a fixed upper plate. Compaction was applied according to predefined pressures (2–10 MPa, depending on the test group). Once demolded, the CEBs were carefully transferred to plastic freezer bags and cured at room temperature for 28 days to maintain a controlled moisture environment during the curing period. Before testing, the blocks were oven-dried at a controlled temperature until a constant mass was reached to remove any remaining moisture. Three specimens were produced and tested for each experimental condition to ensure consistency and reliability. A schematic flowchart illustrating the complete experimental procedure is presented in Figure 3.

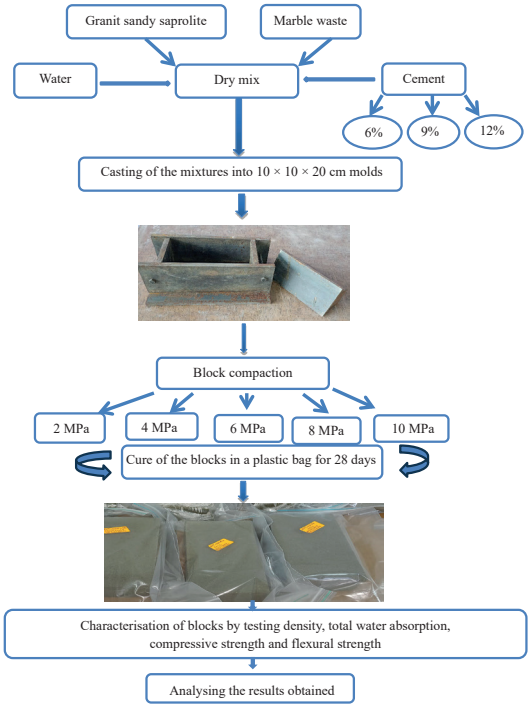

FIGURE 3. A detailed flowchart outlining the various stages of the workflow

Source: own work.

Before being subjected to testing, the CEBs must be oven-dried until a constant mass is achieved. The tests conducted in this study are as follows.

Density test

The density of the blocks was determined in accordance with the French standard XP P 13-901 (AFNOR, 2022). The dry bulk density is obtained by using the following formula:

$$\rho = \frac{M}{V}, \tag{1}$$

where: ρ is the dry bulk density [kg·m^{-3}], M is the dry mass [kg], and V is the brick [m^3].

Total water absorption test

This test was carried out according to the method described by Taallah et al. (2014). It involves fully immersing the blocks in water for 4 days, followed by measuring the weight gain relative to the dry weight. The total water absorption is then calculated using the following formula:

$$Abs = \frac{P_h - P_s}{P_s} 100, \tag{2}$$

where: Abs is the water absorption [%], P_h is the mass of the brick saturated with water [kg], and P_s is the mass of the brick in an absolute dry state [kg].

Flexural and compressive strength test

The dry compressive strength of the CEBs was evaluated in accordance with XP P 13-901. For this test, each specimen consisted of two half-blocks, stacked and bonded with a cement mortar joint. The assembly was subjected to uniaxial compression until failure using a hydraulic press with a capacity of 3,000 kN and a loading rate of 0.02 mm·s^{-1}. This procedure enables the assessment of the mechanical strength of the blocks under dry conditions, a critical parameter for their structural use in construction. The dry compressive strength is calculated using the following formula:

Hamideche, R., Mezhoud, S., Toumi, Y. (2025). Study on the mechanical performance of sustainable earth blocks from sandy granite saprolite and marble waste. *Sci. Rev. Eng. Env. Sci.*, *34* (4), 327–347. DOI 10.22630/srees.10568

$$R = \frac{F}{A}, \tag{3}$$

where: R is the dry compressive strength [MPa], F is the maximum load applied before failure [N], and A is the contact surface of the specimen [mm^2].

In parallel, the flexural tensile strength was determined following the European standard EN 196-1 (CEN, 2016) using the three-point bending test. This test was conducted on block specimens with the same press (3,000 kN capacity) and loading rate (0.02 mm·s^{-1}). The method provides valuable insights into the resistance of blocks to bending stresses, which is essential for evaluating their in-service performance. Together, these two mechanical tests offer a comprehensive characterization of the structural behavior and mechanical reliability of the CEBs. The flexural strength is calculated using the following formula:

$$R = \frac{2FL}{3bd^2}, \tag{4}$$

where: F is the maximum load at failure [N], L is the span length [mm], b is the specimen width [mm], and d^2 is the specimen depth [mm].

The testing procedures are illustrated in Figure 4 for the compressive strength test and Figure 4b for the flexural strength test.

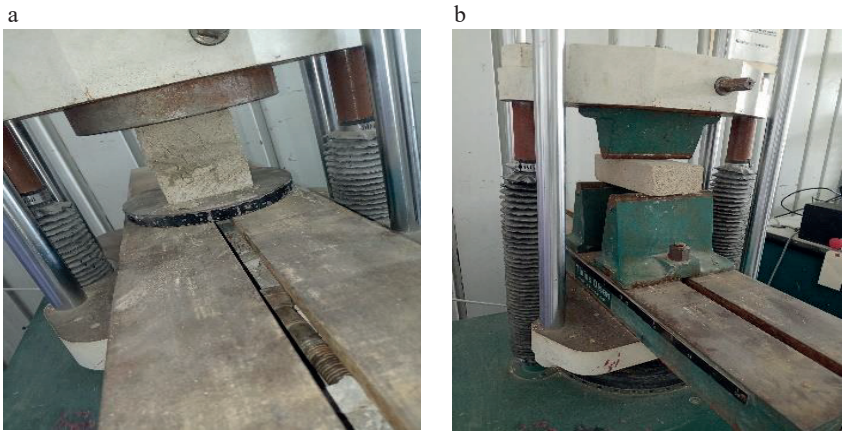

FIGURE 4. Compression test (a) and flexural test (b)
Source: own work.

Results and discussion

Effect of cement content on the properties of compressed earth blocks

In this phase, the effect of cement content on the properties of the CEBs was evaluated. The cement was added to the samples at a constant compaction pressure of 2 MPa.

Dry density. From a structural standpoint, increased density often correlates with enhanced mechanical properties such as compressive and flexural strength, as it reflects a more cohesive and compact material. Figure 5 shows the influence of cement content on the dry density of CEBs. A slight but consistent increase in density was observed as the cement content increased from 6% to 12%, with values ranging between 1,861.29 kg·m^{-3} and 1,877.44 kg·m^{-3}. The density increased from 1861.29 kg·m^{-3} at 6% cement to 1,869.16 kg·m^{-3} at 9%, corresponding to an improvement of approximately 0.42%. A further increase to 12% cement resulted in a density of 1,877.44 kg·m^{-3}, representing an additional 0.44% increase compared to the 9% mixture. Overall, the total increase in density between 6% and 12% of cement was about 0.87%. This trend can be attributed to the formation of cement hydration products, which progressively fill the voids within the soil matrix, leading to a denser internal structure.

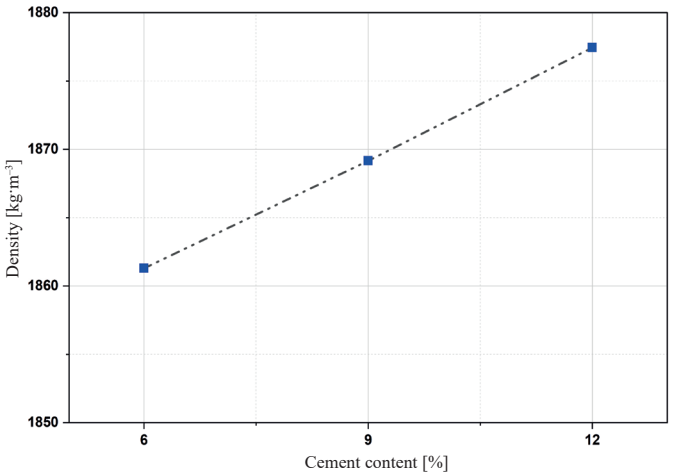

FIGURE 5. Variation of density with cement content

Source: own work.

These findings are in agreement with those reported by Bahar et al. (2004), who found that cement-stabilized soils exhibited higher densities due to improved particle packing and reduced porosity. Similarly, Kerali (2001) demonstrated that cement additions contribute to the densification of the blocks. Riza and Rahman (2015) also reported that typical CEB densities fall within the range of 1,500–2,000 kg·m^{-3}, consistent with the values recorded in the present study.

Similar observations were reported by Kumar and Barbato (2022) in their study on the effects of sugarcane bagasse fibers on the properties of compressed and stabilized earth blocks, where they noted that an increase in cement content leads to denser microstructures and enhanced interparticle cohesion.

The results obtained in this study are consistent with those reported by Elahi et al. (2021) for cement- and fly ash-stabilized earth blocks, whose apparent densities ranged between 1,800 kg·m^{-3} and 1,950 kg·m^{-3}. This similarity confirms that the incorporation of cement within moderate proportions leads to a gradual densification of the matrix, producing compact and structurally coherent blocks comparable to those reported in the literature. The density values obtained in the present study are lower than those reported by Cruz and Bogas (2024) in their research on the durability of CEBs stabilized with recycled cement from concrete waste and incorporating construction and demolition waste, where densities ranging from 2,100 kg·m^{-3} to 2,190 kg·m^{-3} were recorded.

Total water absorption. Figure 6 illustrates the influence of cement content on the total water absorption of CEBs. A clear decreasing trend is observed, with water absorption gradually reducing as cement content increases. After one day of immersion, the total water absorption decreased progressively with increasing cement content. The absorption value dropped from 14.16% at 6% cement to 13.92% at 9%. A further decrease to 13.25% was recorded at 12% cement, indicating a consistent improvement in the blocks' resistance to water penetration with higher cement stabilization. This behavior is consistent with the results reported by Taallah et al. (2014), who demonstrated that cement stabilization improves the water resistance of CEBs. The observed reduction in absorption is primarily attributed to the formation of cement hydration products, which progressively fill the voids within the soil matrix, thereby reducing overall porosity and capillary pathways (Bahar et al., 2004).

The total water absorption values recorded for the tested CEBs remain below the maximum threshold of 15% prescribed by the Indian standard IS 1725 (Bureau of Indian Standards [BIS], 1982). This indicates satisfactory water resistance and compliance with established durability criteria. When compared to conventional masonry materials, these results are particularly encouraging.

For instance, clay bricks typically exhibit water absorption ranging from 10% to 30%, concrete blocks from 4% to 25%, and calcium silicate bricks from 6% to 16% (Taallah, 2014). The lower absorption rates of the studied CEBs highlight their potential as a more water-resistant alternative, especially when stabilized with appropriate cement content and subjected to effective compaction.

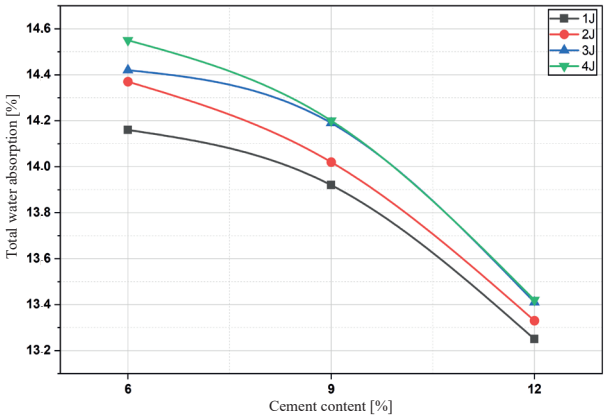

FIGURE 6. Variation of total water absorption with cement content
Source: own work.

Our results are lower than those reported by Kumar and Barbato (2022), who observed a decrease in total water absorption from 24.35% to 20.22% as the cement content increased from 6% to 12%. They attributed this reduction to the enhanced formation of calcium-rich minerals, which promote the densification and homogenization of the soil–cement matrix in CEBs. The lower water absorption values obtained in the present study can be explained using marble waste, a material characterized by a dense crystalline structure and low intrinsic porosity, which makes the blocks more resistant to water penetration compared to those produced from more porous soils.

Dry compressive strength. Figure 7 presents the effect of cement content on the dry compressive strength of CEBs. A clear enhancement in compressive strength is observed as the cement dosage increases from 6% to 12%, with recorded values ranging from 3.39 MPa to 6.39 MPa. All tested formulations exceed the minimum requirement of 2 MPa set by XP P 13-901, confirming their structural suitability. Overall, the compressive strength increased by approximately 88.5% between 6% and 12% cement, highlighting the significant influence of cement stabilization on the improvement of the mechanical performance of CEBs.

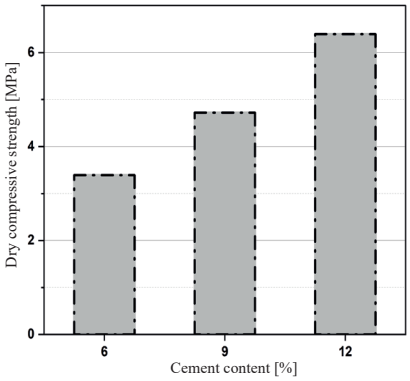

FIGURE 7. Dry compressive strength of compressed earth blocks as a function of cement content
Source: own work.

This strength gain is primarily attributed to the progressive development of cement hydration products, which occupy the pore spaces within the matrix and form rigid interparticle bonds, thereby improving the internal cohesion and load-bearing capacity of the blocks (Bahar et al., 2004). Venkatarama Reddy and Gupta (2005) further support this observation, showing that higher cement content reduces average pore size, contributing to a denser and stronger microstructure. Similar conclusions were reached by Taallah et al. (2014) and Dao et al. (2018), who demonstrated that cement stabilization significantly enhances the mechanical performance of earth--based materials, especially when combined with fine aggregates.

Our results are consistent with those reported by Tripura and Singh (2015), Elahi et al. (2021), and Kumar and Barbato (2022) regarding the influence of cement on the dry compressive strength of CEBs. Tripura and Singh (2015) investigated the properties of cement-stabilized earth blocks and reported compressive strengths ranging from 2.48 MPa to 7.42 MPa for cement contents between 4% and 10%. According to Elahi et al. (2021), increasing the cement content promotes the formation of additional hydration products, which strengthen interparticle bonds and thus enhance the compressive strength of the blocks. The compressive strengths obtained in the present study are higher than those reported by Kumar and Barbato (2022), who recorded values of 1.22 MPa, 1.95 MPa, and 3.70 MPa for cement contents of 0%, 6%, and 12%, respectively.

Flexural strength. Figure 8 illustrates the influence of cement content on the flexural strength of CEBs. The results reveal a clear upward trend, with flexural strength values increasing from 1.80 MPa at 6% cement to 3.04 MPa at 9% and reaching a maximum of 4.02 MPa at 12%. This enhancement is consistent with

the behavior observed in compressive strength and can be attributed to the increased formation of cement hydration products, which fill the pore spaces within the matrix and reinforce the microstructure through the development of strong interparticle bonds. These results also align with findings by Bahar et al. (2004) and Taallah et al. (2014), who reported that higher cement content enhances not only compressive but also tensile and flexural performance due to improved cohesion and reduced porosity.

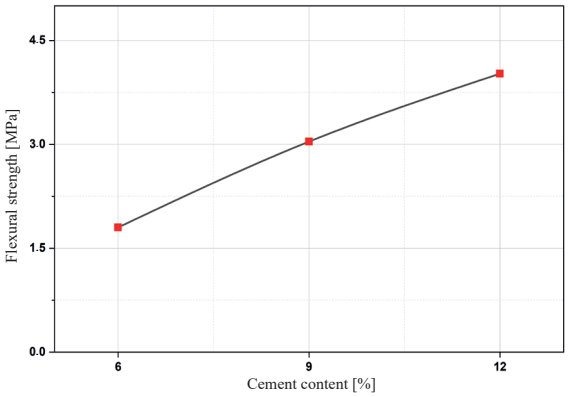

FIGURE 8. Flexural strength of compressed earth blocks as a function of cement content
Source: own work.

The observed values significantly exceed the benchmark of 0.5 MPa proposed by Moevus et al. (2014) as the minimum requirement for earthen construction materials, particularly compacted earth.

The measured values substantially exceed the minimum threshold corresponding to one-tenth of the recommended compressive strength for CEBs (AE & CC, 2022), thereby confirming the satisfactory structural performance of the developed blocks. These findings highlight the efficiency of using locally available materials such as sandy granite saprolite and marble waste, which contribute to improved compactness and particle bonding within the cement-stabilized matrix.

Our results are consistent with those recently reported by Elahi et al. (2021) and Kumar and Barbato (2022) regarding the effect of cement content on the flexural strength of CEBs. However, the values obtained in the present study remain higher than those reported in their works. Elahi et al. (2021) recorded compressive strengths of 0.18 MPa for unstabilized samples, 0.27 MPa for blocks with 3% cement, 0.41 MPa with 5% cement, 0.55 MPa with 7% cement, and 0.66 MPa with 10% cement. Similarly, Kumar and Barbato (2022) reported compressive strengths of 0.29 MPa, 0.47 MPa, and 0.71 MPa for cement contents of 0%, 6%, and 12%, respectively.

Effect of compaction pressure on the properties of compressed earth blocks (at 6% cement content)

From a sustainability standpoint, the excessive use of cement conflicts with the environmental goals of earthen construction, particularly with respect to reducing carbon dioxide emissions and energy consumption. It is, therefore, essential to optimize the binder content to achieve the desired mechanical performance while avoiding unnecessary over-stabilization.

In this study, the results demonstrate that a 6% cement content provides acceptable physical and mechanical properties, in compliance with current regulatory standards. Accordingly, for both economic (lower production costs) and environmental (reduced carbon footprint) considerations, this level of cement can be regarded as an optimal compromise for the formulation of the CEBs investigated.

This section explores the influence of compaction pressure, keeping the cement content fixed at 6%.

Dry density. Figure 9 illustrates the variation in the dry density of CEBs as a function of the applied compaction pressure, at a constant cement content. The results indicate that increasing the compaction pressure leads to a progressive rise in dry density. This behavior is primarily attributed to the reduction in pore volume and improved particle packing, as reported by Taallah et al. (2014). These findings are consistent with those of Kerali (2001), who observed similar increases in density in cement-stabilized blocks, particularly at a cement dosage of 5% and compaction pressures of 6 MPa and 10 MPa. However, it is important to note that the overall increase in density observed in the present study remains relatively modest. This suggests that compaction pressure exerts a more dominant influence on density than cement content alone. These results are consistent with those reported by Tripura and Singh (2015), Elahi et al. (2021) and Atiki (2022). Atiki (2022) reported an increase in the density of CEBs from 1,668.41 $kg \cdot m^{-3}$ to 2,069.57 $kg \cdot m^{-3}$ as the compaction stress increased from 2 MPa to 10 MPa, highlighting the direct effect of compaction pressure on material densification.

Total water absorption. Figure 10 illustrates the evolution of total water absorption in CEBs as a function of the applied compaction pressure. The results reveal a clear downward trend: as compaction pressure increases from 2 MPa to 10 MPa, total water absorption decreases from 14.16% to 10.27% after one day of immersion. This reduction is primarily attributed to the decrease in porosity caused by higher compaction levels, which enhances particle packing and limits capillary pathways for water ingress, as also noted by Taallah (2014).

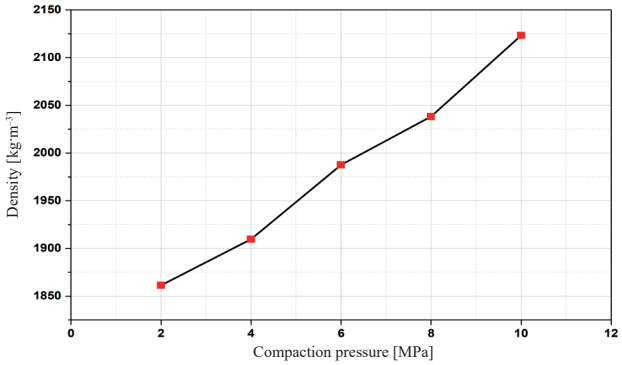

FIGURE 9. Variation in the dry density of compressed earth blocks as a function of the applied compaction pressure

Source: own work.

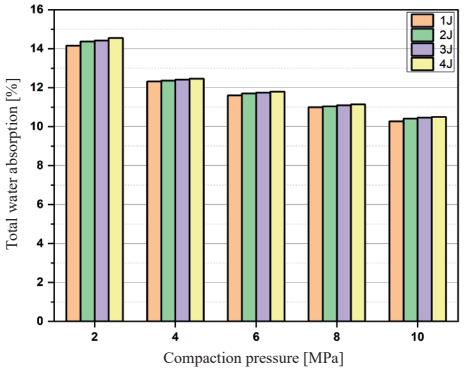

FIGURE 10. Variation of the total water absorption of compressed earth blocks as a function of the applied compaction pressure

Source: own work.

These findings are in agreement with previous studies by Kerali (2001) and Taallah (2014), both of whom demonstrated that compaction plays a critical role in improving the water resistance of stabilized earth blocks. A slight increase in water absorption over time was also observed, reflecting continued pore saturation during prolonged immersion, which is a behavior typical of porous materials.

Importantly, under all tested compaction conditions, the total water absorption values remained below the 15% maximum limit specified by IS 1725, indicating good water durability. Furthermore, blocks compacted at 6 MPa and above

Hamideche, R., Mezhoud, S., Toumi, Y. (2025). Study on the mechanical performance of sustainable earth blocks from sandy granite saprolite and marble waste. *Sci. Rev. Eng. Env. Sci.*, *34* (4), 327–347. DOI 10.22630/srees.10568

exhibited absorption values below 12%, which, according to British technical standards from 1985, corresponds to moderate absorption – a threshold often associated with improved long-term durability (Taallah et al., 2014).

Dry compressive strength. Figure 11 presents the variation in dry compressive strength of CEBs as a function of the applied compaction pressure, at a constant cement content. The results demonstrate a substantial improvement in mechanical performance with increasing compaction pressure. Specifically, the dry compressive strength rises from 3.39 MPa at 2 MPa of compaction to 8.53 MPa at 10 MPa of compaction, more than doubling over the range tested. This enhancement is primarily attributed to the formation of a denser and more uniform internal structure, resulting from the significant reduction in pore volume and improved particle interlocking under higher compaction.

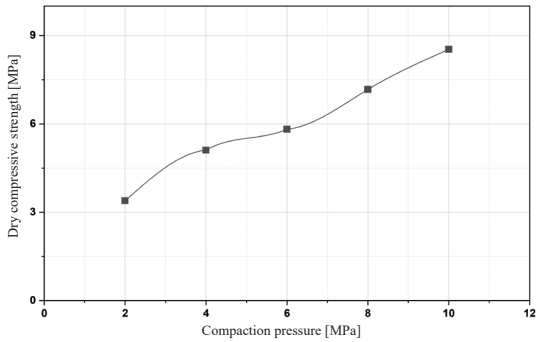

FIGURE 11. Variation in the dry compressive strength of compressed earth blocks as a function of the applied compaction pressure

Source: own work.

These observations are consistent with the findings of Kerali (2001) and Taallah (2014), who emphasized the critical role of compaction in strengthening earth--based materials. By minimizing voids and promoting tighter particle arrangements, higher compaction pressures enhance the load-bearing capacity of CEBs without necessarily increasing binder content.

Furthermore, Figure 12 reveals a strong positive correlation between dry density and compressive strength. The data clearly show that as dry density increases, so does mechanical strength, confirming that densification is a key driver of performance in compressed earth materials. These results are consistent with those reported by Tripura and Singh (2015), Elahi et al. (2021) and Atiki (2022), who also highlighted the positive influence of compaction pressure on the compressive strength of CEBs.

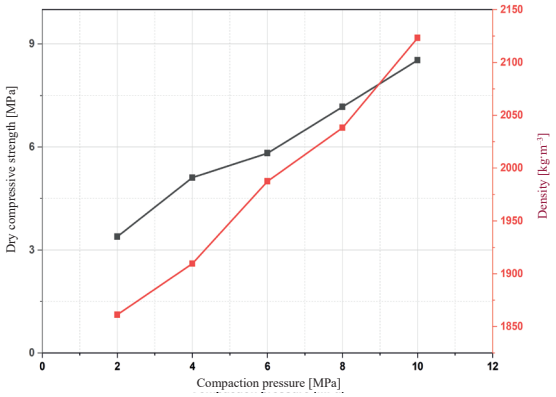

FIGURE 12. Correlation between the dry density and compressive strength of compressed earth blocks as a function of the applied compaction pressure

Source: own work.

Notably, in terms of compressive strength, the blocks compacted at 4 MPa with only 6% cement outperformed those compacted at 2 MPa, even when higher cement contents of 9% and 12% were used. This finding highlights the critical role of densification induced by higher compaction pressure in enhancing the mechanical performance of CEBs.

Flexural strength. Figure 13 illustrates the influence of compaction pressure on the flexural strength of CEBs. The experimental results clearly demonstrate that flexural strength increases significantly with higher compaction pressure.

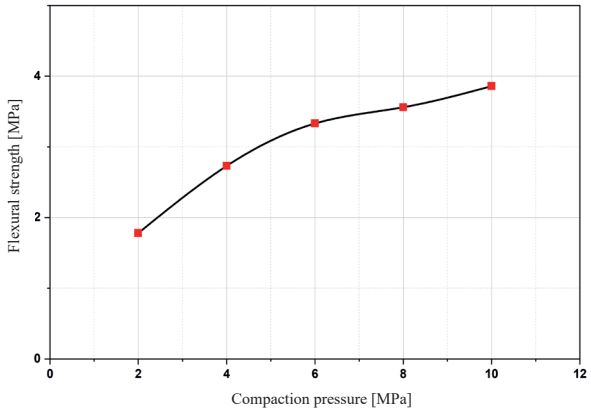

FIGURE 13. Variation in the flexural strength of compressed earth blocks as a function of the applied compaction pressure

Source: own work.

As the applied pressure rises from 2 MPa to 10 MPa, the flexural strength improves from 1.78 MPa to 3.86 MPa, more than doubling over the tested range. These results are consistent with those reported by Atiki (2022), confirming the beneficial effect of increasing compaction pressure on the improvement of CEB properties.

This enhancement is attributed to the same mechanisms that govern improvements in compressive strength, namely, the increased densification of the material and stronger interparticle bonding. Higher compaction reduces internal voids and promotes better particle contact, resulting in a more cohesive matrix capable of resisting tensile stresses associated with bending. These findings are consistent with those reported by Taallah et al. (2014), who emphasized the role of compaction in improving both compressive and tensile strength in earth-based construction materials.

Conclusion

The use of CEBs presents a sustainable and low-carbon alternative to conventional fired clay bricks, primarily due to their lower energy requirements during production and their potential to significantly reduce carbon dioxide emissions. This study investigated the valorization of two locally available and underutilized materials (sandy granite saprolite from Chétaïbi and marble waste) for the formulation of CEBs. The experimental program focused on assessing the effects of cement content and compaction pressure on key physico-mechanical properties, namely dry density, total water absorption, compressive strength, and flexural strength. The main findings can be summarized as follows:

– Both increased cement content and higher compaction pressure positively influenced the mechanical and physical performance of the CEBs. However, compaction pressure proved to be a more efficient and environmentally favorable strategy than increasing binder content.
– The results obtained in this study have significant practical relevance for the development of sustainable construction materials using locally available resources. The combination of sandy granite saprolite and marble waste enabled the production of CEBs exhibiting good mechanical performance and low water absorption, while reducing the environmental impact associated with the extraction of new raw materials. Comparison of these results with the standard requirements for CEBs and with recent studies indicates that the developed blocks can be used as structural masonry units.

– Future work should focus on evaluating long-term durability under real climatic conditions (e.g., wetting-drying, freeze-thaw cycles), as well as exploring alternative low-carbon stabilizers to further improve the sustainability of CEBs in regional construction practices.

References

AE & CC (2022). *Règles professionnelles Blocs de Terre Comprimèe (BTC) Mayotte.* CRAterre. https://doi.org/10.58079/nakf

Association Française de Normalisation [AFNOR]. (1941). *Concrete: preparation. Batching water for structural concrete* (NF P18-303).

Association Française de Normalisation [AFNOR]. (1990). *Aggregates. Measurement of densities, porosity, absorption coefficient and water content of fine gravel and pebbles* (NF P18-554).

Association Française de Normalisation [AFNOR]. (1991). *Soils: investigation and testing. Determination of particle density. Pycnometer method* (NF P 94-054).

Association Française de Normalisation [AFNOR]. (1992a). *Soils: investigation and testing. Granulometric analysis. Hydrometer method* (NF P 94-056).

Association Française de Normalisation [AFNOR]. (1992b). *Soils: investigation and testing. Granulometric analysis. Hydrometer method* (NF P 94-057).

Association Française de Normalisation [AFNOR]. (1995). *Soils: investigation and testing. Determination of moisture content. Oven drying method* (NF P 94-050).

Association Française de Normalisation [AFNOR]. (1996). *Soil: investigation and testing. Granulometric analysis. Dry sieving method after washing* (NF P 94-056).

Association Française de Normalisation [AFNOR]. (1998). *Soils: investigation and testing. Measuring of the methylene blue adsorption capacity of à rocky soil. Determination of the methylene blue of à soil by means of the stain test* (NF P 94-068).

Association Française de Normalisation [AFNOR]. (2022). *Compressed earth blocks for walls and partitions: definitions. Specifications. Test methods. Delivery acceptance conditions* (XP P 13-901).

Association Française de Normalisation [AFNOR]. (2014). *Soils: investigation and testing. Determination of the compaction reference values of a soil type. Standard proctor test. Modified proctor test* (NF P 94-093).

Atiki, E. (2022). *Formulation et caractérisation des blocs de terre comprimée à base de déchets de palmiers dattiers* [doctoral thesis]. The University of Mohamed Khider Biskra.

Bahar, R., Benazzoug, M., & Kenai, S. (2004). Performance of compacted cement-stabilised soil. *Cement and Concrete Composites*, *26*(7), 811–820. https://doi.org/10.1016/j.cemconcomp.2004.01.003

Bureau of Indian Standards [BIS]. (1982). *Soil based blocks used in general building construction* (*IS 1725).*

Cid-Falceto, J., Mazarrón, F. R., & Cañas, I. (2012). Assessment of compressed earth blocks made in Spain: International durability tests. *Construction and Building Materials*, *37*, 738–745. https://doi.org/10.1016/j.conbuildmat.2012.08.019

Cruz, R., & Bogas, J. A. (2024). Durability of compressed earth blocks stabilised with recycled cement from concrete waste and incorporating construction and demolition waste. *Construction and Building Materials*, *450*, 138673. https://doi.org/10.1016/j.conbuildmat.2024.138673

Dao, K., Ouedraogo, M., Millogo, Y., Aubert, J. E., & Gomina, M. (2018). Thermal, hydric and mechanical behaviours of adobes stabilized with cement. *Construction and Building Materials*, *158*, 84–96. https://doi.org/10.1016/j.conbuildmat.2017.10.001

Elahi, T. E., Shahriar, A. R., & Islam, M. S. (2021). Engineering characteristics of compressed earth blocks stabilized with cement and fly ash. *Construction and Building Materials*, *277*, 122367. https://doi.org/10.1016/j.conbuildmat.2021.122367

European Committee for Standardization [CEN]. (2015). *Tests for geometrical properties of aggregates. Part 8: Assessment of fines. Sand equivalent test* (EN 933-8:2012+A1:2015).

European Committee for Standardization [CEN]. (2016). *Methods of testing cement. Part 1: Determination of strength* (EN 196-1).

European Committee for Standardization [CEN]. (2020). *Tests for geometrical properties of aggregates. Part 2: Determination of particle size distribution. Test sieves, nominal size of apertures* (EN 933-2).

Guettala, A., Abibsi, A., & Houari, H. (2006). Durability study of stabilized earth concrete under both laboratory and climatic conditions exposure. *Construction and Building Materials*, *20*(3), 119–127. https://doi.org/10.1016/j.conbuildmat.2005.02.001

Institut Algérien de Normalisation [IANOR]. (2013). *Composition, spécifications et critères de conformité des ciments courants* (NA 442-2013).

Kerali, A. G. (2001). *Durability of compressed and cement-stabilised building blocks* [doctoral thesis]. The University of Warwick, Coventry.

Kumar, N., & Barbato, M. (2022). Effects of sugarcane bagasse fibers on the properties of compressed and stabilized earth blocks. *Construction and Building Materials*, *315*, 125552. https://doi.org/10.1016/j.conbuildmat.2021.125552

Moevus, M., Anger, R., & Fontaine, L. (2012, April 22-27). *Hygro-thermo-mechanical properties of earthen materials for construction: a literature review*. Terra 2012, XIth International Conference on the Study and Conservation of Earthen Architectural Heritage, Lima, Peru. https://hal.science/hal-01005948v1/document

Muhwezi, L., & Achanit, S. E. (2019). Effect of sand on the properties of compressed soil-cement stabilized blocks. *Colloid and Surface Science*, *4*(1), 1–6. https://doi.org/10.11648/j.css.20190401.11

Poullain, P., Leklou, N., Laibi, A. B., & Gomina, M. (2019). Propriétés des briques de terre compressées réalisées àpartir de matériaux traditionnels du Bénin [Properties of compressed earth blocks made of traditional materials from Benin]. *Journal of Composite & Advanced Materials/Revue des Composites et des Matériaux Avancés*, *29*(4), 233–241.

Riza, F. V., & Rahman, I. A. (2015). The properties of compressed earth-based (CEB) masonry blocks. *Eco-efficient Masonry Bricks and Blocks: Design, Properties and Durability*, *2015*, 379–392. https://doi.org/10.1016/B978-1-78242-305-8.00017-6

Taallah, B. (2014). *Etude du comportement physico-mécanique du bloc de terre comprimée avec fibres* [doctoral thesis]. The University of Mohamed Khider Biskra. http://thesis.univ-biskra.dz/1173/1/Geni_civil_d4_2014.pdf

Taallah, B., Guettala, A., Guettala, S., & Kriker, A. (2014). Mechanical properties and hygroscopicity behavior of compressed earth block filled by date palm fibers. *Construction and Building Materials*, *59*, 161–168. https://doi.org/10.1016/j.conbuildmat.2014.02.058

Tripura, D. D., & Singh, K. D. (2015). Characteristic properties of cement-stabilized rammed earth blocks. *Journal of Materials in Civil Engineering*, *27*(7), 1–8. https://doi.org/10.1061/(asce)mt.1943-5533.0001170

Venkatarama Reddy, B. V., & Gupta, A. (2005). Characteristics of soil-cement blocks using highly sandy soils. *Materials and Structures/Materiaux et Constructions*, *38*(280), 651–658. https://doi.org/10.1617/14265

Venkatarama Reddy, B. V., & Latha, M. S. (2014). Influence of soil grading on the characteristics of cement stabilised soil compacts. *Materials and Structures/Materiaux et Constructions*, *47*(10), 1633–1645. https://doi.org/10.1617/s11527-013-0142-1

Walker, P. J. (1995). Strength, durability and shrinkage characteristics of cement stabilised soil blocks. *Cement and Concrete Composites*, *17*(4), 301–310. https://doi.org/10.1016/0958-9465(95)00019-9

Summary

Study on the mechanical performance of sustainable earth blocks from sandy granite saprolite and marble waste. In the pursuit of sustainable and energy-efficient construction materials, earth-based technologies such as compressed earth blocks (CEBs) offer a promising alternative to conventional fired bricks. This study investigates the physico-mechanical performance of CEBs formulated with 85% sandy granite saprolite from Chétaïbi and 15% marble waste, stabilized with varying cement contents (6%, 9%, and 12% by weight) and subjected to different compaction pressures. The produced blocks were evaluated in terms of dry density, total water absorption, compressive strength, and flexural strength. Results indicate that increasing the cement content significantly improves the mechanical properties while reducing water absorption. All formulations exceeded the minimum compressive strength of 2 MPa required by the French standard XP P 13-901, and water absorption values remained below the 15% threshold established by the Indian standard IS 1725. These findings confirm the potential of these blocks as a viable, low-impact alternative to traditional masonry units, supporting the development of more environmentally responsible construction practices.

Scientific Review Engineering and Environmental Sciences (2025), 34 (4), 348–361

Sci. Rev. Eng. Env. Sci. (2025), 34 (4) https://srees.sggw.edu.pl

ISSN 1732-9353 (suspended) eISSN 2543-7496 DOI 10.22630/srees.10744

Received: 19.08.2025
Accepted: 03.11.2025

Irwan LAKAWA✉
SUFRIANTO
HUJIYANTO
Agung SEPTIAWAN

Universitas Sulawesi Tenggara, Faculty of Engineering, Civil Engineering Department, Indonesia

Dynamic analysis of traffic noise across various land uses based on real-time data

Keywords: noise mapping, traffic, land use, real-time data

Introduction

One type of environmental pollution that significantly affects people's health and quality of life in big cities is traffic noise. The distribution of noise tends to vary depending on land use factors, such as residential, commercial, and industrial areas. At present, noise has become a serious environmental issue that must be taken into account in sustainable development policies (Othman et al., 2024). Therefore, understanding the distribution of noise across various types of land use is crucial for designing more effective environmental management policies. According to Lakawa et al. (2023), physical road characteristics, traffic volume, and roadside environmental conditions are some of the elements that can be used as indications of what causes traffic noise in metropolitan settings.

Traffic noise has become one of the strategic transportation issues in urban areas due to the increasing growth of motor vehicles (Graziuso et al., 2022; Meller et al., 2023). This condition is also observed in Kendari City. According to data,

✉ironelakawa@gmail.com

the growth rate of motor vehicles in Kendari City averages 9.3% per year (BPS – Statistics Kendari Municipality, 2024). Traffic activity resulting from this growth inevitably triggers traffic noise. The volume of heavy vehicles is the main variable affecting noise levels (Khedaywi et al., 2021).

Previous studies on several road segments in Kendari City found that noise levels had reached 70.5 dB (Lakawa et al., 2023). This figure has already exceeded the environmental noise threshold applicable in Indonesia (Keputusan KEP-48/MENLH/11/1996). At certain intensities, noise not only disrupts hearing but can also affect the physical and psychological health of residents and road users themselves (Sonaviya & Tandel, 2019; Dewi et al., 2023). High noise levels not only endanger human hearing but can also affect safety and work productivity (Starke et al., 2024). Therefore, it is necessary to predict traffic noise levels in the event of land use development (Alam et al., 2020).

Studies integrating real-time data with noise mapping across various land uses are still very limited. In general, research on traffic noise tends not to provide a comprehensive picture and does not take into account the dynamic relationship between noise and land use characteristics. The distribution of traffic noise across various land uses in Kendari City has never been comprehensively mapped, especially using technology based on real-time data. With technological advancements, real-time traffic noise data collection has become more feasible. The use of noise sensors can help accurately map noise distribution. The results of this study are expected to serve as a reference for the Kendari City Government in designing more environmentally friendly and sustainable transportation and spatial planning policies, particularly in noise control.

Materials and methods

Literature review

The noise characteristics of each road segment will naturally differ. This variation is influenced by numerous factors, such as differences in the types of motor vehicles, the proportion of heavy vehicles, vehicle speed, road conditions, and the surrounding environment. The effect of road service level on traffic noise is 31.1% (Lakawa et al., 2024). Therefore, further investigation is needed to identify the patterns of noise distribution across various land uses. According to Adza et al. (2022), traffic control and engineering systems are strategies that can be applied to reduce noise levels. These strategies include imposing vehicle speed limits, providing pedestrian-only zones, and installing traffic lights.

Lakawa, I., Sufrianto, Hujiyanto, Septiawan, A. (2025). Dynamic analysis of traffic noise across various land uses based on real-time data. *Sci. Rev. Eng. Env. Sci.*, *34* (4), 348–361. DOI 10.22630/srees.10744

Numerous large cities worldwide have undertaken studies on traffic noise. However, there is still a dearth of research, especially in small and medium--sized cities, that examines the distribution of noise across different land uses by combining real-time data with GIS-based mapping. Some related studies include mapping noise based on volunteered geographic information and Web mapping technology. Noise data were collected from residents using mobile devices to obtain subjective perceptions of noise in the community (Sofianopoulos et al., 2024).

Ibili et al. (2021) developed a model for interpreting traffic noise, including variations in assumptions. They discovered that the source, the line of sound transmission, and the noise receivers should all be the focus of efficient traffic noise control. Lee et al. (2022) mapped noise across all road types, where computational time efficiency was measured using grid methods and receiver height. Helal et al. (2019) performed real-time 3D noise mapping using 900 autonomous noise sensors, which measured all surrounding noise types such as vehicle sounds, sirens, and human conversations. This approach proved highly effective in improving strategies and policies to reduce urban environmental noise.

Zambon et al. (2018) investigated noise using the Dynamap method, which was developed to predict traffic noise in large urban areas. This system provided an accurate depiction of road traffic noise. Liu et al. (2025) combined geographical models and multi-source data to model noise utilizing IoT technologies. This approach combines a number of data sets, including ADS-B, meteorological, and noise data. The analysis results showed that the noise monitoring method used could effectively interpret noise distribution patterns.

The biggest factor affecting noise intensity is traffic density, which is followed by vehicle volume and speed (Lakawa et al., 2023). Increases in the number of motor vehicles on the road will lead to higher noise levels. Similarly, vehicle speed affects noise intensity-the faster the vehicle, the higher the noise level (Subramani et al., 2012). However, in cities with heterogeneous traffic characteristics, a phenomenon occurs where low vehicle speeds and traffic congestion actually increase traffic noise levels due to the common practice of drivers honking their horns (Lakawa et al., 2015).

Data collection and analysis

In general, the investigation and data analysis process is divided into three stages: data collection, data input/coding, and analysis with discussion. Traffic surveys (vehicle volume and speed) were conducted during peak hours

in the morning (06:00–09:00), midday (11:00–14:00), and afternoon (16:00–19:00). Simultaneously, real-time noise measurements were conducted across various land uses using a sound level meter (SLM) integrated with computer software. At each sampling point, two noise measurement units were placed: one at 1 m and the other at 10 m from the roadside. The SLM was installed at a height of 1.2 m above ground level. Subsequently, the coordinates for each noise point were digitized using GPS (Fig. 1). At a certain distance, noise intensity decreases with increasing distance from the roadside (Lakawa et al., 2022).

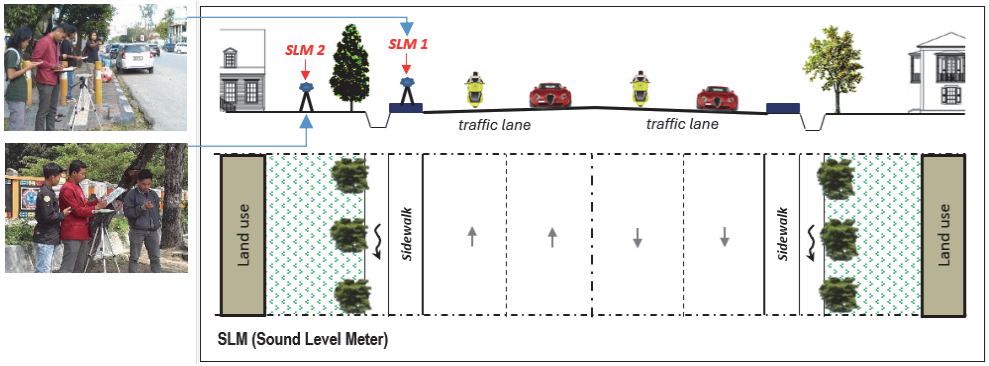

FIGURE 1. Schematic placement of SLM microphones for traffic noise measurement (SLM_1 at 1 m from the roadside, SLM_2 at 10 m from the roadside)

Source: own work.

A mathematical formula is used to determine the equivalent noise level (L_{eq}) based on field data:

$$L_{eq} = L_{50} + 0.43\ (L_1 - L_{50}), \tag{1}$$

where: L_{50} is the 50% noise indicator [dB], L_1 is the 1% noise indicator [dB], and L_{eq} is the equivalent noise level [dB].

An overlay was then performed according to the coordinate points to identify critical noise distribution. The validation stage involved comparing the analysis results with the noise quality standards set by Decree KEP-48/MENLH/11/1996 of the Minister of State for the Environment of the Republic of Indonesia (Table 1).

Lakawa, I., Sufrianto, Hujiyanto, Septiawan, A. (2025). Dynamic analysis of traffic noise across various land uses based on real-time data. *Sci. Rev. Eng. Env. Sci.*, *34* (4), 348–361. DOI 10.22630/srees.10744

TABLE 1. Noise level standards

Type of land use	Noise level [dB]
Land use designation	
Housing and settlements	55
Trade and services	70
Office and commerce	65
Green open space	50
Industry	70
Government and public facilities	60
Recreation	70
Special	
airport[a]	
railway station[a]	
seaport	70
cultural heritage	60
Surrounding activity	
Hospital or the like	55
School or the like	55
Place of prayer or the like	55

[a]Adjusted to the provisions of the Minister of Transportation.

Source: Decree KEP-48/MENLH/11/1996 of the Minister of State for the Environment of the Republic of Indonesia.

The highest amount of noise that can be released into the atmosphere without endangering public health or environmental comfort is known as the noise threshold value. The average sound pressure level during a certain time period can be expressed using the concept of equivalent noise level (L_{eq}). The sound generated by numerous vibrations dispersed in all directions is known as motor vehicle noise on roadways (Fig. 2).

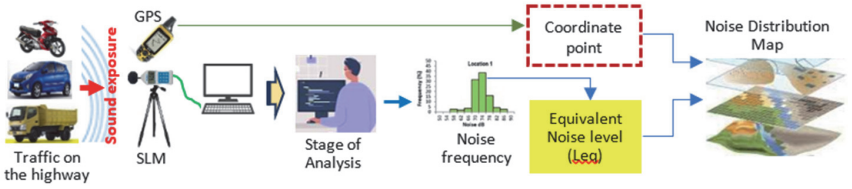

FIGURE 2. Flowchart of the noise monitoring and data analysis process

Source: own work.

Results and discussion

Traffic noise in Kendari City is considerably significant, with most areas exceeding the permissible threshold. Careful attention is required in spatial planning and traffic management to mitigate the impact of noise. Policy implementation is necessary in regulating traffic flow, operational hours for heavy vehicles, and the application of noise-reducing technologies on major roads as potential solutions to reduce noise impacts. This analysis compares noise levels at the roadside and within building yards. Noise levels tend to vary depending on the type of land use.

Figure 3 illustrates the probability distribution of noise levels for various land uses, both at the roadside and within building yards. These values vary according to the type of land use. A probability plot was used to assess whether the noise distribution data follow a normal distribution. The analysis's findings demonstrate that the data are normally distributed since the p-value is higher than 0.05.

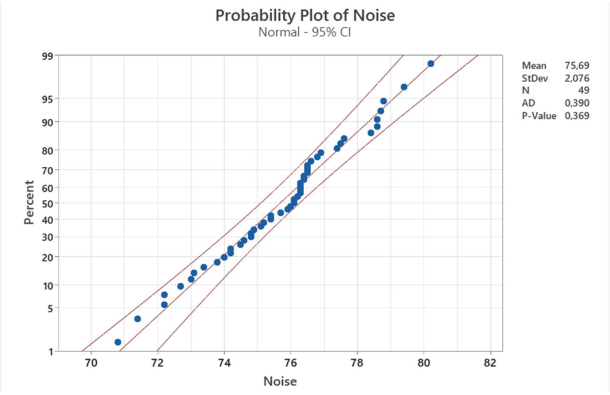

FIGURE 3. Probability of noise levels across various land uses
Source: own work.

Traffic noise was measured using the equivalent noise level (L_{eq}), which serves as a metric for assessing environmental noise caused by road traffic. Statistical analysis of noise levels at each sampling point across various land uses yielded L_{eq} values at the roadside (1 m from the roadside) and within yards (10 m from the roadside).

Traffic noise levels in Kendari City have exceeded the environmental noise thresholds for residential areas, schools, commercial areas, service areas, and public facilities. The average noise level at the roadside was 75.4 dB, while

Lakawa, I., Sufrianto, Hujiyanto, Septiawan, A. (2025). Dynamic analysis of traffic noise across various land uses based on real-time data. *Sci. Rev. Eng. Env. Sci.*, *34* (4), 348–361. DOI 10.22630/srees.10744

at 10 m from the roadside (yard) it was 71.1 dB. The difference in noise intensity between the roadside and the yard was 4.3 dB (Fig. 4). These levels are classified as high and may cause disturbances if exposure is continuous. Service, commercial, and office areas, which function as social activity centers, showed higher noise levels compared to residential areas, schools, and public facilities.

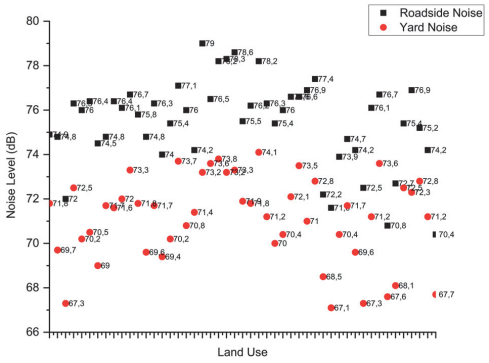

FIGURE 4. Results of the noise level analysis by land use (roadside and yard)
Source: own work.

Nearly all categories of land use in Kendari City are subject to traffic noise levels surpassing the limits established by Decree KEP-48/MENLH/11/1996 of the Minister of State for the Environment of the Republic of Indonesia. This indicates that traffic noise exposure is an aspect that must be taken seriously in spatial planning and transportation system management. Traffic management considerations should include measures such as one-way traffic systems and restrictions on heavy vehicles on certain roads.

Figure 5 illustrates the dynamic relationship between noise, speed, and traffic volume. The graph explains the interaction between traffic factors and noise levels on major roads in Kendari City. The fluctuation of variable values provides insight into how changes in traffic volume and vehicle speed contribute to noise intensity. This dynamic behavior indicates that the higher the traffic volume on a given road, the higher the resulting noise level. This is due to the greater number of vehicles moving along the road, which increases noise generated from vehicle engines, tire-road friction, and horn use. At the same time, vehicle speed tends to decrease due to traffic congestion. This is a logical outcome, as higher traffic volumes and congestion naturally result in reduced speeds. Land uses located along main roads with high traffic volumes will experience higher noise intensities compared to those situated farther from the roadside.

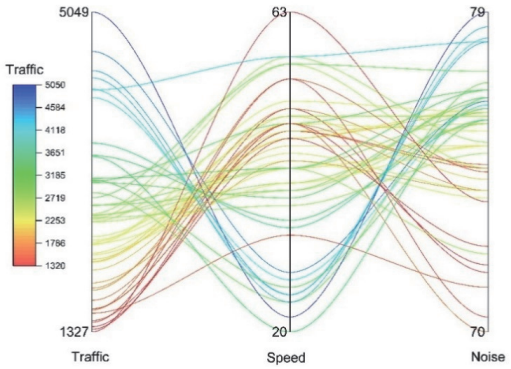

FIGURE 5. Dynamic behavior of traffic characteristics and noise levels
Source: own work.

Figure 6 depicts the critical noise exposure areas in Kendari City as a result of land development. These areas indicate zones that are likely to be affected by traffic noise exceeding environmental thresholds. Critical noise exposure generally occurs in areas with high traffic volumes. Infrastructure development, such as the expansion of commercial areas, can exacerbate this condition. Increased human activity in land use areas that is not balanced with adequate transportation management will result in heightened noise impacts.

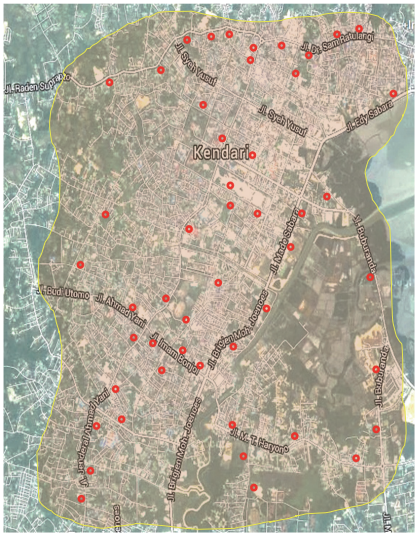

FIGURE 6. Critical noise exposure areas due to land development
Source: own work.

Lakawa, I., Sufrianto, Hujiyanto, Septiawan, A. (2025). Dynamic analysis of traffic noise across various land uses based on real-time data. *Sci. Rev. Eng. Env. Sci.*, *34* (4), 348–361. DOI 10.22630/srees.10744

Several areas experiencing critical noise exposure are strategic points connecting various community activity centers. Land development that fails to consider noise aspects can worsen environmental quality and create high-risk zones for residents, especially those living in residential areas close to main roads. Air pollution and noise constitute significant challenges in urban planning. Industrial zones and highways constitute the principal sources of air and environmental noise pollution (Govea et al., 2024). Wise transportation management policies are urgently needed to mitigate the negative impacts of noise in the future.

The highest noise exposure was recorded in service areas at 76.9 dB, followed by commercial areas at 76.1 dB, office areas at 75.8 dB, school areas at 75.4 dB, residential areas at 74.6 dB, and the lowest in public facility areas at 73.4 dB. High noise exposure in each land use type is influenced by the high trip generation rate of community activities. Additionally, location plays a role – these land uses are strategically situated along roads connecting several nearby community activity centers (Figs. 7 and 8).

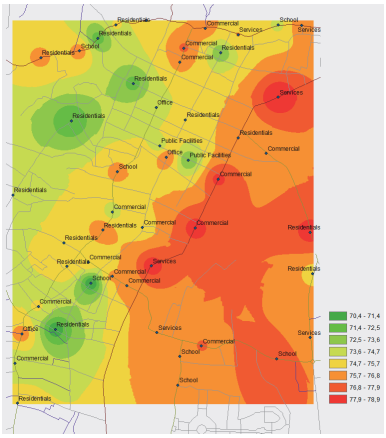

FIGURE 7. Distribution of traffic noise across various land uses
Source: own work.

The findings indicate that noise distribution is influenced not only by traffic volume and vehicle speed but also by the location of land near community activity centers. This phenomenon demonstrates that high-activity areas, such as service, commercial, and office zones, experience higher noise exposure compared to other areas. There is a significant relationship between land use, activity, and noise sources in urban areas (Margaritis et al., 2020). The influence of land use on noise levels is often considered secondary compared to traffic volume and other

noise sources. However, the results of this study reveal that the type and location of land use contribute to trip generation, which in turn triggers surrounding traffic noise. Commercial and densely serviced areas are the most affected by extreme noise levels.

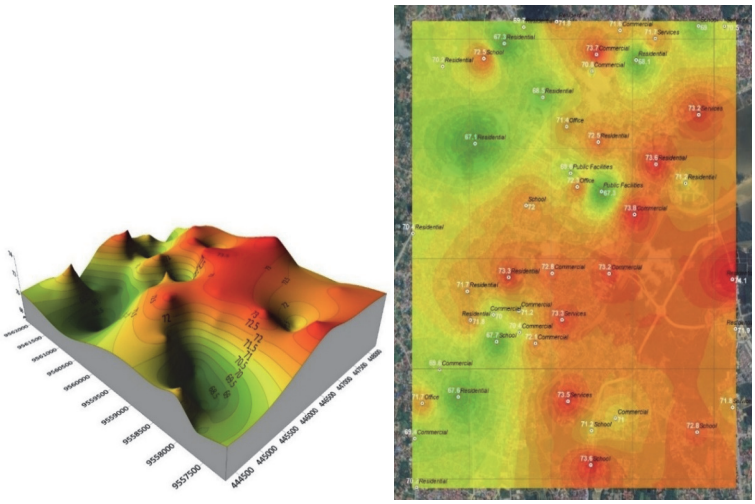

FIGURE 8. Traffic noise exposure at 10 m from the roadside
Source: own work.

Having noise maps facilitates the investigation and identification of problematic locations for urban residents (Lezhneva et al., 2019). Effective spatial planning and transportation system management should be considered to reduce traffic noise, especially in areas with high noise levels. Land use characteristics and traffic patterns inevitably differ between small and large cities. The use of real-time data enables dynamic noise monitoring, allowing changes in traffic conditions and external factors to be accounted for. This study not only measures noise based on traffic zones but also considers various land use types that influence noise levels holistically.

Conclusions

Traffic noise levels in Kendari City have exceeded the thresholds set by the Ministry of Environment of the Republic of Indonesia. The average noise level at the roadside reached 75.4 dB, while at 10 m from the roadside (yard) it was

71.1 dB. The main factors contributing to high noise levels are vehicle volume and the location of land used close to social activity centers. Noise levels vary depending on the type of land use. Office, service, and commercial areas have higher noise levels compared to residential areas, schools, and public facilities. The dynamic noise behavior observed shows that the higher the traffic volume, the greater the noise level produced.

The increase in noise intensity can endanger the health and comfort of residents living near roads. To mitigate noise impacts, integrated spatial policies are required in conjunction with transportation planning and management, such as regulating traffic circulation patterns and implementing green zones along roads. The Kendari City Government must take noise aspects into account in spatial planning, paying attention to the arrangement of green zones in accordance with noise potential. The implementation of green zones along roads, using natural barriers, can help reduce exposure to traffic noise.

The novelty of this research lies in the real-time data integration approach to map the distribution of traffic noise by land use types. This study not only measures noise levels statistically, but also considers the dynamic relationship between traffic volume, vehicle speed, and land use characteristics.

Acknowledgments

This article is an output of our research under the BIMA 2025 program. Therefore, we would like to express our gratitude to the Ministry of Higher Education, Science, and Technology of the Republic of Indonesia (Kemdiktisaintek) and the Directorate of Research and Community Service (DPPM) for providing the BIMA 2025 research grant. This research was funded through the PFR (Regular Fundamental Research) scheme under the Main Contract Number: 130/C3/DT.05.00/PL/2025 dated May 28, 2025, the Derivative Contract Number: 700/LL.9/PG/2025 dated June 3, 2025, and the Contract between the Research and Community Service Institute (LPPM) of the Universitas Sulawesi Tenggara and the researcher Number: 09/N/Kontrak-Penelitian/VI/2025 dated June 5, 2025. We also express our highest appreciation to the Rector and the Dean of the Faculty of Engineering, Universitas Sulawesi Tenggara, for their support and encouragement, which enabled the completion of this research. Special thanks are extended to all members of the research team for their collaboration from the preparation stage, data collection, data analysis, and preparation of the final report.

References

Adza, W. K., Hursthouse, A. S., Miller, J., & Boakye, D. (2022). Exploring the combined association between road traffic noise and air quality using QGIS. *International Journal of Environmental Research and Public Health*, *19*(24), 17057. https://doi.org/10.3390/ijerph192417057

Alam, P., Ahmad, K., Afsar, S. S., & Akhtar, N. (2020). Noise monitoring, mapping, and modelling Studies – A review. *Journal of Ecological Engineering*, *21*(4), 82–93. https://doi.org/10.12911/22998993/119804

BPS – Statistics Kendari Municipality (2024). *Kendari municipality in figures 2024*. BPS – Statistics Kendari Municipality.

Dewi, P. M., Prasetyo, L. B. B., & Armijaya, H. (2023). Analisis tingkat kebisingan lalu lintas berdasarkan variasi guna lahan (Studi kasus: Jalan AH Nasution Kota Metro). *Jurnal TESLINK: Teknik Sipil Dan Lingkungan*, *5*(1), 91–98. https://doi.org/10.52005/teslink.v5i1.156

Govea, J., Gaibor-Naranjo, W., Sanchez-Viteri, S., & Villegas-Ch, W. (2024). Integration of data and predictive models for the evaluation of air quality and noise in urban environments. *Sensors*, *24*(2), 1–18. https://doi.org/10.3390/s24020311

Graziuso, G., Francavilla, A. B., Mancini, S., & Guarnaccia, C. (2022). Application of the Harmonica Index for noise assessment in different spatial contexts. *Journal of Physics: Conference Series*, *2162*(1), 1–10. https://doi.org/10.1088/1742-6596/2162/1/012006

Helal, D., Dubouloz, S., Mortensen, J., Baldi, P., & Royo, P. (2019). Real-time 3D environmental noise monitoring and mapping using a large-scale Internet of Things. *INTER-NOISE and NOISE-CON Congress and Conference Proceedings*, *259*(2), 7937–7948.

Ibili, F., Adanu, E. K., Adams, C. A., Andam-Akorful, S. A., Turay, S. S., & Ajayi, S. A. (2021). Traffic noise models and noise guidelines: A review. *Noise & Vibration Worldwide*, *53*(1–2), 65–79. https://doi.org/10.1177/09574565211052693

Keputusan Menteri Negara Lingkungan Hidup Nomor KEP-48/MENLH/11/1996. Tentang Baku Tingkat Kebisingan [Decree of the State Minister of Environment of the Republic of Indonesia 48/MENLH/11/1996 concerning noise level standards].

Khedaywi, T., Alkofahi, N., & Alomari, L. (2021). Development of a statistical model for predicting traffic noise (case study: Irbid-Jordan). *Jordan Journal of Civil Engineering*, *15*(4), 551–561.

Lakawa, I., Hujiyanto, Sulaiman, & Haryono. (2022). The determination of noise area criteria based on prediction distance. *International Journal of Development Research*, *12*(11), 60589–60593.

Lakawa, I., Hujiyanto, & Haryono. (2023). A study of heterogeneous traffic noise trigger parameters for urban areas. *Technium: Romanian Journal of Applied Sciences and Technology*, *13*, 79–87. https://doi.org/10.47577/technium.v13i.9572

Lakawa, I, Sammang, L., Selintung, M., & Hustim, M. (2015, October 7–8). *Perilaku Hubungan Interaksi antara Kepadatan Lalu Lintas, Kecepatan, dan Kebisingan (Studi Kasus: Jalan Arteri dan Kolektor Kota Kendari)*. Prosiding Konferensi Nasional Teknik Sipil, Makassar.

Lakawa, I., Sufrianto, S., Syamsuddin, S. & Rahman, I. (2023). Pengaruh Karakteristik Lalu Lintas Terhadap Kebisingan Jalan Raya. *Sultra Civil Engineering Journal*, *4*(2), 123–132. https://doi.org/10.54297/sciej.v4i2.525

Lakawa, I., Syamsuddin, Hujiyanto, & Ilham, V. A. (2023). Noise mapping due to motor vehicle activities in the by-pass ring road area of the City of Kendari. *Scientific Review Engineering and Environmental Sciences*, *32*(4), 392–406. https://doi.org/10.22630/srees.5550

Lakawa, I., Syamsuddin, & Sudarta. (2024). The influence of road service quality on traffic noise levels. *International Journal of Management and Education in Human Development*, *4*(4), 1439–1445.

Lee, H. M., Luo, W., Xie, J., & Lee, H. P. (2022). Urban traffic noise mapping using building simplification in the Panyu District of Guangzhou City, China. *Sustainability*, *14*(8), 4465. https://doi.org/10.3390/su14084465

Lezhneva, E., Vakulenko, K., & Galkin, A. (2019). Assessment of traffic noise pollution due to urban residential road transport. *Romanian Journal of Transport Infrastructure*, *8*(1), 34–52. https://doi.org/10.2478/rjti-2019-0002

Liu, J., Sun, S., Tang, K., Fan, X., Lv, J., Fu, Y., Feng, X., & Zeng, L. (2025). IoT-based airport noise perception and monitoring: multi-source data fusion, spatial distribution modeling, and analysis. *Sensors*, *25*(8), 1–29. https://doi.org/10.3390/s25082347

Margaritis, E., Kang, J., Aletta, F., & Axelsson, Ö. (2020). On the relationship between land use and sound sources in the urban environment. *Journal of Urban Design*, *25*(5), 626–642. https://doi.org/10.1080/13574809.2020.1730691

Meller, G., Lourenço, W. M. de, Melo, V. S. G. de, & Campos Grigoletti, G. de (2023). Use of noise prediction models for road noise mapping in locations that do not have a standardized model: A short systematic review. *Environmental Monitoring and Assessment*, *195*(6), 740. https://doi.org/10.1007/s10661-023-11268-9

Othman, E., Cibilić, I., Poslončec-Petrić, V., & Saadallah, D. (2024). Investigating noise mapping in cities to associate noise levels with sources of noise using crowdsourcing applications. *Urban Science*, *8*(1), 13. https://doi.org/10.3390/urbansci8010013

Sofianopoulos, S., Stigas, S., Stratakos, E., Tserpes, K., Faka, A., & Chalkias, C. (2024). Citizens as environmental sensors: noise mapping and assessment on Lemnos Island, Greece, using VGI and web technologies. *European Journal of Geography*, *15*(2), 106–119. https://doi.org/10.48088/ejg.s.sof.15.2.106.119

Sonaviya, D. R., & Tandel, B. N. (2019). A review on GIS-based approach for road traffic noise mapping. *Indian Journal of Science and Technology*, *14*(12), 1–6. https://doi.org/10.17485/ijst/2019/v12i14/132481

Starke, R. A., Gerges, R. N. C., Dias, R. A., Noll, V., Hamad, A. F., Laporte, J. V. F., & Ratola, F. C. (2024). Real time industrial noise mapping with IoT Systems. *International Journal of Computer Applications*, *186*(43), 33–39.

Subramani, T., Kavitha, M., & Sivaraj, K. P. (2012). Modelling of traffic noise pollution. *International Journal of Engineering Research and Applications*, *2*(3), 3175–3182.

Zambon, G., Roman, H. E., Smiraglia, M., & Benocci, R. (2018). Monitoring and prediction of traffic noise in large urban areas. *Applied Sciences*, *8*(2), 1–17. https://doi.org/10.3390/app8020251

Summary

Dynamic analysis of traffic noise across various land uses based on real-time data. Traffic noise is one of the most significant forms of environmental pollution in urban areas. It can have negative impacts on both road users and residents living near highways. The high growth rate of motor vehicles from year to year in Kendari City has triggered an increase in traffic noise levels. This study aims to analyze the distribution of traffic noise across various land uses by utilizing real-time data. Noise measurements were conducted using a sound level meter (SLM) at several sampling points representing residential, commercial, service, office, school, and public facility areas. The SLM was positioned 1 m and 10 m away from the edge of the road. According to the findings of the analysis, Kendari City's traffic noise levels have exceeded the environmental noise threshold. The study found that the main factors contributing to high noise levels are traffic volume and low vehicle speed. Areas with high traffic volumes, such as service, commercial, and office zones, produce higher noise exposure compared to other land use types. Land uses located near social activity centers are significantly impacted by noise exposure. Real-time data--based noise mapping is highly effective in designing sustainable urban transportation and spatial planning policies in cities with heterogeneous traffic categories.

Scientific Review Engineering and Environmental Sciences (2025), 34 (4), 362–375

Sci. Rev. Eng. Env. Sci. (2025), 34 (4) https://srees.sggw.edu.pl

ISSN 1732-9353 (suspended) eISSN 2543-7496 DOI 10.22630/srees.10540

Received: 01.07.2025
Accepted: 13.10.2025

Tom OKOT✉

Universidad Latinoamericana de Ciencia y Tecnología, Costa Rica

Bridging sustainability awareness and housing preferences: insights from Generation Z in Costa Rica

Keywords: Generation Z, sustainable housing, green building certification, environmental attitude, Costa Rica, green mortgage

Introduction

Urban population growth, climate change, and the increasing scarcity of natural resources have placed substantial pressure on housing systems worldwide, especially in the Global South (Van Noorloos et al., 2020). In response, sustainable construction practices have gained prominence, seeking to reduce environmental impacts while improving building efficiency and long-term livability. Costa Rica, known for its strong environmental policies and progressive green agendas, presents a unique opportunity to study how younger generations perceive and engage with these sustainable housing options (Conejo et al., 2023). The sustainable construction movement arose from life-cycle thinking and resource efficiency principles (reduce, reuse, recycle), and early scholarship emphasized environmental assessment tools and whole-building sustainability evaluation (Ding, 2008; Bragança et al., 2010). Modern certification systems grew from these early frameworks.

✉tokot199@ulacit.ed.cr

In this paper, "Generation Z (Gen Z)" refers to individuals born between 1996 and 2010 (age cohort 22–28 in the present study). This cohort is characterized by high digital connectivity, early labor-market entry, and heightened exposure to environmental discourse via social media and formal education attributes that shape distinct consumption preferences and expectations for product transparency and sustainability (Dragolea et al., 2023).

In recent years, the construction sector has been recognized as one of the primary contributors to environmental degradation, accounting for 39% of global energy--related carbon dioxide emissions (Min et al., 2022). Latin American countries have begun implementing sustainability strategies in urban planning and housing development, including energy efficiency, water conservation, bioclimatic architecture, and the use of environmentally responsible materials (Nassary et al., 2022). Certification systems such as Leadership in Energy and Environmental Design (LEED) and Excellence in Design for Greater Efficiencies (EDGE) have played a pivotal role in operationalizing these goals, offering structured guidelines to assess the sustainability of real estate projects (Isimbi & Park, 2022).

This study focuses on LEED and EDGE, two internationally recognized certification systems with growing relevance in Costa Rica. LEED is a credit-based framework widely used worldwide, while EDGE is tailored for housing markets in emerging economies and emphasizes cost-effective efficiency measures. Both involve registration and review fees that increase initial project costs, but these are often offset by operational savings and higher market appeal. In Costa Rica, EDGE has recently been promoted through the Green Building Council (GBCCR) and financial institutions as part of green mortgage programs.

However, despite these advancements, the adoption of green construction practices remains limited, especially in residential real estate. One of the factors influencing this gap is consumer demand, or lack thereof, for sustainable features. While green technologies may offer long-term financial and ecological benefits, their uptake largely depends on whether potential buyers understand and value these attributes. This is particularly relevant for emerging buyer segments such as Gen Z, whose members are entering the housing market with distinct values and preferences shaped by digital exposure, climate change discourse, and educational access (Okot et al., 2022).

This study is grounded in two complementary theoretical frameworks: the theory of planned behavior (TPB) and the norm activation model (NAM). TPB posits that behavioral intentions are driven by attitudes toward the behavior, subjective norms, and perceived behavioral control (Ajzen, 2020). In the context of sustainable housing, this suggests that Gen Z consumers are more likely to consider eco-friendly

features if they perceive them as beneficial, socially endorsed, and within their purchasing power. NAM, on the other hand, emphasizes the role of personal norms activated by problem awareness and a sense of responsibility (Park & Ha, 2014). Applied to this context, it suggests that Gen Z individuals may feel morally compelled to support sustainable housing if they understand its environmental impact and feel personally accountable.

Costa Rica offers an ideal empirical setting to investigate these dynamics. The country has demonstrated a commitment to sustainability through national strategies such as the Decarbonization Plan 2018–2050, urban planning initiatives supporting green infrastructure, and its early adoption of renewable energy, which already powers over 98% of its electricity grid (Godínez-Zamora et al., 2020). However, residential projects still face challenges in balancing sustainability, affordability, and market appeal. Given that Costa Rican cities are experiencing densification, particularly in the greater metropolitan area (GAM), real estate developers are increasingly targeting younger buyers with vertical housing solutions, including apartments and mixed-use buildings.

Building on this context, the study seeks to answer the following questions:

1. Research questions:

– To what extent does Gen Z in Costa Rica value sustainable housing attributes in their residential purchase or rental decisions?
– What is the level of awareness and perceived importance of environmental certifications among Gen Z in the Costa Rican housing context?
– How do attitudes, perceived behavioral control, and personal norms influence Gen Z's preference for sustainable housing?

2. Research hypotheses:

– H1: Gen Z's positive attitudes toward sustainability significantly influence their preference for green-certified housing.
– H2: Higher levels of perceived behavioral control increase the likelihood of preferring sustainable housing options.
– H3: Personal environmental norms positively influence the perceived attractiveness of sustainable residential features.
– H4: Awareness of environmental certifications (e.g., EDGE, LEED) moderates the relationship between attitudes and housing preference.

To test these hypotheses, a quantitative survey was administered to members of Gen Z in Costa Rica, whose responses form the empirical basis of this research. The findings aim to inform both public policy and the real estate sector on how

to design and market residential projects that align with the values and expectations of the emerging Gen Z demographic, potentially accelerating the mainstreaming of sustainable construction in Latin America. Figure 1 summarizes the research design, instrument, and sampling, and the sequence of data cleaning and statistical analyses.

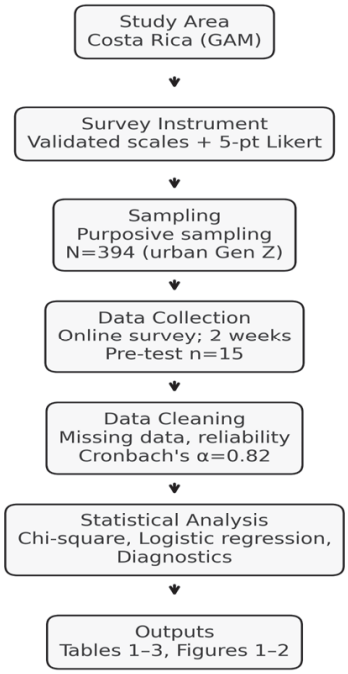

FIGURE 1. Methodological flow diagram
Source: own work.

Material and methods

Study area

The study was carried out in Costa Rica's GAM, which includes San José, Heredia, Alajuela, and Cartago. The GAM concentrates over 70% of the country's urban population and is the primary housing market targeted by new vertical developments (Instituto Nacional de Estadística y Censos [INEC], 2023).

Survey instrument and data collection

We used a structured online questionnaire, built from validated scales in TPB and NAM literature. Guided by TPB (Ajzen, 2020) and NAM (Le & Nguyen, 2022; Kim, 2023), the research aimed to test behavioral and normative predictors of interest in sustainable housing. The survey was designed based on validated instruments from existing literature on sustainable housing preferences (Aule et al., 2022; Isimbi & Park, 2022) and aligned with TPB and NAM constructs. The instrument consisted of: (a) sociodemographic items, (b) familiarity with certification systems (LEED, EDGE, and national initiatives), (c) importance ratings for 10 sustainable housing attributes (five-point Likert), and (d) items measuring attitudes, subjective norms, perceived behavioral control, and personal norms (five-point Likert). The questionnaire was pre-tested with 15 participants, and minor wording and flow edits were applied. The final survey was administered online for two weeks, distributed via university mailing lists, alumni networks, and social media. Participation was voluntary and anonymous, and informed consent was obtained. Ethical clearance was granted by Universidad Latinoamericana de Ciencia y Tecnología (ULACIT).

Sampling and sample characteristics

Inclusion criteria: age 22–28, current residence in the urban GAM, and basic internet access. Purposive sampling targeted digitally-accessible Gen Z respondents across multiple cantons in the GAM. Using Cochran's formula and a 95% confidence level, the required minimum sample was 385; after data cleaning, $N = 394$ valid responses remained (no missing key outcome data) (Mardia et al., 2024). The sample skews towards tertiary-educated respondents (67% university students or graduates), which we note as a limitation regarding representativeness.

Data analysis

Data processing and statistical analyses were conducted using IBM SPSS v27. Descriptive statistics summarized respondent profiles and attribute importance. Chi-square tests examined categorical associations (e.g., certification familiarity × × preference). Binary logistic regression tested predictors of preference for green--certified housing (dependent variable: preference for certified housing equals 1,

otherwise 0). Model checks included multicollinearity [variance inflation factor (*VIF*) below 2.0], linearity of continuous predictors with logit (Box–Tidwell test), influential observation checks (Cook's distance), and goodness-of-fit tests (Hosmer–Lemeshow). Results are reported with beta coefficients (β), standard errors (*SE*), Wald statistics, odds ratios [exp(β)], 95% confidence intervals, and model fit indices (Nagelkerke R^2). Statistical significance was set at $p < 0.05$.

Results and discussion

Descriptive statistics and participant profile

A total of 394 valid responses were collected from individuals aged 22 to 28 residing in urban areas of Costa Rica. Of these, 53% identified as female, 46% as male, and 1% as non-binary. The majority of respondents (67%) reported having a university degree or being currently enrolled in a tertiary program. Income distribution was relatively even, with 49% reporting a middle-income status and 31% identifying as lower-middle income.

Regarding environmental attitudes, 100% of respondents stated that environmental sustainability is "important" or "very important" to them, confirming a strong baseline environmental awareness in this generational cohort.

Awareness and perceived relevance of certifications

Despite the high degree of environmental concern, only 31% of participants reported familiarity with green housing certifications such as LEED or EDGE. Among those familiar, 72% associated these certifications with energy efficiency, and 54% with environmental health and air quality. However, nearly 70% of respondents could not explain the specific criteria or benefits associated with these certifications.

This finding suggests some knowledge–intention gap, where pro-environmental attitudes are not supported by functional knowledge, echoing similar patterns observed in sustainable consumption literature (Dimitrova et al., 2022). It aligns with NAM's premise that unless awareness is sufficiently activated, personal norms may not translate into action (Park & Ha, 2014; Table 1).

TABLE 1. Awareness and perceived value of green certifications among participants

Certification awareness	Familiar	Consider it important
	%	
LEED	29	66
EDGE	18	71
Not familiar with any	69	–

Source: own work based on survey responses.

Preference for sustainable housing attributes

Participants were asked to rank the importance of ten sustainable features using a five-point Likert scale (1 = not important, 5 = very important). The top three features were:

– energy efficiency ($\bar{x}$ = 4.61, *SD* = 0.48),
– quality of indoor environment ($\bar{x}$ = 4.44, *SD* = 0.53),
– bioclimatic design ($\bar{x}$ = 4.26, *SD* = 0.57).

Lower-rated attributes included the use of locally sourced materials ($\bar{x}$ = 3.41) and connection to graywater treatment systems ($\bar{x}$ = 3.52). While these latter features have strong environmental implications, they may lack perceptual immediacy or be poorly understood, reinforcing the role of perceived behavioral control and awareness, per TPB (Ajzen, 2020; Fig. 2).

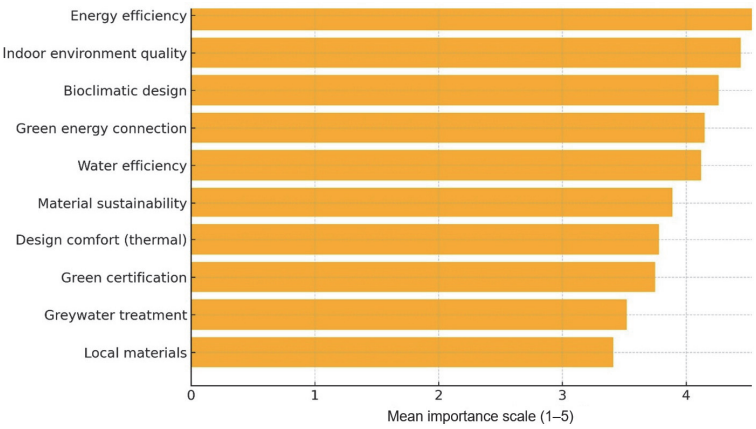

FIGURE 2. Sustainable housing attributes ranked by mean importance

Source: own work.

Model diagnostics and fit

The logistic regression model met assumptions and showed an acceptable fit. Multicollinearity diagnostics indicated *VIF* < 2.0 for all predictors, ruling out problematic collinearity. Linearity of the logit for continuous predictors was verified using the Box–Tidwell test (all $p > 0.05$), and no influential observations were detected (maximum Cook's distance < 1.0). Goodness-of-fit was satisfactory (Hosmer–Lemeshow $\chi^2 = 7.82$, $df = 8$, $p = 0.45$). The model explained approximately 26% of the variance in preference for certified housing (Nagelkerke $R^2 = 0.26$). Odds ratios and 95% confidence intervals are reported in Table 2, indicating that environmental attitudes (*OR* = 1.79, 95% *CI* [1.36, 2.37]), perceived behavioral control (*OR* = 1.55, 95% *CI* [1.09, 2.20]), personal norms (*OR* = 2.03, 95% *CI* [1.48, 2.80]), and certification awareness (*OR* = 1.43, 95% *CI* [1.03, 1.99]) significantly increased the likelihood of preferring green-certified housing.

TABLE 2. Logistic regression results predicting preference for green-certified housing ($n = 394$)

Predictor variable	β (*SE*)	Wald χ^2	p	*OR* [exp(β)]	95% *CI* for *OR*
Environmental attitude (H1)	0.58 (0.14)	17.14	0.000**	1.79	[1.36, 2.37]
Perceived behavioral control (H2)	0.44 (0.18)	6.00	0.014*	1.55	[1.09, 2.20]
Personal norms (H3)	0.71 (0.16)	19.72	0.000**	2.03	[1.48, 2.80]
Certification awareness × attitude (H4)	0.36 (0.17)	4.48	0.034*	1.43	[1.03, 1.99]

*$p < 0.05$; **$p < 0.01$.

Source: own work.

Regression analysis confirmed that environmental attitudes, perceived behavioral control, and personal norms significantly predict preference for certified green housing. Awareness of certification systems positively moderated this relationship. Table 3 presents a synthesis of the four tested hypotheses, including their theoretical basis, effect sizes (β), and significance levels. All hypotheses were statistically supported within the logistic regression model.

TABLE 3. Summary of hypotheses and regression results

Hypothesis	Statement	Supported?	β	p
H1	Environmental attitudes positively influence preference	supported	0.58	< 0.01
H2	Perceived behavioral control positively influences preference	supported	0.44	< 0.05
H3	Personal environmental norms increase preference likelihood	strongly supported	0.71	< 0.001
H4	Certification awareness moderates the attitude–preference relationship	supported	0.36	< 0.05

Source: own work.

Interpretation and theoretical contributions

These results confirm that attitudinal and normative drivers, as described in TPB and NAM, are central to Gen Z's housing preferences in Costa Rica. While prior studies have discussed environmental concerns abstractly (Dragolea et al., 2023), this paper provides empirical validation in the residential housing context, specifically among first-time market entrants in Latin America.

The observed moderating effect of certification awareness provides an actionable insight: promoting education on certification systems may significantly boost sustainable housing uptake. This is particularly relevant in a region where technical information is often fragmented, and green building literacy is low (Isimbi & Park, 2022).

Interestingly, while personal norms exhibited the strongest effect size, less tangible attributes like locally sourced materials or graywater treatment were less appreciated, likely due to limited visibility or knowledge. These findings support the notion that moral responsibility alone is insufficient without targeted awareness – a key implication for policymakers and developers (Levy, 2014).

Comparative insights and regional applicability

While this research focuses on Costa Rica, its insights are highly relevant across Latin America, where youth-led environmentalism is rising, yet housing markets remain slow to adapt. In countries like Colombia, Chile, and Mexico, similar generational demand patterns for eco-efficient housing are emerging, but adoption is limited by cost concerns, lack of awareness, and institutional inertia (Bungau et al., 2022).

A key differentiator between Millennials and Gen Z lies in digital fluency and immediacy of environmental urgency. While Millennials laid the foundation for sustainable consumption, Gen Z exhibits a sharper demand for transparency and long-term ecological value in purchasing decisions (Jasrotia et al., 2023). These preferences must be matched with responsive design and financing models, especially in urban peripheries where sustainable options are rare or unaffordable.

For housing developers across the region, market readiness remains uneven. While large firms are beginning to adopt green design principles, SMEs and cooperatives still face barriers in accessing certification systems or financing retrofits (Iwuanyanwu et al., 2024). Regional coordination through platforms like the Inter-American Development Bank's green housing initiatives or national climate financing programs could catalyze systemic change (Almeida et al., 2022).

Beyond Costa Rica, similar challenges and opportunities shape sustainable housing adoption across Latin America. In Mexico, progress has been constrained by limited access to green mortgage instruments, which restricts younger consumers' ability to finance certified housing. In Colombia, the uptake of certification has been hindered by cost barriers for small and medium-sized developers, limiting the diffusion of sustainable practices beyond high-end projects. In Chile, uneven regulatory incentives across municipalities have created disparities in sustainable housing implementation, despite national-level commitments to climate goals. Regional initiatives provide a counterbalance: the Inter-American Development Bank has piloted green housing financing programs that lower upfront cost barriers, and their regional case studies demonstrate how certification uptake can follow different pathways depending on local institutional support. These comparative insights highlight that Costa Rican Gen Z consumers display a strong preference for certified housing, yet regional constraints in financing, certification cost structures, and uneven policy incentives remain critical barriers to widespread adoption (Almeida et al., 2022).

Overall, scaling green housing adoption in Latin America will require not only policy harmonization but also active partnerships between developers, youth-oriented civil society groups, and multilateral funding sources. The Costa Rican case can serve as a blueprint for designing policy bundles and outreach strategies aligned with the values of environmentally engaged youth.

Conclusions

While the findings of this study contribute meaningful insights into Gen Z's housing preferences and sustainability attitudes in Costa Rica, several limitations should be acknowledged.

First, the use of non-probabilistic, purposive sampling, while effective for reaching a digitally connected urban Gen Z cohort, limits the generalizability of results. Participants were largely drawn from university networks and online platforms, potentially overrepresenting individuals with higher levels of education and sustainability exposure. As a result, the findings may not fully capture the perspectives of less connected or rural young adults, or those without a tertiary education.

Second, the study's cross-sectional design restricts the ability to draw causal conclusions or assess changes over time. Environmental awareness and housing market dynamics are evolving rapidly, particularly in response to climate-related

policies and economic volatility. Future studies employing longitudinal methods could help track the stability of green housing preferences as Gen Z transitions into different life stages or as housing affordability shifts in response to policy incentives.

Third, while the study applied validated theoretical models (TPB and NAM), it relied on self-reported intentions rather than actual housing decisions. Although intentions are meaningful predictors of behavior, future research would benefit from incorporating behavioral data, such as home purchase patterns or rental choices among green-certified versus conventional units.

Additionally, the study was geographically limited to Costa Rica, which, while a leader in sustainability policy, may differ significantly from other Latin American nations in terms of housing finance systems, urban infrastructure, and environmental regulation. Comparative studies across countries like Colombia, Mexico, or Brazil could offer valuable cross-cultural insights and test the robustness of the TPB–NAM framework in diverse institutional environments.

Finally, future research could explore intergenerational comparisons, such as differences between Millennials, Gen X, and Gen Z in how they perceive and act upon green housing opportunities. These insights could support segmentation strategies for developers and inform policy design that reflects the diverse environmental motivations across age groups.

By addressing these limitations, future research can expand the external validity and practical utility of green housing studies in Latin America and beyond.

This study explored the preferences of Costa Rica's Gen Z regarding sustainable residential housing, with a focus on the perceived value of green building attributes and environmental certifications. The findings confirm that members of this demographic cohort exhibit strong pro-environmental attitudes, prioritizing features such as energy efficiency, indoor environmental quality, and bioclimatic design when considering housing options. These results are consistent with the increasing global awareness among younger generations about climate change and resource depletion and reflect Costa Rica's longstanding commitment to sustainability.

Despite this interest, the study identified a significant knowledge gap concerning green housing certifications, as only 31% of respondents were familiar with systems like LEED or EDGE. This disconnect between environmental concern and technical awareness represents a barrier to informed housing decisions and highlights the need for targeted communication strategies. Developers and policymakers must work to translate sustainability into accessible, visible, and trusted information, particularly through certification education and labeling.

The application of TPB and NAM provided strong theoretical grounding for understanding the behavioral mechanisms driving these preferences. Statistical

analysis showed that environmental attitudes, perceived behavioral control, and personal environmental norms were all significant predictors of preference for certified green housing. Furthermore, awareness of certification systems moderates the relationship between attitudes and housing preference, suggesting that education and exposure can significantly enhance sustainable decision-making.

These results have important implications for housing developers, urban planners, and public institutions. Promoting green certifications, offering financing incentives such as green mortgages, and embedding sustainability into housing policy frameworks are key steps toward aligning market offerings with the values of a new generation of buyers. Additionally, this research underscores the importance of investing in sustainability literacy campaigns that go beyond general awareness to provide clear, actionable knowledge.

By bridging the gap between environmental values and technical understanding, Costa Rica can lead by example in the Latin American region. Empowering Gen Z with tools to act on their sustainable preferences may not only transform housing markets but also contribute to broader environmental and social resilience.

References

Ajzen, I. (2020). The theory of planned behavior: Frequently asked questions. *Human Behavior and Emerging Technologies*, *2*(4), 314–324. https://doi.org/10.1002/hbe2.195

Almeida, M. D., Eguino, H., Gómez Reino, J. L., & Radics, A. (2022). *Decentralized governance and climate change in Latin America and the Caribbean. Inter-American Development Bank Regional Chapter.* Paper presented at the Decentralized Governance and Climate Change Conference, Georgia State University, Atlanta, GA, USA.

Aule, T. T., Majid, R. B. A., & Jusan, M. B. M. D. (2022). Exploring cultural values and sustainability preferences in housing development: A structural equation modeling approach. *Scientific Review Engineering and Environmental Sciences*, *31*(3), 149–160. https://doi.org/10.22630/srees.2971

Bragança, L., Mateus, R., & Koukkari, H. (2010). Building sustainability assessment. *Sustainability*, *2*(7), 2010–2023. https://doi.org/10.3390/su2072010

Bungau, C. C., Bungau, T., Prada, I. F., & Prada, M. F. (2022). Green buildings as a necessity for sustainable environment development: dilemmas and challenges. *Sustainability*, *14*(20), 13121. https://doi.org/10.3390/su142013121

Conejo, F. J., Rojas, W., Zamora, A. L., & Young, C. E. (2023). Really, that sustainable? Exploring Costa Ricans' green product involvement. *Journal of Macromarketing*, *43*(2), 215–232. https://doi.org/10.1177/02761467231153573

Dimitrova, T., Ilieva, I., & Stanev, V. (2022). I consume, therefore I am? Hyperconsumption behavior: Scale development and validation. *Social Sciences*, *11*(11), 532. https://doi.org/10.3390/socsci11110532

Ding, G. K. (2008). Sustainable construction – The role of environmental assessment tools. *Journal of Environmental Management*, *86*(3), 451–464. https://doi.org/10.1016/j.jenvman.2006.12.025

Dragolea, L-L., Butnaru, G. I., Kot, S., Zamfir, C. G., Nuţă, A-C., Nuţă, F-M., Cristea, D. S., & Ştefănică, M. (2023). Determining factors in shaping the sustainable behavior of the Generation Z consumer. *Frontiers in Environmental Science*, *11*, 1096183. https://doi.org/10.3389/fenvs.2023.1096183

Godínez-Zamora, G., Victor-Gallardo, L., Angulo-Paniagua, J., Ramos, E., Howells, M., Usher, W., De León, F., Meza, A., & Quirós-Tortós, J. (2020). Decarbonising the transport and energy sectors: Technical feasibility and socioeconomic impacts in Costa Rica. *Energy Strategy Reviews*, *32*, 100573. https://doi.org/10.1016/j.esr.2020.100573

IBM Corp. (2020). *IBM SPSS Statistics (Version 27.0)*. IBM Corp.

Instituto Nacional de Estadística y Censos [INEC]. (2023). *Anuario de Estadísticas demográficas 2023*. Costa Rica.

Isimbi, D., & Park, J. (2022). The analysis of the EDGE certification system on residential complexes to improve sustainability and affordability. *Buildings*, *12*(10), 1729. https://doi.org/10.3390/buildings12101729

Iwuanyanwu, O., Gil-Ozoudeh, I., Okwandu, A. C., & Ike, C. S. (2024). Retrofitting existing buildings for sustainability: Challenges and innovations. *Engineering Science & Technology Journal*, *5*(8), 2616–2631. https://doi.org/10.51594/estj.v5i8.1515

Jasrotia, S. S., Darda, P., & Pandey, S. (2023). Changing values of millennials and centennials towards responsible consumption and a sustainable society. *Society and Business Review*, *18*(2), 244–263. https://doi.org/10.1108/SBR-01-2022-0013

Kim, Y. (2023). A study of the integrated model with norm activation model and theory of planned behavior: applying the green hotel's corporate social responsibilities. *Sustainability*, *15*(5), 4680. https://doi.org/10.3390/su15054680

Le, M. H., & Nguyen, P. M. (2022). Integrating the theory of planned behavior and the norm activation model to investigate organic food purchase intention: evidence from Vietnam. *Sustainability*, *14*(2), 816. https://doi.org/10.3390/su14020816

Levy, N. (2014). *Consciousness and moral responsibility*. Oxford University Press (UK).

Mardia, K. V., Kent, J. T., & Taylor, C. C. (2024). *Multivariate analysis* (2nd ed.). John Wiley & Sons.

Min, J., Yan, G., Abed, A. M., Elattar, S., Khadimallah, M. A., Jan, A., & Ali, H. E. (2022). The effect of carbon dioxide emissions on the building energy efficiency. *Fuel*, *326*, 124842. https://doi.org/10.1016/j.fuel.2022.124842

Nassary, E. K., Msomba, B. H., Masele, W. E., Ndaki, P. M., & Kahangwa, C. A. (2022). Exploring urban green packages as part of Nature-based Solutions for climate change adaptation measures in rapidly growing cities of the Global South. *Journal of Environmental Management*, *310*, 114786. https://doi.org/10.1016/j.jenvman.2022.114786

Okot, T., Hernandez, E., Zumbado, C., López, E., & Navarro, V. (2022). Construction and Real Estate Sustainability Management: Costa Rican Prospects 2016–2021. *Baltic Journal of Real Estate Economics and Construction Management*, *10*(1), 1–15. https://doi.org/10.2478/bjreecm-2022-0001

Park, J., & Ha, S. (2014). Understanding consumer recycling behavior: Combining the theory of planned behavior and the norm activation model. *Family and Consumer Sciences Research Journal*, *42*(3), 278–291. https://doi.org/10.1111/fcsr.12061

Van Noorloos, F., Cirolia, L. R., Friendly, A., Jukur, S., Schramm, S., Steel, G., & Valenzuela, L. (2020). Incremental housing as a node for intersecting flows of city-making: rethinking the housing shortage in the global South. *Environment and Urbanization*, *32*(1), 37–54. https://doi.org/10.1177/0956247819887679

Summary

Bridging sustainability awareness and housing preferences: insights from Generation Z in Costa Rica. This study investigates how Generation Z perceives and values sustainable residential housing, with a focus on environmental attitudes, personal norms, and awareness of green building certifications. This study is situated in Costa Rica, one of Latin America's sustainability leaders. It applies the theory of planned behavior (TPB) and the norm activation model (NAM) to explore the behavioral and normative drivers of housing preferences. A structured survey of 394 urban residents aged 22–28 was conducted, and responses were analyzed using descriptive statistics and binary logistic regression with diagnostic tests. Findings show that energy efficiency, indoor environmental quality, and bioclimatic design are the most valued features. Although environmental concern is nearly universal among respondents, only 31% are familiar with certifications such as LEED or EDGE, revealing a critical awareness gap. Regression analysis confirms that pro-environmental attitudes, perceived behavioral control, and personal norms significantly influence preference for green-certified housing, and certification awareness strengthens this relationship. These insights highlight the need for targeted sustainability education and clearer communication of certification systems. The study offers practical guidance for developers, urban planners, and policymakers aiming to align residential products with the values of environmentally conscious young adults in Costa Rica and comparable markets.

Scientific Review Engineering and Environmental Sciences (2025), 34 (4), 376–397

Sci. Rev. Eng. Env. Sci. (2025), 34 (4) https://srees.sggw.edu.pl

ISSN 1732-9353 (suspended) eISSN 2543-7496 DOI 10.22630/srees.10809

Received: 16.09.2025
Accepted: 11.11.2025

Michael MANTON[1]✉
Vaidotas GRIGALIŪNAS[2]
Leonas JARAŠIUS[3]
Jūratė SENDŽIKAITĖ[3, 4]
Gabija TAMULAITYTĖ[1]
Maria GRODZKA-ŁUKASZEWSKA[5]

[1]Vytautas Magnus University, Bioeconomy Research Institute, Lithuania
[2]Directorate of Žemaitija Protected Areas, Lithuania
[3]Foundation for Peatland Restoration and Conservation, Lithuania
[4]Vilniaus Kolegija, Faculty of Agrotechnologies, Lithuania
[5]Warsaw University of Technology, Faculty of Environmental Engineering, Poland

Drained and forgotten peat extraction sites: economic and carbon impacts of peat and water loss in spontaneously forested Lithuanian peatlands

Keywords: nature conservation, drained peatlands, soil carbon, rewetting, wetlands, ecosystem services

Introduction

Peatlands are globally important ecosystems that cover only around 3% of the Earth's land surface; however, they store nearly one-third of the world's soil carbon (United Nations Environment Programme [UNEP], 2022). This exceptional

✉michael.manton@vdu.lt

capacity results from the accumulation of partially decomposed organic material under persistently wet, oxygen-poor conditions, which slows microbial activity and allows carbon to build up over time (Craft, 2015).

Beyond carbon storage, peatlands provide a range of ecosystem services, including water regulation, nutrient retention, and support for specialized biodiversity (Joosten & Clarke, 2002; Tanneberger & Wichtmann, 2011). Their stable hydrological regimes help mitigate floods and droughts, while their organic soils are suitable for distinctive plant and animal communities. Peatlands also serve as valuable witnesses of historical nature development and are a part of local cultural heritage.

Despite these values, many peatlands across Europe have been drained and degraded due to agricultural expansion, forestry, and peat extraction (Joosten, 2009). Widespread drainage for peat mining and land use conversion has led to a loss of the acrotelm (the active peat-forming layer) and disrupted hydrological conditions and has triggered long-term carbon emissions (Leifeld & Menichetti, 2018). As an example, peat extraction has affected 4.2% of the raised bogs in the Baltic States (Hofer et al., 2012; Karofeld et al., 2016). The European Union's consumption of peat has drawn criticism for its unsustainable nature and lack of long-term resource management strategies (Patel et al., 2025). The cessation of peat extraction without subsequent restoration efforts can lead to the collapse of the peatland ecosystem, with degraded sites often remaining drained, resulting in continued peat decomposition, subsidence, and impaired vegetation recovery (Rydin et al., 2013). Natural recovery and regeneration of associated peatland vegetation is typically limited by persistent low water levels, altered nutrient regimes, and vegetation shifts toward non-peat-forming species (Boers et al., 2006; Manton et al., 2021). Although spontaneous tree colonization may stabilize the soil, it does not restore natural ecosystem processes and functions of peatland and thus may, in fact, increase greenhouse gas (GHG) emissions (Craft, 2015; Kamocki et al., 2025). In managed but continuously drained peatland forests, carbon accumulation in biomass and litter input does not compensate for carbon losses(Mander et al., 2024). Afforesting drained peatlands also fails to reestablish their native biodiversity and ecological functions (Haapalehto et al., 2017; Jurasinski et al., 2024). Moreover, such interventions may increase the vulnerability of these landscapes to wildfires (Kohlenberg et al., 2018; Zheng et al., 2023).

Recognizing the climate and ecological impacts of peatland degradation, the European Union has placed restoration at the core of several key policy instruments. The EU Biodiversity Strategy for 2030, the Soil Strategy, and the Nature Restoration Law all identify the rewetting of drained peatlands as a critical measure

Manton, M., Grigaliūnas, V., Jarašius, L., Sendžikaitė, J., Tamulaitytė, G., Grodzka-Łukaszewska, M. (2025). Drained and forgotten peat extraction sites: economic and carbon impacts of peat and water loss in spontaneously forested Lithuanian peatlands. *Sci. Rev. Eng. Env. Sci.*, *34* (4), 376–397. DOI 10.22630/srees.10809

for meeting climate and biodiversity goals (Communication COM/2020/380, Communication COM/2021/699, Regulation (EU) 2022/869). Regulation (EU) 2018/841 highlights the importance of restoring organic soils, including peatlands, to enhance carbon removals in the land-use sector. Recent studies have emphasized that afforestation of drained peatlands, in the absence of hydrological restoration, is unlikely to deliver climate benefits and may even exacerbate GHG emissions (Jurasinski et al., 2024; Mander et al., 2024). Instead, rewetting and ecological restoration, such as through paludiculture or the reintroduction of peat-forming vegetation, are increasingly recognized as effective nature-based solutions (Wichmann & Nordt, 2024).

In this study, we assess the ecological condition and restoration potential of abandoned peat extraction sites in Lithuania. Focusing on forested post-extraction peatlands, we quantify peat volume loss, hydrological alterations, and associated carbon emissions. By evaluating degradation levels and the extent of ecosystem service loss, we aim to support site-specific restoration strategies that align with EU policy objectives. Our findings provide a basis for targeted rewetting efforts to reduce GHG emissions, improve ecological function, and contribute to national and European peatland restoration commitments.

Material and methods

Study area and spatial data analysis

Peatlands are an integral component of Lithuania's landscape, covering approx. 640,000 ha (10% of the country), and represent one of the country's most hydrologically and ecologically significant ecosystems (Valatka et al., 2018). Based on their geological origin and trophic status, peatlands in Lithuania comprise three main types: fens (78%), minerotrophic systems fed by mineral-rich groundwater, surface runoff, and precipitation; raised bogs (8%), oligotrophic peatlands elevated above the surrounding terrain and sustained purely by precipitation; and transitional mires (14%), which exhibit intermediate characteristics of both fens and bogs (Mitsch & Gosselink, 2015; Manton et al., 2021).

Historically, peat extraction has played a major role in the rural economy, beginning in the early 20th century and expanding rapidly during the Soviet industrial period (1950–1990) (Paavilainen & Päivänen, 1995). Currently, approx. 70% of Lithuania's peatlands have been drained and show evidence of human disturbance (Jarašius et al., 2015; Valatka et al., 2018). In total, peat extraction

sites cover 20,533 hectares of which 60% are overgrown by secondary forests (Grigaliunas et al., 2023). The abandonment of drained and or extracted peatlands generally undergo spontaneous succession, typically colonized by pioneer woody species such as *Betula pubescens*, *Pinus sylvestris*, and *Salix* spp., resulting in the formation of secondary forests with altered hydrological regimes (Manton et al., 2021; Jarašius et al., 2022). Although these peatlands are degraded, they provide valuable opportunities for understanding hydrological recovery, vegetation succession, and ecosystem service restoration in peatland landscapes (Makrickas et al., 2023).

This study focuses on 33 abandoned peatland quarries (3,854 ha) in Lithuania, Northern Europe (Fig. 1).

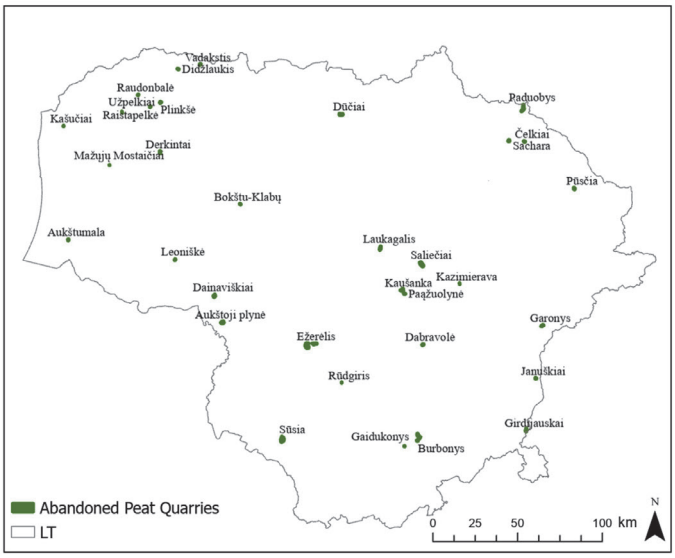

FIGURE 1. Distribution of abandoned peatlands in the territory of the country and location of the areas investigated during field research

Source: own work.

To identify and characterize degraded peatlands in forested areas across Lithuania, we first conducted a GIS-based spatial analysis to identify the spatial components of the peatlands (i.e., location, area, elevation). We used data from three national data sources: the Lithuanian mire and peatlands database (Agricultural Data Center [ŽŪDC], 2025), the cadastral database (Lithuanian State Forest Service [VMU], 2021), and the Lithuanian database of biodiversity (Valstybinė saugomų teritorijų tarnyba prie Aplinkos ministerijos [VSTT], 2025).

Manton, M., Grigaliūnas, V., Jarašius, L., Sendžikaitė, J., Tamulaitytė, G., Grodzka-Łukaszewska, M. (2025). Drained and forgotten peat extraction sites: economic and carbon impacts of peat and water loss in spontaneously forested Lithuanian peatlands. *Sci. Rev. Eng. Env. Sci.*, *34* (4), 376–397. DOI 10.22630/srees.10809

The selection of the 33 abandoned peatland quarries was based on the presence of historical peat extraction data, spatial representation throughout Lithuania and a range of ecological conditions (i.e., peatland type, peat depth, water level, vegetation type, woody biomass, etc.) (Fig. 2).

FIGURE 2. Three samples of abandoned peatland quarries showing the range of ecological conditions found in Lithuania

Source: photos by J. Sendžikaitė.

Field investigations

The representative 33 abandoned peatland quarries were selected for field investigations, which were conducted between 2022 and 2023. At each site, we assessed peat depth, soil acidity (pH), carbon-to-nitrogen ratio (C : N), water table level (depth), and wood volume to determine the condition of the abandoned peatlands.

Peat depth was measured by applying a minimum of 10 sampling points along a standardized 100 m sampling transect using a standard peat corer following national peat survey guidelines (Saulėnas, 1993). We collected three samples at each site from the upper peat layer (5–15 cm) for laboratory analysis. The samples were analyzed for pH (measured in a 1 : 2.5 peat–water suspension), total organic carbon (by wet oxidation or spectrophotometry), and total Kjeldahl nitrogen, allowing us to calculate the C : N ratio. Trophic status (oligotrophic, mesotrophic, or eutrophic) was estimated based on the C : N and vegetation composition, following the classification system of Succow and Stegmann (2001),

while the degree of peat decomposition was assessed in the field using the von Post humification scale (H1–H10).

Water table levels were recorded at the same locations as the peat depth measurements, and we supplemented the water table levels with long-term data from automated loggers at five sites (Aukštumala, Sachara, Pūsčia, Plinkšiai and Užpelkiai). Based on Koska et al. (2001), we classified site moisture regimes into six categories, from dry to lower eulittoral. For analysis, we used a threshold depth of 35 cm below the surface. Sites with an average water table deeper than this were considered to have unfavorable conditions for natural peat formation and thus considered degraded.

The analysis of wood volume on abandoned peatland quarries can help assess ecosystem recovery and carbon sequestration, as tree biomass reflects post--extraction succession. Increased wood volume also indicates peatland degradation, such as drying or nutrient enrichment, making it a useful but context-dependent indicator of peatland condition (Makrickas et al., 2023). Therefore, we used the cadastral database (VMU, 2021) to estimate the tree wood volume for each of the 33 abandoned peatland quarries.

Data analysis – principal component analysis

Using past statistics (Hammer, 2023) we normalized the five peatland characteristic data (peat depth, soil pH, C : N, water depth, and wood volume) and performed a multivariate principal component analysis (PCA) using a variance––covariance matrix. The PCA was performed to reduce the complexity of the dataset by transforming the five correlated environmental variables (C : N, pH, peat depth, water level and wood volume) into components that capture the main ecological gradients. We also performed a cluster analysis. These analyses produced a clearer visualization of site differences and identified key drivers like acidity, hydrology, and forest volume across peatland types.

Estimation of ecosystem service value

Peat

To evaluate the extent of peatland degradation, we estimated the volume of peat loss by comparing current and presumed natural historical surface elevations prior to peat extraction for each of the 33 sites. The analysis combined vector data representing peatland boundaries with raster-based surface elevation data.

Polygons delineating peatland areas in a shapefile format were used. For each site, a digital elevation model containing values representing the current peat surface altitude in meters above sea level was defined. All spatial data were projected to the Lithuanian Coordinate System of 1992 (LKS-92) to ensure geometric compatibility.

To estimate the original peat surface before drainage or subsidence, we used a two-meter buffer ring around each polygon. The outer buffer (expanded by 2 m) and the inner buffer (contracted by 2 m) defined a ring-shaped area approximating the undisturbed rim. The mean elevation value within this rim was taken as the reference historical surface level. The current average surface elevation was then calculated using raster values within each peatland polygon.

The difference between historical and current averages provided an estimate of surface lowering and thus the loss of peat through both extraction and subsequent subsidence following abandonment. Subsequently, we used the average peat market price of €116 per ton (t) to estimate the carbon loss value of each of the 33 peatlands (IndexBox, 2025).

We applied the following equation to estimate the value of peat loss: value [€] = = peat volume [m^3] × bulk density [$t \cdot m^{-3}$] × price [$€ \cdot t^{-1}$], where: bulk density is 0.1 $t \cdot m^{-3}$ and price is €116 per ton.

Water

To estimate the reduction in water retention capacity, we assumed that the field capacity of peat is up to 80% of its volume in water (Holden, 2005). Thus, every cubic meter of peat lost corresponds to 0.8 m^3 of water storage capacity lost. To provide an indicative economic value, we used a rate of €0.54 per m^3 of water, based on benefit transfer values from regional studies (e.g., Stachowicz et al., 2022; Makrickas et al., 2023). This allowed us to estimate the value of lost hydrological services. We emphasize that these estimates are general and should be treated as indicative rather than site-specific.

Carbon

Carbon loss from peat extraction was estimated by converting the volume of removed peat into dry mass, applying a carbon fraction, and expressing the result as both tons of carbon (t C) and carbon dioxide equivalents (t CO_2) using the following equations (Intergovernmental Panel on Climate Change [IPCC], 2014):

– Peat mass [kg] was calculated as: $M_{peat} = V \times \rho_{peat}$, where: V is peat volume [m^3] and ρ_{peat} is bulk density [$kg \cdot m^{-3}$].

– Carbon stock [t C] was then estimated as: $C = \frac{V \times \rho_{peat} \times fC}{1{,}000}$, where: *fC* is the carbon fraction of peat.

– Carbon dioxide equivalents [t CO_2] were derived as: $CO_2\,eq. = \frac{V \times \rho_{peat} \times fC}{1{,}000\left(\frac{44}{12}\right)}$, where: ρ_{peat} is 100 kg·m^{-3} (mid-range of 60–150 kg·m^{-3}) (Parish et al., 2008) and carbon fraction (*fC*) is 0.50 (mid-range of 0.45–0.55) (Gorham, 1991; Joosten & Clarke, 2002).

It should be noted that this mid-range approach assumes uniform peat properties across the extracted peat quarries, as site-specific variability in bulk density or decomposition state was not available. It also represents carbon removed as stock (Turetsky et al., 2015). This stock-based approach is widely applied in peatland carbon accounting when direct flux data are lacking (Gorham, 1991; Joosten & Clarke, 2002; Turetsky et al., 2015).

Finally, we used the average carbon dioxide emission market price of €57.24 (VICAP) (from 1 January 2024 to 5 September 2025) to estimate the carbon loss value of each of the 33 peatlands (International Carbon Action Partnership [ICAP], 2025).

Rewetting

Rewetting represents a fundamental initial phase of peatland restoration, undertaken to enhance the provision of ecosystem services and their contributions to human well-being (Stachowicz et al., 2022). In drained peatlands, this process is primarily achieved through the closure of anthropogenic drainage networks. Therefore, we estimated the cost (€2,400 per ha) to rewet the 33 abandoned peatland quarries, following Stachowicz et al. (2022) and Makrickas et al. (2023).

Results and discussion

Peat properties and ecological status of studied sites

A total of 33 peatland sites (3,854 ha) were assessed, displaying a broad range of ecological conditions (Fig. 2). Despite historical peat extraction, all still contain at least 30 cm of peat and thus meet the formal definition of peatland. The mean peat

depth varied from as little as 0.5 m (Saliečiai) to a maximum of 7 m (Užpelkiai), with the majority clustered around 2 m. This indicates that large volumes of peat are still present (Table 1).

The examination of water levels across 33 peatland sites indicates that the majority exhibit low hydrological conditions, with 14 sites (42%) falling into the lowest category, "2–", suggesting considerable drainage. Intermediate water levels (categories "2+" to "3+") are observed in 13 sites (39%), while only six peatlands (18%) demonstrate high water levels rated as "4+". Notably, all sites with a water level of "4+" have been classified as being in satisfactory condition, and several have undergone restoration. Notably, peatlands such as Aukštumala, Plinkšė, Pūsčia, Sachara and Užpelkiai have undergone restoration, displaying higher water levels. This pattern suggests a clear relationship between restoration efforts and improved hydrological conditions, underlining the importance of active water level management in peatland conservation and carbon retention strategies (Table 1).

Soil acidity, measured as pH, ranged from very acidic (pH 2.73 in Plinkšiai) to near-neutral values (pH 7.00 in Girdijauskai), indicating diverse geochemical profiles. However, most pH samples were below 4.5, particularly in sites originally classified as raised bogs (Table 1).

The carbon-to-nitrogen ratio, a proxy for peat decomposition and quality, spanned from 20.6 (Paduobys) to 83.0 (Vadakstis), with higher values often associated with lower peat mineralization. Most sites also showed high C : N, suggesting low nutrient availability and slow decomposition. Peat decomposition ranged from weak (H3) in wetter areas to moderate or strong (H6–H7) in more degraded locations. Many samples fell in the H4–H5 range, which reflects ongoing aerobic decay due to low water tables (Table 1). Oligotrophic peatlands typically exhibit low pH values (< 4.2) and are dominated by acid-tolerant, nutrient-poor vegetation. Mesotrophic sites showed intermediate pH values (4.2–5.5) and supported a more diverse flora, including brown mosses and sedges (Jarašius et al., 2022). Eutrophic peatlands were identified by higher pH levels (> 5.5) and the presence of nutrient-demanding species such as *Carex*, *Phragmites*, and/or *Typha*. Together, these indicators provided insight into both the nutrient regime and the degree of peat decomposition at each site.

Aboveground woody biomass ranged widely, from 10.18 $m^3 \cdot ha^{-1}$ (Aukštumala) to 207.93 $m^3 \cdot ha^{-1}$ (Rūdgiris), reflecting both natural forest development and afforestation in some sites. Several sites in poor peatland condition (i.e., Sachara) were also recorded with high wood volumes. This raises concerns about the role of spontaneous tree encroachment in inhibiting restoration outcomes (Table 1).

TABLE 1. Overview of the peatland characteristic of the 33 extracted quarries in Lithuania

Peatland	Peatland type	Area [ha]	Mean peat depth [m]	pH	C : N	Water level	Wood volume [$M^3 \cdot ha^{-1}$]	Ecological condition	Restoration
Aukštoji plynė	raised bog	190	2.0	3.29	53.1	2−	124.82	bad	
Aukštumala	raised bog	66	2.0	3.06	55.0	3+	10.18	satisfactory	yes
Bokštų – Klabų	fen / transitional mire	48	2.0	3.55	47.2	2−	90.76	bad	
Burbonys	raised bog	225	1.6	3.13	64.5	2−	69.57	bad	
Čelkiai	fen	65	2.0	3.28	73.8	2−	130.75	bad	
Dabravolė	raised bog	71	2.0	2.95	60.0	2−	102.50	bad	
Dainaviškiai	raised bog	153	2.0	3.19	58.2	2+	206.96	satisfactory	
Derkintai	fen / transitional mire	75	2.0	6.05	25.0	4+	69.90	satisfactory	
Didžlaukis	fen / raised bog	63	1.4	3.03	72.8	2−	63.07	bad	
Dūčiai	fen / transitional mire	185	0.7	5.62	27.3	2−	64.65	bad	
Ežerėlis	fen / transitional mire	581	1.0	3.08	38.7	2−	82.43	bad	
Gaidukonys	fen	26	2.0	3.28	42.9	3+	157.13	satisfactory	
Garonys	raised bog	80	2.5	3.04	70.3	2+	54.47	bad	
Girdijauskai	fen	84	1.8	7.00	20.7	3−	17.79	bad	
Januškiai	fen	60	2.0	5.76	26.0	4+	75.75	satisfactory	
Kašučiai	raised bog	20	1.2	3.22	47.9	2−	121.41	bad	
Kaušanka	fen / raised bog	88	2.0	4.39	56.0	2−	110.20	bad	
Kazimierava	raised bog	19	2.0	2.82	56.1	3+	114.29	satisfactory	
Laukagalis	raised bog	144	1.7	4.48	46.9	2−	75.38	bad	
Leoniškė	raised bog	52	1.4	3.35	72.1	4+	125.46	satisfactory	
Mažieji Mostaičiai	fen	10	1.0	3.74	23.8	3−	148.50	satisfactory	
Paąžuolynė	raised bog	55	2.0	3.31	42.4	2+	119.32	satisfactory	
Paduobys	fen	268	1.5	5.56	20.6	2+	79.26	satisfactory	
Plinkšė	raised bog	70	2.0	2.73	68.2	3+	85.83	satisfactory	yes
Pūsčia	raised bog	87	6.0	3.56	52.2	3+	73.42	satisfactory	yes
Raistapelkė	transitional mire	44	2.0	5.56	23.3	4+	41.78	satisfactory	
Raudonbalė	raised bog	36	2.0	3.06	61.1	2+	114.87	satisfactory	
Rūdgiris	raised bog	21	2.0	3.34	32.6	2+	207.93	satisfactory	
Sachara	raised bog	93	1.5	2.84	62.1	3+	121.04	satisfactory	yes
Saliečiai	fen	345	0.5	4.37	39.7	2−	94.42	bad	
Sūsia	fen	455	1.2	4.37	39.7	2−	60.10	bad	
Užpelkiai	raised bog	17	7.0	3.55	37.6	4+	23.45	satisfactory	yes
Vadakstis	raised bog	58	2.0	3.45	83.0	3+	71.23	bad	
Total area		3,854							

Source: own work.

Peatland condition was classified as "satisfactory" for 17 sites and "bad" for 16, suggesting that nearly 50% of sites remain heavily degraded with deep drainage, heavily decomposed peat, and dominance of non-peat-forming vegetation. This was supported by water level data, where most degraded sites exhibited a low water table (2−), potentially limiting peat-forming processes, increasing GHG emissions and forming unnatural mire vegetation communities. The 16 peatlands deemed satisfactory were nonetheless moderately degraded but retained patches of semi-natural vegetation or higher water levels. None of the sites were in a good or near-natural condition. Restoration measures were reported in only a few sites, notably Aukštumala, Plinkšė, Pūsčia, Sachara, and Užpelkiai, highlighting the limited but targeted application of rewetting efforts (Table 1). Both the least disturbed sites and rewetted sites require further active restoration efforts to recover peat-forming processes.

Principal component analysis

The results of the PCA analysis showed that the first two principal components (PC1 and PC2) accounted for a cumulative 67.83% of the total variance, with PC1 explaining 37.98% and PC2 explaining 29.85%. The remaining components contributed progressively less, with PC3, PC4, and PC5 explaining 17.68%, 10.66%, and 3.83%, respectively (Table 2).

PC1 was primarily associated with C : N (loading = 0.617) and pH (loading = −0.682), indicating a strong gradient between organic matter quality and acidity. PC2 was dominated by peat depth (0.702) and water level (0.618), reflecting hydrological and vertical structural variation across sites. PC3 was most influenced by wood volume (0.749), suggesting a link to forest biomass accumulation. The remaining components (PC4 and PC5) showed mixed contributions but were less influential in explaining overall variance (Table 3).

TABLE 2. Summary result values from the principal component analysis

PC	Eigenvalue	Variance [%]
1	1.899	37.982
2	1.492	29.852
3	0.883	17.675
4	0.533	10.663
5	0.191	3.827

Source: own work.

TABLE 3. Summary result values from the principal component analysis loading values

Specification	PC1	PC2	PC3	PC4	PC5
C : N	0.617	0.023	−0.423	0.312	0.584
pH	−0.682	0.011	0.097	0.151	0.709
Peat depth	0.077	0.702	−0.050	−0.673	0.214
Water level	0.110	0.618	0.498	0.591	−0.097
Wood volume	0.368	−0.352	0.749	−0.280	0.317

Source: own work.

The biplot (Fig. 3) illustrates the spatial distribution of the sampling sites and variable loadings. Sites with high C : N and low pH values were clustered along the positive axis of PC1, while deeper peat and higher water levels aligned with a positive PC2. Wood volume showed a strong association with PC3 and was orthogonal to the hydrological gradient, indicating distinct ecological drivers.

Overall, the PCA revealed clear separation among peatland types based on chemical, hydrological, and structural attributes, supporting the classification of peatland condition and guiding restoration prioritization.

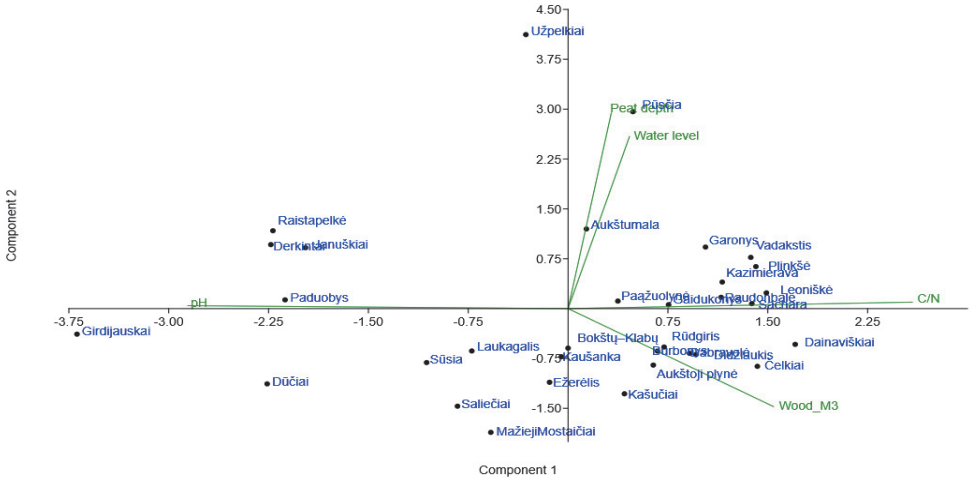

FIGURE 3. Results from principal component analysis based on variance-covariance matrix analysis of 5 variables representing 33 peatlands in Lithuania

Source: own work.

Visual inspection of the dendrogram from the hierarchical cluster analysis (Fig. 4) revealed distinct groupings among the peatland sites based on environmental variables. The hierarchical cluster analysis identified four major groupings among

Manton, M., Grigaliūnas, V., Jarašius, L., Sendžikaitė, J., Tamulaitytė, G., Grodzka-Łukaszewska, M. (2025). Drained and forgotten peat extraction sites: economic and carbon impacts of peat and water loss in spontaneously forested Lithuanian peatlands. *Sci. Rev. Eng. Env. Sci.*, *34* (4), 376–397. DOI 10.22630/srees.10809

the 33 peatland sites, based on environmental variables such as C : N, water level, peat depth and wood volume. Dividing the dendrogram at a linkage distance of approximately seven revealed the following clusters:

– Cluster 1 (9 sites): Includes Paduobys through to Sūsia peatlands (see: Fig. 4). These sites share similar topographic, hydrological and pH characteristics, likely representing moderately degraded peatlands with spontaneously revegetated vegetation.
– Cluster 2 (2 sites): The Pūsčia and Užpelkiai peatlands, characterized by relatively intact peatland conditions, with consistent water regimes and a deeper peat depth.
– Cluster 3 (8 sites): Includes the Dainaviškas – Leoniškė peatlands. These sites appear to occupy an intermediate ecological position, possibly reflecting mixed land use impacts and variable restoration potential with similar C : N and wood volumes.
– Cluster 4 (14 sites): Includes the Kašučiai – Garonys peatlands. These peatlands are more ecologically distinct, showing signs of advanced degradation and disturbed hydrological regimes with increased seasonal variability and impaired water retention capacity.

This four-cluster PCA result provides a clearer ecological stratification of the former peatland quarry sites, thus offering a valuable framework for prioritizing conservation and restoration efforts based on shared site characteristics (Fig. 4).

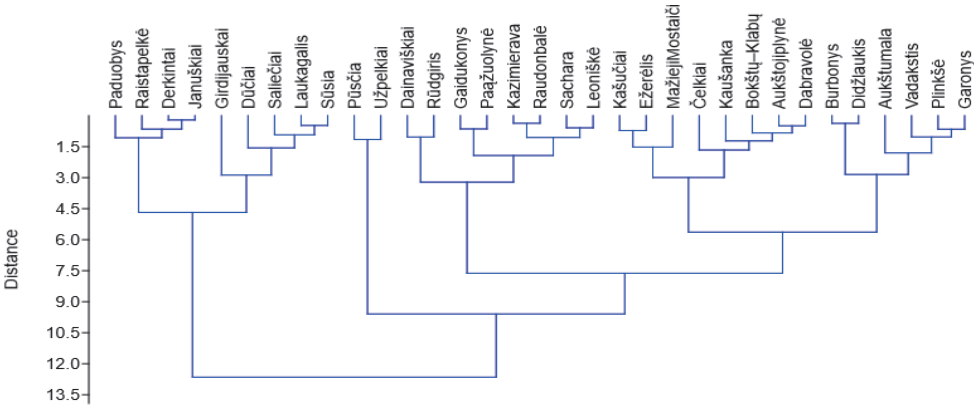

FIGURE 4. Results of the cluster analysis identified four main peatland clusters; from left to right, these represent clearer ecological stratification of the peatland sites

Source: own work.

Estimation of ecosystem service value associated with peat extraction

Peat

The assessment of the 33 abandoned Lithuanian peatland sites subjected to peat extraction revealed significant peat removal, surface subsidence, and volume reduction (Table 4). The average surface lowering ranges from 0.03 m (Dainaviškiai) to 4.97 m (Paduobys), with a mean lowering of approx. 1.81 m. These vertical losses reflect the cumulative effects of mechanical extraction, drainage, and compaction over time. The resulting peat volume losses are substantial, with site-specific estimates ranging from 33,261 m^3 (Mažieji Mostaičiai) to over 8.3 million m^3 (Saliečiai). Major extraction sites such as Saliečiai and Sūsia have each lost more than 12 million m^3 of peat, primarily due to their large surface areas and sustained extraction intensity. Collectively, the total peat volume loss across all surveyed peatlands exceeds 53.4 million m^3, underscoring the extensive alteration of peatland morphology and carbon storage capacity resulting from industrial-scale extraction activities. In addition to direct removal, long-term drainage and peat oxidation have contributed to continued surface subsidence, a process typically occurring at rates of approx. 0.5–2.0 cm annually in peatlands (Grzywna, 2017; Oleszczuk et al., 2022; Ghezelayagh et al., 2024). However, given that the lowering in the analyzed sites reaches 4.97 m, this natural subsidence component represents only a minor share of the total vertical loss.

Water

Peatland drainage and peat extraction lead to both physical removal of organic material and significant water volume loss, as peatland drainage lowers the water table and accelerates oxidation (Table 4). Across the 33 sites, estimated water volume losses range from 26.6 m^3 (Mažieji Mostaičiai) to over 6.6 million m^3 (Saliečiai). The total estimated water volume lost across all extraction sites is close to 62 million m^3, reflecting both direct hydrological drainage and secondary subsidence impacts. These losses illustrate the extensive hydrological disruption caused by peat extraction and emphasize the need for post-extraction rewetting and ecological restoration to mitigate further degradation and re-establish peatland functions.

Carbon

The analysis of the 33 abandoned peatland quarries revealed highly variable carbon losses and associated economic values (Table 4). Individual carbon stock losses ranged from as low as 5,355 t C at Leoniskė to over 666,352 t C at Paduobys.

This carbon loss translates into a wide range of estimated carbon values, from €19,636 at Leoniskė to more than €139.9 million at Paduobys. These results underline both the scale of past carbon emissions and the significant potential economic value of restoring and conserving remaining peat carbon stocks.

Rewetting

The rewetting cost estimates for the 33 abandoned peatland quarries show large variation across sites, reflecting differences in areas and degradation extents (Table 4). The largest peatlands, such as Paduobys (2.67 million m²) and Plinkšė (3.5 million m²), have correspondingly high estimated rewetting costs of €642,948 and €1.06 million, respectively. In contrast, smaller peatlands such as Mažieji Mostaičiai (101,278 m²) and Kašučiai (19,583 m²) require far lower investments of only €24,307 and €34,575, respectively. Several medium-sized sites, like Burbonys (2.24 million m²) and Kazimierava (187,681 m²), show intermediate costs (€539,780 and €45,043, respectively). These results highlight how peatland size strongly influences the estimated financial needs for restoration through rewetting.

Balance

The analysis of 33 abandoned peatland quarries revealed substantial peat, water, and carbon loss (Table 4). Across a total surveyed area of 3.85 million m², peat volume loss amounted to approx. 77.5 million m^3, accompanied by a water volume loss of 61.9 million m^3. The estimated carbon stock loss reached 3.87 million t C. This is equivalent to 14.2 million t CO_2 emissions. In economic terms, the total value of peat loss was estimated at €898.8 million, with additional losses of €33.5 million in water and €813.1 million in carbon. The costs associated with rewetting all 33 abandoned peatland quarries were estimated at €9.25 million, resulting in a net balance of approx. €42.97 million. These results highlight both the magnitude of the historic degradation and the considerable potential benefits of restoration for climate mitigation and ecosystem service recovery.

It should be noted that the extrapolation of peat loss and subsidence is a complex task due to its nonlinearity (Ikkala et al., 2021) and the different subsidence dynamics in forested versus agricultural peatlands (Liu et al., 2020). Moreover, the analysis of ecosystem services only focused on the once-off loss of peat extraction and rewetting, but not the scale and accumulated losses since abandonment or benefits of rewetting. As an example, the abandonment of peatland ranged from 1940 to 2020, and some peatlands are under restoration. Thus, our general estimates are a transient process.

TABLE 4. Estimated peatland extraction losses in terms of volume and monetary value for peat, water and carbon

Peatland	Area [m^2]	Average lowering [m]	Peat volume lost [m^3]	Water volume lost [m^3]	Carbon stock [t C]	CO_2 eq. [t CO_2]	Peat value [€]	Water value [€]	Carbon value [€]	Rewetting [€]	Balance [€]
Aukštoji plynė	1,897,398	0.99	1,884,403	1,507,522	94,220	345,477	21,859,073	814,062	19,775,104	455,376	814,532
Aukštumala	660,029	1.00	660,029	528,023	33,001	121,006	7,656,336	285,132	6,926,407	158,407	286,390
Bokštų – Klabų	479,576	0.50	239,788	191,830	11,989	43,962	2,781,541	103,588	2,516,358	115,098	46,496
Burbonys	2,249,084	2.68	6,020,396	4,816,317	301,020	1,103,749	69,836,588	2,600,811	63,178,605	539,780	3,517,392
Dabravolė	707,745	0.40	280,998	224,798	14,050	51,517	3,259,575	121,391	2,948,818	169,859	19,507
Dainaviškiai	1527519	0.03	4,8171	38,537	2,409	8,831	558,784	20,810	505,511	366,605	−334,142
Derkintai	753,770	3.35	2,527,243	2,021,794	126,362	463,332	29,316,019	1,091,769	26,521,129	180,905	1,522,216
Didžlaukis	628,759	0.66	412,802	330,242	20,640	75,681	4,788,508	178,331	4,331,988	150,902	127,287
Dūčiai	1,854,022	2.36	4,379,285	3,503,428	218,964	802,876	50,799,706	1,891,851	45,956,635	444,965	2,506,255
Ežerėlis	5,809,552	0.60	3,485,731	2,788,585	174,287	639,057	40,434,482	1,505,836	36,579,596	1,394,292	954,758
Garonys	803,448	2.68	2,1503,21	1,720,257	107,516	394,229	24,943,727	928,939	22,565,676	192,828	1,256,284
Geidukonys	262,586	0.83	217,177	173,741	10,859	39,816	2,519,249	93,820	2,279,073	63,021	83,336
Girdijauskai	837,204	2.95	2,468,046	1,974,437	123,402	452,479	28,629,331	1,066,196	25,899,908	200,929	1,462,298
Januškiai	603,841	3.51	2,120,003	1,696,002	106,000	388,671	24,592,035	915,841	22,247,514	144,922	1,283,758
Kašučiai	198,535	0.62	122,455	97,964	6,123	22,450	1,420,478	52,901	1,285,054	47,648	34,875
Kaušanka	878,596	2.24	1,971,236	1,576,989	98,562	361,397	22,866,339	851,574	20,686,340	210,863	1,117,562
Kazimierava	187,681	3.15	591,366	473,093	29,568	108,418	6,859,844	255,470	6,205,850	45,043	353,481
Laukagalis	1,441,621	0.87	1,246,935	997,548	62,347	228,607	14,464,446	538,676	13,085,455	345,989	494,326
Leoniškė	521,081	0.21	107,104	85,683	5,355	19,636	1,242,406	46,269	1,123,959	125,059	−52,882
Mažieji Mostaičiai	101,278	0.33	3,3261	26,609	1,663	6,098	385,828	14,369	349,044	24,307	−1,892
Čelkiai	649,624	2.78	1,805,635	1,444,508	90,282	331,036	20,945,370	780,035	18,948,510	155,910	1,060,916
Paąžuolynė	552,464	2.61	1,443,053	1,154,443	72,153	264,562	16,739,416	623,399	15,143,537	132,591	839,889
Paduobys	2,678,952	4.97	13,327,034	10,661,627	666,352	2,443,312	154,593,594	5,757,279	139,855,166	642,948	8,338,201
Plinkšė	697,250	0.50	349,546	279,637	17,477	64,084	4,054,733	151,004	3,668,168	167,340	68,221
Pūsčia	871,503	3.46	3014,593	2,411,674	150,730	552,680	34,969,276	1,302,304	31,635,424	209,161	1,822,387
Raistapelkė	442,392	2.54	1,121,856	897,485	56,093	205,675	13,013,528	484,642	11,772,863	106,174	649,850
Raudonbalė	356,677	0.29	104,145	83,316	5,207	19,093	1,208,077	44,990	1,092,903	85,602	−15,419
Rūdgiris	208,626	3.05	635,275	508,220	31,764	116,468	7,369,194	274,439	6,666,640	50,070	378,045
Sachara	925,314	0.87	801,704	641,363	40,085	146,980	9,299,763	346,336	8,413,155	222,075	318,196
Saliečiai	3,446,981	3.48	11,995,418	9,596,335	599,771	2,199,180	139,146,849	5,182,021	125,881,061	827,275	7,256,492
Sūsia	4,552,531	2.42	11,040,897	8,832,718	552,045	2,024,183	128,074,405	4,769,668	115,864,226	1,092,607	6,347,904
Užpelkiai	169,299	1.74	293,655	234,924	14,683	53,837	3,406,401	126,859	3,081,647	40,632	157,264
Vadakstis	580,904	1.00	580,346	464,277	29,017	106,398	6,732,015	250,710	6,090,208	139,417	251,681
Total	38,535,842	1.81	77,479,906	61,983,925	3,873,995	14,204,779	898,766,915	33,471,320	813,081,530	9,248,602	42,965,463

Source: own work.

Manton, M., Grigaliūnas, V., Jarašius, L., Sendžikaitė, J., Tamulaitytė, G., Grodzka-Łukaszewska, M. (2025). Drained and forgotten peat extraction sites: economic and carbon impacts of peat and water loss in spontaneously forested Lithuanian peatlands. *Sci. Rev. Eng. Env. Sci.*, *34* (4), 376–397. DOI 10.22630/srees.10809

Conclusions

This study highlights the scale of ecological and climate-related degradation associated with abandoned peat extraction sites in Lithuania. Despite the end of mining activities in many of these areas, they remain in a drained state that continues to drive peat loss, carbon emissions, and limited ecosystem function.

Our main findings are:

– Peat loss estimates from extraction at 33 abandoned peatland quarries totaled 77.5 million m^3, which equates to a current value of €899 million in revenue. Nonetheless, the abandoned peatland quarries still host peat deposits ranging from 0.5 m to 2 m in average depth. Thus, rewetting is needed.
– The drying and degradation of peatlands also reduced the water storage capacity across the 33 study sites, with an estimated loss of approx. 62 million liters of water, equaling approx. €33 million. This affects local hydrology and increases the vulnerability to drought, fire, flood and natural biodiversity.
– Soil carbon losses from these sites are substantial. We estimate approx. 14.2 t CO_2 emissions equaling €813 million were lost from peat extraction alone. These emissions are largely unaccounted for in land-use sector reporting and undermine climate targets.
– The rewetting of the 33 abandoned peatland quarries is estimated to cost approx. €9.2 million. Given these findings, we argue that rewetting and restoring Lithuania's drained peatlands should be a clear environmental priority. Blocking drainage ditches, raising water tables, and reintroducing peat-forming vegetation would help halt further degradation. Over a long timeframe, these sites could shift from being net carbon sources to functioning wetlands that support biodiversity and store water. This creates an opportunity to align restoration efforts with conservation policies and EU climate goals. Our results support current EU initiatives that call for the restoration of organic soils, particularly under the Nature Restoration Law and rules for the land use, land-use change and forestry (LULUCF) (Regulation (EU) 2018/841).

In conclusion, "drained and forgotten" peatlands are hotspots of avoidable carbon and water service loss. Restoration offers a clear, cost-effective path to reversing this trend. By quantifying peat loss, carbon emissions, and hydrological impacts, this study provides the evidence base needed to support targeted, science--based restoration strategies. We recommend prioritizing the rewetting of these areas within national and EU restoration programs, and monitoring outcomes to track improvements in carbon and water dynamics over time.

References

Agricultural Data Center [ŽŪDC]. (2025). *Dirv_DR10LT – spatial data set of soil of the territory of the Republic of Lithuania at scale 1:10 000* [Data set]. http://data.europa.eu/88u/dataset/https-data-gov-lt-datasets-2965-

Boers, A. M., Frieswyk, C. B., Verhoeven, J. T. A., & Zedler, J. B. (2006). Contrasting approaches to the restoration of diverse vegetation in herbaceous wetlands. In R. Bobbink, B. Beltman, J. T. A. Verhoeven, & D. F. Whigham (Eds.), *Wetlands: functioning, biodiversity conservation, and restoration* (pp. 225–246). Springer.

Communication from the Commission to the European Parliament, the Council, the European economic and social committee and the committee of the regions. EU Biodiversity Strategy for 2030: Bringing nature back into our lives (COM/2020/380 final). Brussels, 20.5.2020.

Communication from the Commission to the European Parliament, the Council, the European economic and social committee and the committee of the regions. EU Soil Strategy for 2030: Reaping the benefits of healthy soils for people, food, nature and climate (COM/2021/699 final). Brussels, 17.11.2021.

Craft, C. (2015). *Creating and restoring wetlands: From theory to practice*. Elsevier.

Ghezelayagh, P., Oleszczuk, R., Stachowicz, M., Eini, M. R., Kamocki, A., Banaszuk, P., & Grygoruk, M. (2024). Developing a remote-sensing-based indicator for peat soil vertical displacement: A case study in the Biebrza Valley, Poland. *Ecological Indicators*, *166*, 112305. https://doi.org/10.1016/j.ecolind.2024.112305

Gorham, E. (1991). Northern peatlands: role in the carbon cycle and probable responses to climatic warming. *Ecological Applications*, *1*(2), 182–195. https://doi.org/10.2307/1941811

Grigaliunas, V., Jarašius, L., Zableckis, N., Dapkuniene, K., Manton, M., Kazanaviciute, V., & Sendžikaitė, J. (2023). *Miškuose esančių pažeistų durpynų sutvarkymo galimybių studija*. Miško Mokslo Darbas. https://am.lrv.lt/media/viesa/saugykla/2024/1/UeLJMXgcIl8.pdf

Grzywna, A. (2017). The degree of peatland subsidence resulting from drainage of land. *Environmental Earth Sciences*, *76*(16), 559. https://doi.org/10.1007/s12665-017-6869-1

Haapalehto, T., Juutinen, R., Kareksela, S., Kuitunen, M., Tahvanainen, T., Vuori, H., & Kotiaho, J. S. (2017). Recovery of plant communities after ecological restoration of forestry-drained peatlands. *Ecology and Evolution*, *7*(19), 7848–7858. https://doi.org/10.1002/ece3.3243

Hammer, Ø. (2023). *Reference manual. Paleontological Statistics (PAST) Version 4.13*. Natural History Museum, University of Oslo.

Hofer, B., Huwald, G., & Lehmann, J. (2012). Studie zur Situation des Torfabbaus im Baltikum. *TELMA-Berichte der Deutschen Gesellschaft für Moor-und Torfkunde*, *42*, 43–56. https://e-docs.geo-leo.de/server/api/core/bitstreams/3c3cfebd-c05b-440d-b100-51841a51c1fc/content

Holden, J. (2005). Peatland hydrology and carbon release: Why small-scale process matters. *Philosophical Transactions of the Royal Society A: Mathematical, Physical and Engineering Sciences*, *363*(1837), 2891–2913. https://doi.org/10.1098/rsta.2005.1671

Ikkala, L., Ronkanen, A. K., Utriainen, O., Kløve, B., & Marttila, H. (2021). Peatland subsidence enhances cultivated lowland flood risk. *Soil and Tillage Research*, *212*, 105078. https://doi.org/10.1016/j.still.2021.105078

IndexBox. (2024). *Lithuania – Peat – Market Analysis, Forecast, Size, Trends and Insights*. https://www.indexbox.io/store/lithuania-peat-market-analysis-forecast-size-trends-and-insights/

Intergovernmental Panel on Climate Change [IPCC]. (2014). *2013 Supplement to the 2006 IPCC Guidelines for National Greenhouse Gas Inventories: Wetlands*. IPCC. https://www.ipcc-nggip.iges.or.jp/public/wetlands/

International Carbon Action Partnership [ICAP]. (2025) *ICAP Allowance Price Explorer*. https://icapcarbonaction.com/en/ets-prices

Jarašius, L., Etzold, J., Truus, L., Purre, A-H., Sendžikaitė, J., Strazdiņa, L., Zableckis, N., Pakalne, M., Bociąg, K., Ilomets, M., Herrmann, A., Kirschey, T., Pajula, R., Pawlaczyk, P., Chlost, I., Cieśliński, R., Gos, K., Libauers, K., Sinkevičius, Z., & Jurema, L. (2022). *Handbook for assessment of greenhouse gas emissions from peatlands*. Lithuanian Fund for Nature.

Jarašius, L., Lygis, V., Sendžikaitė, J., & Pakalnis, R. (2015). Effect of different hydrological restoration measures in Aukštumala raised bog damaged by peat harvesting activities. *Baltic Forestry*, *21*(2), 192−203.

Joosten, H. (2009). 30 human impacts: Farming, fire, forestry and fuel. In E. Maltby & T. Barker (Eds.), *The wetlands handbook*. Blackwell Science.

Joosten, H., & Clarke, D. (2002). *Wise use of mires and peatlands: Background and principles including a framework for decision-making*. International Mire Conservation Group and International Peat Society.

Jurasinski, G., Barthelmes, A., Byrne, K. A., Chojnicki, B. H., Christiansen, J. R., Decleer, K., Fritz, Ch., Günther, A. B., Huth, V., Joosten, H., Juszczak, R., Juutinen, S., Kasimir, A., Klemedtsson, L., Koebsch, F., Kotowski, W., Kull, A., Lamentowicz, M., Lindgren, A., Lindsay, R., Linkevičienė, Lohila, A., Mander, Ü., Manton, M., Minkkinen, K., Peters, J., Renou-Wilson, F., Sendžikaitė, J., Šimanauskienė, R., Taminskas, J., Tanneberger, F., Tegetmeyer, C., Diggelen, R. van, Vasander, H., Wilson, D., Zableckis, N., Zak, D. H., & Couwenberg, J. (2024). Active afforestation of drained peatlands is not a viable option under the EU Nature Restoration Law. *Ambio*, *53*(7), 970–983. https://doi.org/10.1007/s13280-024-02016-5

Kamocki, A. K., Manton, M., Rudbeck Jepsen, M., Stachowicz, M., Antochów, A., Grygoruk, M., & Banaszuk, P. (2025). *Estimations of GHG emissions from drained peatlands: Accountability in the trans-border Neman River basin.* https://dx.doi.org/10.2139/ssrn.5144113

Karofeld, E., Jarašius, L., Priede, A., & Sendžikaitė, J. (2017). On the after-use and restoration of abandoned extracted peatlands in the Baltic countries. *Restoration Ecology*, *25*(2), 293–300. https://doi.org/10.1111/rec.12436

Kohlenberg, A. J., Turetsky, M. R., Thompson, D. K., Branfireun, B. A., & Mitchell, C. P. (2018). Controls on boreal peat combustion and resulting emissions of carbon and mercury. *Environmental Research Letters*, *13*(3), 035005. https://doi.org/10.1088/1748-9326/aa9ea8

Koska, I., Succow, M., Clausnitzer, U., Timmermann, T., & Roth, S. (2001). Vegetationskundliche Kennzeichnung von Mooren (topische Betrachtung). In M. Succow & H. Joosten (Eds.), *Landschaftsökologische Moorkunde* (pp. 112–184). Schweizerbart.

Leifeld, J. & Menichetti, L. (2018). The underappreciated potential of peatlands in global climate change mitigation strategies. *Nature Communications*, *9*(1). https://doi.org/10.1038/s41467-018-03406-6

Lithuanian State Forest Service [VMU]. (2021). *Cadastral GIS database*.

Liu, H., Price, J., Rezanezhad, F., & Lennartz, B. (2020). Centennial-scale shifts in hydrophysical properties of peat induced by drainage. *Water Resources Research*, *56*(10), e2020WR027538. https://doi.org/10.1029/2020WR027538

Makrickas, E., Manton, M., Angelstam, P., & Grygoruk, M. (2023). Trading wood for water and carbon in peatland forests? Rewetting is worth more than wood production. *Journal of Environmental Management*, *341*, 117952. https://doi.org/10.1016/j.jenvman.2023.117952

Mander, Ü., Espenberg, M., Melling, L., & Kull, A. (2024). Peatland restoration pathways to mitigate greenhouse gas emissions and retain peat carbon. *Biogeochemistry*, *167*(4), 523–543. https://doi.org/10.1007/s10533-023-01103-1

Manton, M., Makrickas, E., Banaszuk, P., Kołos, A., Kamocki, A., Grygoruk, M., Stachowicz, M., Jarašius, L., Zableckis, N., Sendžikaitė, J., Peters, J., Napreenko, M., Wichtmann, W., & Angelstam, P. (2021). Assessment and spatial planning for peatland conservation and restoration: Europe's trans-border Neman River basin as a case study. *Land*, *10*(2), 174. https://doi.org/10.3390/land10020174

Mitsch, W. J., & Gosselink, J. G. (2015). *Wetlands*. Wiley.

Oleszczuk, R., Łachacz, A., & Kalisz, B. (2022). Measurements versus estimates of soil subsidence and mineralization rates at peatland over 50 years (1966–2016). *Sustainability*, *14*(24), 16459. https://doi.org/10.3390/su142416459

Paavilainen, E., & Päivänen, J. (1995). *Peatland forestry: Ecology and principles.* Springer. https://doi.org/10.1007/978-3-662-03125-4

Parish, F., Sirin, A., Charman, D., Joosten, H., Minayeva, T., Silvius, M., & Stringer, L. (2008). *Assessment on peatlands, biodiversity and climate change: Main report*. Global Environment Centre, Kuala Lumpur and Wetlands International.

Patel, N., Ieviņa, B., Kažmēre, D., Feofilovs, M., Kamenders, A., & Romagnoli, F. (2025). Towards resilient peatlands: integrating ecosystem-based strategies, policy frameworks, and management approaches for sustainable transformation. *Sustainability*, *17*(8), 3419. https://doi.org/10.3390/su17083419

Regulation (EU) 2018/841 of the European Parliament and of the Council of 30 May 2018 on the inclusion of greenhouse gas emissions and removals from land use, land use change and forestry in the 2030 climate and energy framework, and amending Regulation (EU) No 525/2013 and Decision No 529/2013/EU. OJ L 156, 19.6.2018, pp. 1–25.

Regulation of the European Parliament and of the Council on Nature Restoration and Amending Regulation (EU) 2022/869. OJ L, 2024/1991, 29.7.2024.

Rydin, H., Jeglum, J. K. & Bennett, K.D. (2013). *The Biology of Peatlands*. Oxford University Press.

Saulėnas, V. (1993). *Durpės telkinių tyrimų ir išteklių klasifikavimo rekomendacijos. Valstybinė geologijos tarnyba prie statybos ir urbanistikos ministerijos*. https://lgt.lrv.lt/media/viesa/saugykla/2024/2/yF1ekPwJPoI.pdf

Stachowicz, M., Manton, M., Abramchuk, M., Banaszuk, P., Jarašius, L., Kamocki, A., Povilaitis, A., Samerkhanova, A., Schäfer, A., Sendžikaitė, J., Wichtmann, W., Zableckis, N., & Grygoruk, M. (2022). To store or to drain – To lose or to gain? Rewetting drained peatlands as a measure for increasing water storage in the transboundary Neman River Basin. *Science of The Total Environment*, *829*, 154560. https://doi.org/10.1016/j.scitotenv.2022.154560

Succow, M., & Stegmann, H. (2001). *Succow's peatland classification*. Greifswald University.

Tanneberger, F., & Wichtmann, W. (Eds.). (2011). *Carbon credits from peatland rewetting: climate, biodiversity, land use*. Schweizerbart Science Publishers.

Turetsky, M. R., Benscoter, B., Page, S., Rein, G., Van Der Werf, G. R., & Watts, A. (2015). Global vulnerability of peatlands to fire and carbon loss. *Nature Geoscience*, *8*(1), 11–14. https://doi.org/10.1038/ngeo2325

United Nations Environment Programme [UNEP]. (2022). *Global peatlands assessment: The state of the world's peatlands*. *Evidence for Action toward the Conservation, Restoration, and Sustainable Management of Peatlands*. Global Peatlands Initiative. United Nations Environment Programme. https://doi.org/10.59117/20.500.11822/41222

Valatka, S., Stoškus, A., & Pileckas, M. (2018). *Lietuvos Durpynai. Kiek Jų Turime, Ar Racionaliai Naudojame?* Gamtos paveldo fondas.

Valstybinė saugomų teritorijų tarnyba prie Aplinkos ministerijos [VSTT]. (2025). *Biologinės Įvairovės Duomenų Bazė*. https://www.biomon.lt/

Wichmann, S., & Nordt, A. (2024). Unlocking the potential of peatlands and paludiculture to achieve Germany's climate targets: obstacles and major fields of action. *Frontiers in Climate*, *6*, 1380625. https://doi.org/10.3389/fclim.2024.1380625

Zheng, B., Ciais, P., Chevallier, F., Yang, H., Canadell, J. G., Chen, Y., Velde, I. R. van der, Aben, I., Chuvieco, E., Davis, S. J., Deeter, M., Hong, Ch., Kong, Y., Li, H., Lin, X., He, K., & Zhang, Q. (2023). Record-high CO_2 emissions from boreal fires in 2021. *Science*, *379*(6635), 912–917. https://doi.org/10.1126/science.ade0805

Summary

Drained and forgotten peat extraction sites: economic and carbon impacts of peat and water loss in spontaneously forested Lithuanian peatlands. This study examines the condition and environmental impact of abandoned peatland quarries in Lithuania. Using spatial data and field investigations, we identified 33 abandoned peat quarry sites covering over 3,854 ha, which were abandoned between 1940 and 2020. Detailed field assessments were conducted at each abandoned peatland quarry to evaluate the peat depth, pH, carbon-to-nitrogen ratio, decomposition, water table levels, and wood volume. Despite past extraction, many sites still contain substantial peat layers along with significant carbon and water storage potential. However, ongoing drainage continues to drive peat loss and carbon dioxide emissions. We estimate that peat loss from extraction totaled 77.5 million m^3, which equates to a current value of €899 million in revenue. Nonetheless,

the abandoned peatland quarries still host peat deposits ranging from 0.5 m to 2 m in depth. The drying and degradation of the peatlands has also reduced the water storage capacity across the 33 study sites. This loss is estimated at approx. 62 million liters of water, which equals approx. €33 million. This substantially affects local hydrology and increases the vulnerability to drought, fire, flood and natural biodiversity. Carbon emissions from drained peat soils are also substantial. We estimate approx. 14.2 t CO_2 emissions equaling €813 million were lost from peat extraction alone. These emissions are often unreported if such areas are classified simply as "forests." Our findings highlight the need for active restoration, particularly rewetting, to stop further degradation. Rewetting would reduce emissions, improve water retention, and support biodiversity recovery while offering clear opportunities to align peatland restoration with EU climate and nature goals.

Scientific Review Engineering and Environmental Sciences (2025), 34 (4), 398–416

Sci. Rev. Eng. Env. Sci. (2025), 34 (4) https://srees.sggw.edu.pl

ISSN 1732-9353 (suspended) eISSN 2543-7496 DOI 10.22630/srees.10421

Received: 30.04.2025
Accepted: 25.11.2025

Muhammad Umar ALI
Mateusz GRYGORUK✉
Warsaw University of Life Sciences – SGGW, Centre for Climate Research, Poland

Hydrological analysis of the Oder droughts for the period 1950–2022 in the context of the 2022 river disaster

Keywords: trend analysis, low flow, Poland, water management

Introduction

History has demonstrated how susceptible places on Earth are to severe and prolonged droughts, which can harm the environment, society, and economy. The growing population, increased demand for water due to irrigation and industrial uses, and global warming have all increased awareness of our susceptibility to drought. In many regions of the world, the frequency and severity of drought have increased due to climate change (Tallaksen & van Lanen, 2023). In terms of the number of people harmed and the financial cost, drought is one of the most damaging natural disasters (Van Loon, 2015). According to the United Nations Convention to Combat Desertification report, by 2030, an estimated 700 million people will be at risk of displacement due to drought (UNCCD, 2022).

Such is the case of one of the European rivers – the Oder. Among the many worrying pictures of the impact of severe droughts across Europe, July and August 2022 were the times when, unexpectedly, about 249 tons of dead fish were

✉mateusz_grygoruk@sggw.edu.pl

retrieved from the waters of the Oder, according to the report of the 'Polish Team for the Situation on the Oder' (Zespół ds. Sytuacji powstałej na rzece Odrze) (Kolada, 2022). Toxins produced by the algae species *Prymnesium parvum* caused the mass extinction of aquatic life. This situation resulted from the accumulation of unfavorable factors (atmospheric, hydrological, and nutrient concentrations), which led to an algae bloom in the waters of the Oder (Absalon et al., 2023). A key factor that enabled the proliferation of this species was the high salinity of the Oder during this period, likely due, at least in part, to discharges of industrial wastewater with a high salt content, such as from mining activities. Other contributing factors included the drought and the resulting low water levels, which reduced dilution and flow, as well as hydromorphological modifications to the river. A combination of meteorological conditions, including prolonged periods of high temperatures and a lack of precipitation, as well as human activities such as water extraction and altered land use, contributed to the hydrological alterations observed during this event. This incident highlighted the Oder system's vulnerability to severe weather and underscored the need for enhanced water resource management and effective drought protection measures. This study aims to conduct a comprehensive hydrological analysis of the Oder, with a particular focus on the catastrophic events that occurred in 2022. The overall goal of this paper was to reveal the trends and specifics of droughts along the Oder in its upper, middle, and lower courses, providing background for the analysis of the 2022 drought, which is suspected to remain one of the leading causes of the Oder disaster. The specific objectives of this paper were (1) to analyze and reveal the drought criteria expressed by the average value of the annual lowest discharges of the Oder in three different water gauging stations: Chałupki (upper course of the Oder), Połęcko (middle course of the Oder), and Gozdowice (lower course of the Oder); (2) to calculate and analyze durations of droughts in the three listed gauging stations; (3) to calculate trends of droughts, with a special focus on their changing lengths and discharge deficits; and (4) to analyze the 2022 drought as a possible trigger of the extensive *Prymnesium parvum* bloom and related exposure of the aquatic ecosystems of the Oder to the toxic enzyme prymnesine, produced by the blooming *Prymnesium parvum*.

Materials and methods

The Oder (Fig. 1) is one of the largest rivers in Central Europe. It originates in the Oder Mountains (Oderské Vrchy), at an elevation of around 634 m a.s.l., and spans approximately 854 km, making it Poland's third-longest river and a major

Ali, M. U., Grygoruk, M. (2025). Hydrological analysis of the Oder droughts for the period 1950–2022 in the context of the 2022 river disaster. *Sci. Rev. Eng. Env. Sci.*, *34* (4), 398–416. DOI 10.22630/srees.10421

waterway in the region (Sługocki & Czerniawski, 2023). The Oder river basin spans 118,938 km², covering three countries: Poland (86%), Germany (9%), and the Czech Republic (5%). The river basin has a population of approximately 16 million (2015), with 50.4% of the area being agricultural farmland (Joint Research Centre [JRC], 2020).

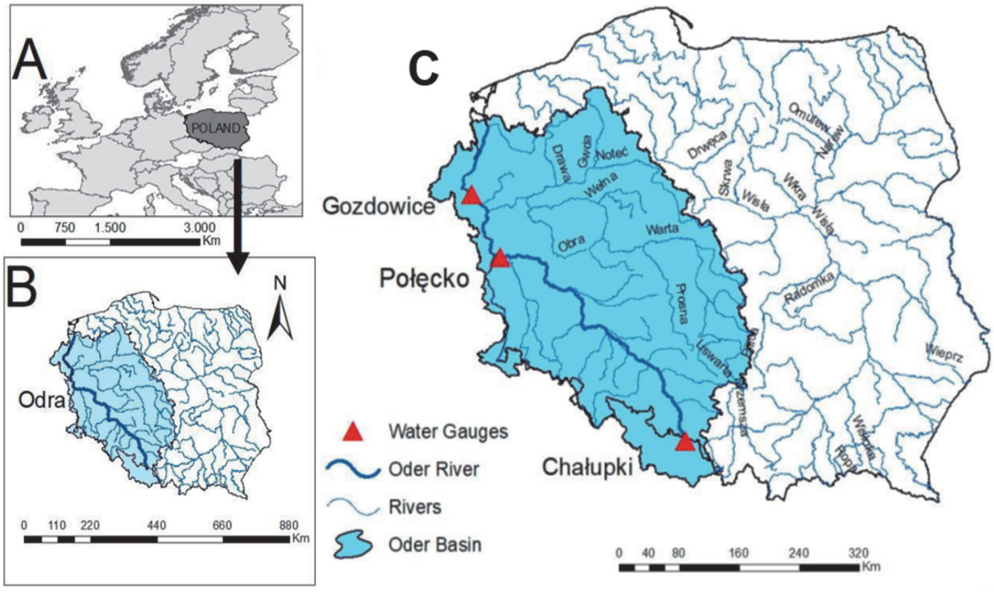

FIGURE 1. Location of the Oder river basin in Poland
Source: own work.

The Oder is primarily a lowland river with a hydrological regime characterized by a mix of pluvial and groundwater, and its catchment area covers approximately 33% of Poland. Its mean annual flow ranges from 41 $m^3 \cdot s^{-1}$ in the upper course to 535 $m^3 \cdot s^{-1}$ near the river mouth (Wrzesiński, 2021). The channel slope drops from 0.7% close to the border between Poland and the Czech Republic to 0.38% in the middle course, 0.25% in the lower course, and 0.04% at the mouth of the river (Absalon et al., 2023). The Oder river basin has a moderate climate, with notable seasonal fluctuations in temperature and precipitation. Winters are usually cold, with average temperatures ranging from −1°C to −5°C, while summers are temperate to warm, with average temperatures ranging from 18°C to 25°C (Sayegh & Żabnieńska, 2019). The basin receives an average of 500 mm of rainfall annually in the lowlands and over 1,200 mm in the higher regions (Graf & Wrzesiński, 2020). The average discharge at the river's mouth is approximately 574 $m^3 \cdot s^{-1}$; however,

it may vary depending on seasonal and meteorological circumstances. The river flow usually reaches its maximum in the spring and early summer due to snowmelt from the Sudetes and Carpathian Mountains, as well as increasing precipitation. At certain times, the flow rate in the middle and lower sections of the river exceeds 1,000 $m^3 \cdot s^{-1}$ (Kreienkamp et al., 2021).

In this study, daily discharge data are analyzed based on river discharge data retrieved from the Institute of Meteorology and Water Management – National Research Institute (IMGW-PIB). In the first step, the lowest annual discharges were selected for each of the three water gauges for every year of analysis. Next, the average of these yearly values for each gauging station was calculated as a criterion for drought occurrence, referred to as the average low discharge, hereafter referred to as the average annual minimum flow (SNQ). It was calculated as an arithmetic average of the lowest annual discharges recorded in the Oder at each of the three gauging stations analyzed over the period 1950–2022. In the next step, river discharge hydrographs (daily discharge values) were analyzed to extract the days when daily discharges were lower than the SNQ value in each of the three gauges analyzed. This analysis allowed us to extract all the droughts (daily discharge lower than the assumed threshold discharge SNQ). The analysis included trend analysis using the Mann–Kendall test, a non-parametric method employed to detect trends in time series data (Shah & Kiran, 2021). It is beneficial for hydrological data where assumptions of normality may not hold (Zhou et al., 2020).

Results

The lowest annual discharges of the Oder (Fig. 2) are decreasing the most steeply in Gozdowice and Połęcko. In Chałupki, we can see that the SNQ was recorded at 4.22 $m^3 \cdot s^{-1}$ in 1954, while the highest was 22.1 $m^3 \cdot s^{-1}$ in 2010. Over the period from 1950 to 2022, the SNQ of Chałupki was 9.72 $m^3 \cdot s^{-1}$. With a *p*-value of 0.9922, Chałupki shows no significant trend in the long-term lowest discharges. This implies that Chałupki's low-flow conditions have stayed mostly constant over time. On the other hand, in Połęcko, the lowest annual discharge was 53.1 $m^3 \cdot s^{-1}$ in 2015, and the highest was 194 $m^3 \cdot s^{-1}$ in 1977. The SNQ of Połęcko over the period 1950–2022 was 106 $m^3 \cdot s^{-1}$, and the *p*-value for Połęcko was 0.8975, also indicating no significant trend. This implies that low-flow conditions at the station have fluctuated over time without showing any signs of permanent alteration. In Gozdowice, the lowest discharge was 124 $m^3 \cdot s^{-1}$ in 2015, and the highest SNQ

Ali, M. U., Grygoruk, M. (2025). Hydrological analysis of the Oder droughts for the period 1950–2022 in the context of the 2022 river disaster. *Sci. Rev. Eng. Env. Sci.*, *34* (4), 398–416. DOI 10.22630/srees.10421

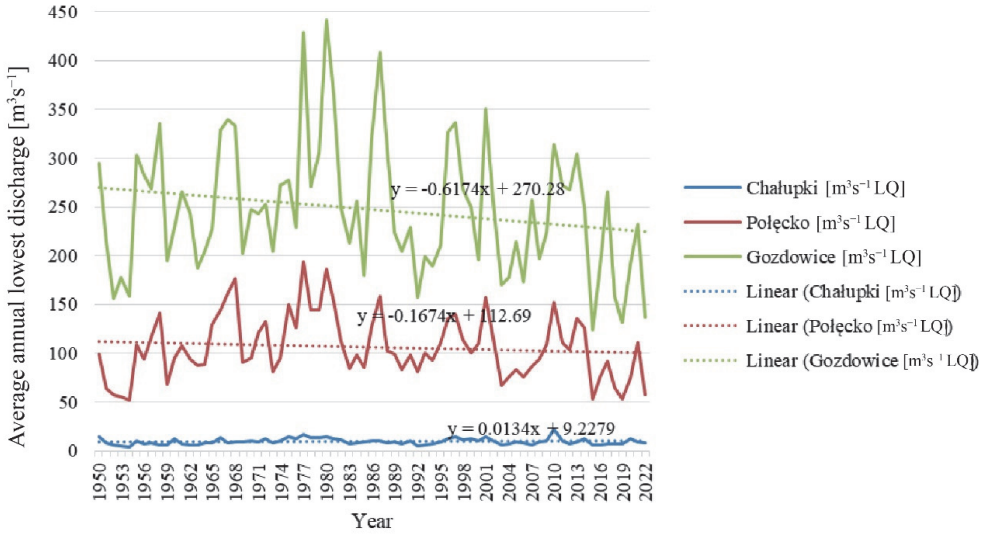

FIGURE 2. Lowest annual discharges of the Oder at three water gauging stations in the period of 1950–2022

Source: own work based on data of the Institute of Meteorology and Water Management – National Research Institute (IMGW-PIB).

was 441 $m^3 \cdot s^{-1}$ in 1980. The SNQ of Gozdowice over the period 1950–2022 was 247 $m^3 \cdot s^{-1}$. Like the other stations, the *p*-value of Gozdowice, which is 0.9563, shows no significant pattern in the lowest discharges over time. The lowest monthly discharges of the Oder in Chałupki generally show an increasing trend (Fig. 3). However, in April, May, June, July, and August, the lowest monthly discharges appear to be decreasing, whereas in January, February, March, and October, they are increasing. However, the trends are not statistically significant. The steepest decreasing changes of the lowest monthly discharges were recorded in June and September, while the steepest increasing tendencies of the lowest monthly discharges of the Oder in Chałupki were recorded in November and December. Overall, the lowest monthly discharges occur in summer and spring, and the highest in winter and autumn. On the other hand, the lowest monthly discharges of the Oder in Połęcko have generally been decreasing (Fig. 4). In the April to August period, the lowest monthly discharges appear to be decreasing; however, there is a slight increase in January, February, and March. Significant trends are found from April to August. The pronounced trends in spring and summer months underscore the impact of prolonged dry periods, which can potentially lead to reduced river discharge and exacerbate drought conditions.

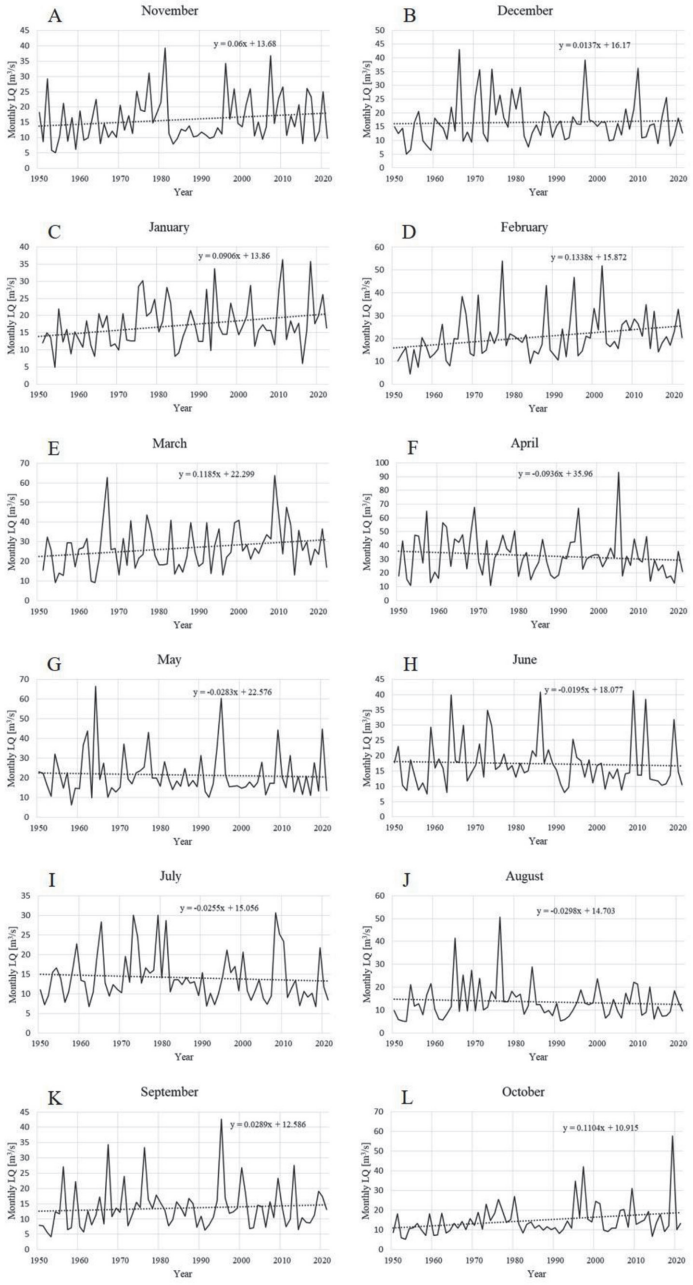

FIGURE 3. Lowest monthly flows of the Oder in Chałupki in the period of 1950–2022

Source: own work based on data of the Institute of Meteorology and Water Management – National Research Institute (IMGW-PIB).

Ali, M. U., Grygoruk, M. (2025). Hydrological analysis of the Oder droughts for the period 1950–2022 in the context of the 2022 river disaster. *Sci. Rev. Eng. Env. Sci.*, *34* (4), 398–416. DOI 10.22630/srees.10421

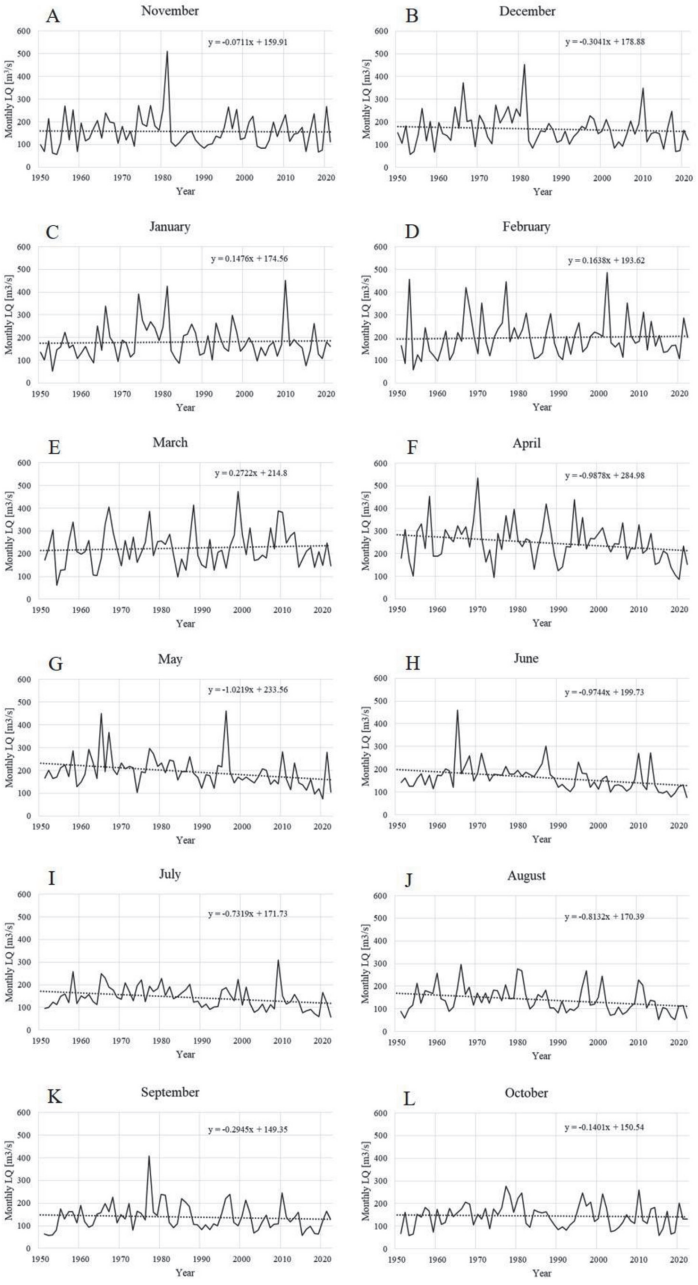

FIGURE 4. Lowest monthly flows of the Oder in Połęcko in the period of 1950–2022

Source: own work based on data of the Institute of Meteorology and Water Management – National Research Institute (IMGW-PIB).

Depending on the particular months, the graph displays both growing and declining patterns in the lowest monthly flows. These patterns suggest that various factors may be influencing the river's flow near Połęcko, including seasonal precipitation patterns, temperature fluctuations, and water management practices. Overall, the lowest monthly discharges are becoming lower in summer and spring. Similarly, in Gozdowice, increasing and decreasing trends are observed (Fig. 5). In January, February, and March, it appears that the lowest monthly discharges are increasing; however, in the other months from April to September, the lowest monthly discharges are decreasing. However, the trends are not statistically significant. In Gozdowice, like in Połęcko, declining trends throughout the summer months signify a rise in the intensity of low discharge intervals, which is associated with drought conditions. These results highlight the Oder's susceptibility to reduced discharge at critical times, which may impact downstream water availability and the health of the ecosystem. The monthly lowest discharge data from several months across the three water gauges show notable trends. According to the Mann–Kendall test results, the significant value is $p = 0.05$. The p-values below indicate notable and statistically significant trends. The resulting p-values are presented in Table 1. From the analysis, we can see that the strongest trends are observed in Chałupki in January ($p = 0.019$), February ($p = 0.001$), and October ($p = 0.032$). These patterns could indicate a worsening of the winter and late fall droughts, which would impact water availability during these months. In Połęcko, significant trends are observed in April ($p = 0.032$), May ($p = 0.001$), June ($p = 0.0002$), July ($p = 0.003$), and August ($p = 0.003$). The effects of prolonged dry spells are highlighted by the patterns in spring and summer, which can result in decreased river discharge and exacerbate drought conditions. On the other hand, the noteworthy patterns in Gozdowice for May ($p = 0.007$), June ($p = 0.002$), July ($p = 0.015$), and August ($p = 0.008$) support Połęcko's findings. Over the period analyzed, the average duration of the Oder drought in Chałupki was 22 days (daily discharge was lower than the SNQ of 9.72 $m^3 \cdot s^{-1}$). Droughts at this gauging station lasted a total of 1,586 days (6.03% of the analyzed period) (Fig. 6). The majority of droughts occurred in August and September. The fewest number of droughts was recorded in January and February.

Ali, M. U., Grygoruk, M. (2025). Hydrological analysis of the Oder droughts for the period 1950–2022 in the context of the 2022 river disaster. *Sci. Rev. Eng. Env. Sci.*, *34* (4), 398–416. DOI 10.22630/srees.10421

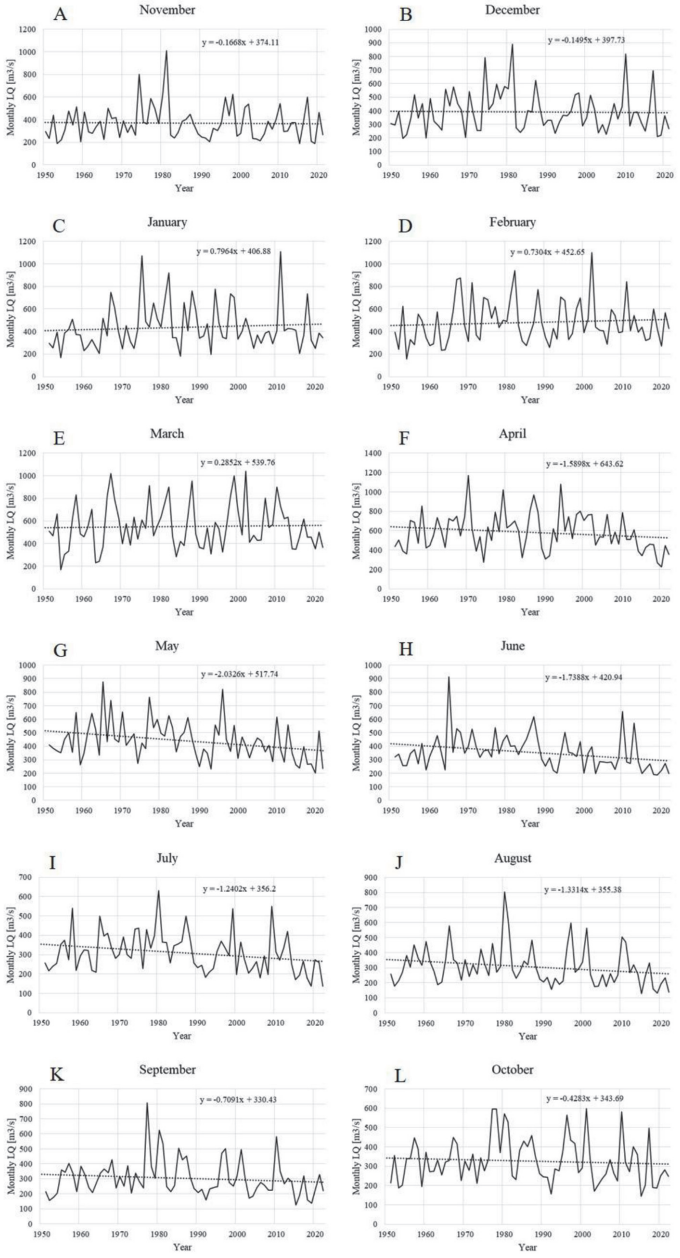

FIGURE 5. Lowest monthly flows of the Oder in Gozdowice in the period of 1950–2022

Source: own work based on data of the Institute of Meteorology and Water Management – National Research Institute (IMGW-PIB).

TABLE 1. *p*-values of the Mann–Kendall test for the lowest monthly discharges of the Oder in a particular month over the period of 1950–2022

Water gauge	Month											
	NOV	DEC	JAN	FEB	MAR	APR	MAY	JUN	JUL	AUG	SEP	OCT
Chałupki	0.071	0.506	0.019	0.001	0.054	0.181	0.553	0.159	0.184	1.000	0.199	0.032
Połęcko	0.710	0.388	0.797	0.384	0.669	0.032	0.001	0.0002	0.003	0.003	0.326	0.617
Gozdowice	0.770	0.548	0.509	0.384	0.984	0.145	0.007	0.002	0.015	0.008	0.210	0.338

Note: The blue background indicates a statistically significant increasing trend in average annual minimum flow (SNQ), while the red background indicates a statistically significant decreasing trend in SNQ.

Source: own work.

Over the period analyzed, the average duration of the Oder drought in Połęcko was 29 days (daily discharge was lower than the SNQ of 106 $m^3 \cdot s^{-1}$). Droughts at this gauging station lasted a total of 2,076 days (7.9% of the analyzed period) (Fig. 6). The majority of droughts occurred in August and September. The fewest number of droughts was recorded in January and April. Over the period analyzed, the average duration of the Oder drought in Gozdowice was 36 days (daily discharge was lower than the SNQ of 247 $m^3 \cdot s^{-1}$). Droughts at this gauging station totaled 2,584 days (9.8% of the total period analyzed) (Fig. 6). The majority of droughts occurred in August and September. The fewest number of droughts was recorded in January and May. It was revealed that the number and duration of droughts increase along the course of the Oder.

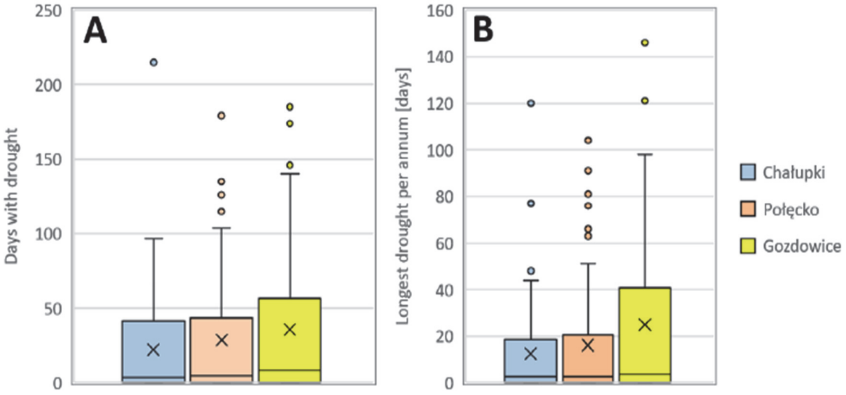

FIGURE 6. Distribution of droughts in three gauging profiles analyzed: A – the number of days of drought; B – the duration of the longest drought per annum

Source: own work.

Ali, M. U., Grygoruk, M. (2025). Hydrological analysis of the Oder droughts for the period 1950–2022 in the context of the 2022 river disaster. *Sci. Rev. Eng. Env. Sci.*, *34* (4), 398–416. DOI 10.22630/srees.10421

Over the period analyzed, the average duration of the Oder drought in Chałupki was 22 days (daily discharge was lower than the SNQ of 9.72 $m^3 \cdot s^{-1}$). Droughts at this gauging station lasted a total of 1,586 days (6.03% of the analyzed period) (Fig. 6). The majority of droughts occurred in August and September. The fewest number of droughts was recorded in January and February. Over the period analyzed, the average duration of the Oder drought in Połęcko was 29 days (daily discharge was lower than the SNQ of 106 $m^3 \cdot s^{-1}$). Droughts at this gauging station lasted a total of 2,076 days (7.9% of the analyzed period) (Fig. 6). The majority of droughts occurred in August and September. The fewest number of droughts was recorded in January and April. Over the period analyzed, the average duration of the Oder drought in Gozdowice was 36 days (daily discharge was lower than the SNQ of 247 $m^3 \cdot s^{-1}$). Droughts at this gauging station totaled 2,584 days (9.8% of the total length of the analyzed period) (Fig. 6). The majority of droughts occurred in August and September. The fewest number of droughts was recorded in January and May. It was revealed that the number and duration of droughts increase along the course of the Oder. Analysis of the durations of droughts on the Oder suggests that their dynamics differ when comparing the upper, middle, and lower courses of the river. In Chałupki, the number of days with drought is decreasing, suggesting that the inflow of water to Poland from the Czech Republic, along with the course of the Oder, is not subject to a significant increase in drought depths and frequencies. This indicates that the frequency of drought days has decreased over time in this area, which is defined as a daily discharge that is less than the SNQ value. The statistical significance trend is validated by the *p*-value of 0.0093 (Table 2), significantly below the significance level of 0.05. This suggests that the observed decline in drought days is statistically significant and not due to random chance. A similar situation is observed when analyzing the durations of the most extended annual droughts in Chałupki. At Chałupki, the most significant yearly drought durations likewise exhibit a decreasing tendency, indicating that the longest drought each year has been getting shorter over time. The *p*-value is 0.0021 (Table 2), indicating strong statistical significance. Improved mitigation strategies or modifications to weather patterns that reduce prolonged periods of dryness in this area may be associated with shorter drought durations. In the decade of 1950–1960, the longest recorded drought lasted for nearly 120 days, whereas in the most recent years, droughts longer than 40 days occur seldom.

TABLE 2. *p*-values of the Mann–Kendall tests for several days of drought at a particular gauging station and the longest annual drought at a specific gauging station

Profile	Number of days of drought		Longest drought	
	trend	p	trend	p
Chalupki	decreasing	0.0093	decreasing	0.0021
Polecko	increasing	0.5855	increasing	0.7792
Gozdowice	increasing	0.6032	increasing	0.7481

Note: The red background represents the statistical significance of the trend.

Source: own work.

The 2022 Oder drought appears to be unique when compared to other historical droughts. In Chałupki, over the period from 1 March 2022 to 30 September 2022, there were 11 days with drought (river discharge lower than 9.72 $m^3 \cdot s^{-1}$) (Fig. 7A). Discharge deficit (the amount of water required to balance the momentary discharge of the Oder to the threshold discharge SNQ) of the Oder in Chałupki in this period was positive and reached 228.7 Mm^3, meaning that over this period, water resources of the catchment of the Oder could be used to balance the drought. Most of the time, river discharges of the Oder were higher than the drought threshold used in this study. In Połęcko, over the period from 1 March 2022 to 30 September 2022, there were 0 days with drought (river discharge lower than 106 $m^3 \cdot s^{-1}$) (Fig. 7B). Discharge deficit (the amount of water required to balance the momentary discharge of the Oder to the threshold discharge SNQ) of the Oder in Połęcko in this period was positive and reached 3,371 Mm^3, meaning that over this period, water resources of the catchment of the Oder could be used to balance the drought. Most of the time, river discharges of the Oder were higher than the drought threshold used in this study. In Gozdowice, over the period from 1 March 2022 to 30 September 2022, there were 204 days with drought (river discharge lower than 247 $m^3 \cdot s^{-1}$) (Fig. 7C). Discharge deficit (the amount of water required to balance the momentary discharge of the Oder to the threshold discharge SNQ) of the Oder in Gozdowice in this period was negative and reached 1,898 Mm^3, meaning that over this period, water resources of the catchment of the Oder were not enough to balance the drought. Most of the time, river discharges of the Oder were higher than the drought threshold used in this study.

Ali, M. U., Grygoruk, M. (2025). Hydrological analysis of the Oder droughts for the period 1950–2022 in the context of the 2022 river disaster. *Sci. Rev. Eng. Env. Sci.*, *34* (4), 398–416. DOI 10.22630/srees.10421

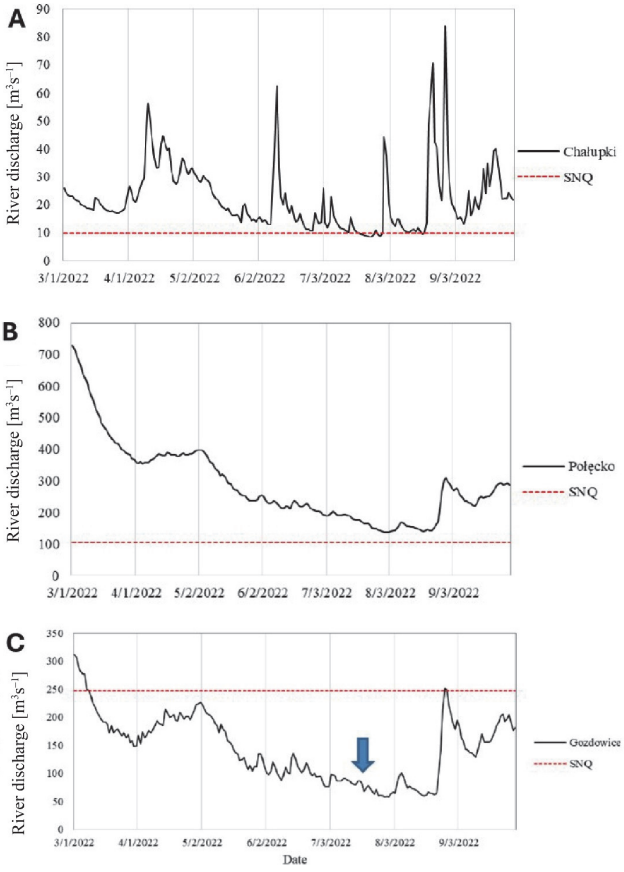

FIGURE 7. Discharge of the Oder in Chałupki (A), Połęcko (B), and Gozdowice (C) in the period from 1 March 2022 to 30 September 2022 (The arrow in Figure 7C represents the time when the Oder disaster occurred; SNQ – average annual minimum flow)

Source: own work based on data of the Institute of Meteorology and Water Management – National Research Institute (IMGW-PIB).

Discussion

Droughts in the middle and lower reaches of the river present several visible trends, including an increase in their duration, particularly during critical summer droughts. This reflects the regional trend in Europe (Parry et al., 2012), which revealed that, similar to the results presented in this study, summer droughts have

increased in duration and discharge deficits over the last five decades. However, comparing the presented patterns to the former studies on droughts in Poland, it appears that the revealed trends in the durations of summer droughts in the middle and lower Oder are significantly larger than those previously reported (Przybylak et al., 2020). As documented, the 2022 drought became increasingly severe along the course of the Oder, particularly in its middle and lower reaches. These results highlight the Oder's susceptibility to decreased discharge during critical periods, which may impact the downstream water supply and ecological health. The statistical analysis reveals significant declining patterns in the monthly lowest discharge statistics, especially in the spring and summer. These patterns indicate that the drought has been worsening over time, which may have contributed to the Oder disaster in 2022.

The lowest yearly discharges at each site fluctuated, but the *p*-values did not show any noticeable long-term patterns. This result suggests that the general hydrological behavior of the Oder in terms of low flow has remained steady over the past few decades, despite brief fluctuations caused by droughts and other hydrological events. This is especially important because rising water demands and climate change have led to significant volatility in the flow of several European rivers (Blöschl, 2022). The seasonal examination of drought events, on the other hand, shows a different picture. All three stations are particularly vulnerable to drought in the late summer and early autumn months (from July to September), with August being the highest month for drought at Chałupki, Połęcko, and Gozdowice. However, in the downstream stations of Połęcko and Gozdowice, the changes are most noticeable, where droughts happen more frequently and stay longer. This pattern aligns with previous research, which demonstrates that the combined effects of land development, precipitation variability, and water extraction typically cause downstream river sections to experience greater hydrological stress (Sperna Weiland et al., 2021). While comparing the upstream station (Chałupki) with the downstream station (Gozdowice), this study found that the intensity and frequency of droughts are higher downstream. This finding is consistent with earlier research that suggests lower reaches of rivers are more vulnerable to water shortages due to a combination of natural and anthropogenic factors (Blauhut et al., 2022). This means that since downstream areas are more severely affected by drought, future attempts to manage water resources should concentrate more on them. Low water levels lead to multiple changes in aquatic ecosystems (Stubbington et al., 2024). In such a case, the reported disaster in the Oder region in 2022 (Szlauer-Łukaszewska et al., 2024) could have been induced by the specific drought that occurred that year. The beginning of the catastrophe

Ali, M. U., Grygoruk, M. (2025). Hydrological analysis of the Oder droughts for the period 1950–2022 in the context of the 2022 river disaster. *Sci. Rev. Eng. Env. Sci.*, *34* (4), 398–416. DOI 10.22630/srees.10421

(12 July 2022) corresponds to the lowest water levels recorded over the discussed 2022 summer drought, so the lack of coincidence of these two phenomena is highly unlikely. The 2022 drought event – the primary focus of this study – falls within a broader pattern of increasing drought occurrences in Europe, a consequence of climate change. Research shows that in recent decades, Europe has seen more frequent and intense droughts. This is primarily due to rising temperatures, altered precipitation patterns, and increased evaporation (Moravec et al., 2021). Similar patterns can be observed in the Oder data, particularly from July through September, when decreased rainfall and warmer temperatures typically result in reduced river flow. Despite the Oder's generally consistent hydrological regime, seasonal drought patterns have worsened in recent years, particularly in areas downstream. This validates the results of Eini et al. (2023), who noted a comparable increase in drought severity in Poland, particularly in areas with high water demand and significant agricultural activities. The findings highlight the fact that, despite the river's total flow not declining significantly, seasonal hydrological stress is rising, which may have more negative effects on ecosystems, agriculture, and water supplies. There are several parallels and gaps between the results of this study and other relevant research conducted on the Oder and similar rivers in Europe. For example, Raczyński and Dyer (2024) found that, similar to the patterns seen in the Oder, low-flow periods are occurring increasingly often in numerous European rivers throughout the summer. On the other hand, the Oder seems to have resisted significant long-term changes in its lowest discharges. In contrast, different rivers, including the Rhine and Danube, have demonstrated more notable long-term variations in flow as a result of climate change. Perhaps this is due to the region's improved water management techniques and the Oder's unique geography. Drought patterns at Połęcko and Gozdowice align with research on the Elbe and Vistula, which has demonstrated comparable downstream escalated situations of drought effects (Piniewski et al., 2022). The results underscore the need for improved water management plans and adaptable methods to mitigate the impacts of droughts and ensure long-term access to sustainable water supplies (Sutanto et al., 2019). Drought deficits revealed for the lowest course of the Oder for the 2022 summer drought (more than 1.8 Mm^3 of water) were much higher than any reasonable reservoir could mitigate. Therefore, future actions aimed at mitigating droughts on the Oder should be based on catchment-scale solutions that can store as much water as possible in the landscape, preferably anticipating the need for restoration of aquatic and wetland ecosystems.

Conclusions

This study examined long-term drought patterns and hydrological conditions in the Oder from 1950 to 2022 using daily discharge data from three gauging stations (Chałupki, Połęcko, and Gozdowice). We identified spatial and temporal trends in drought along the river. Although the lowest annual discharges at all three stations fluctuated, the statistical analysis performed showed no statistically significant long-term trends, indicating that the river's overall low flow capacity has remained stable over the past several decades. However, we revealed a clear increase in drought frequency during summer months, particularly from July to September, with August consistently being the most drought-prone month across all stations. This fulfills the goal of characterizing drought patterns and highlights the increasing hydrological stress during critical warm months. A comparison of the stations revealed that downstream sections of the river experience more frequent and longer droughts than the upstream station at Chałupki.

This spatial variation suggests higher vulnerability downstream, likely due to cumulative upstream water withdrawals, increased human activity, and reduced inflows, addressing the goal of assessing regional differences in hydrological behavior. The analysis of the 2022 drought revealed that extremely low discharges and prolonged drought periods – particularly at Gozdowice – significantly contributed to the environmental disaster that occurred later that year. While hydrological drought may not have been the sole factor, the severe flow reduction likely worsened water temperature, nutrient levels, and algal blooms, acting as a key trigger. This aligns with understanding how drought conditions influenced the 2022 crisis.

Overall, the findings indicate that although the Oder has maintained long-term discharge stability, the increase in seasonal drought events reflects rising sensitivity to climate-related hydrological stress. These results offer valuable insights into drought dynamics in Central European river systems and underscore the need for enhanced adaptive water management, transboundary cooperation, and hazard mitigation strategies, particularly in downstream regions where risks are greatest. Future efforts should focus on enhancing water retention, ecological restoration, and coordinated emergency planning to strengthen resilience against extreme droughts and prevent similar ecological crises.

Acknowledgments

The results presented in this paper were developed in the form of a master's thesis defended at the Faculty of Civil and Environmental Engineering of the Warsaw University of Life Sciences – SGGW, authored by Muhammad Umar Ali, and supervised by Mateusz Grygoruk.

References

Absalon, D., Matysik, M., Woźnica, A., & Janczewska, N. (2023). Detection of changes in the hydrobiological parameters of the Oder River during the ecological disaster in July 2022 based on multi-parameter probe tests and remote sensing methods. *Ecological Indicators*, *148*, 110103. https://doi.org/10.1016/j.ecolind.2023.110103

Blauhut, V., Stoelzle, M., Ahopelto, L., Brunner, M. I., Teutschbein, C., Wendt, D. E., Akstinas, V., Bakke, S. J., Barker, L. J., Bartošová, L., Briede, A., Cammalleri, C., Kalin, K. C., De Stefano, L., Fendeková, M., Finger, D. C., Huysmans, M., Ivanov, M., Jaagus, J., …, & Živković, N. (2022). Lessons from the 2018–2019 European droughts: A collective need for unifying drought risk management. *Natural Hazards and Earth System Sciences*, *22*(6), 2201–2217. https://doi.org/10.5194/nhess-22-2201-2022

Blöschl, G. (2022). Three hypotheses on changing river flood hazards. *Hydrology and Earth System Sciences*, *26*(19), 5015–5033. https://doi.org/10.5194/hess-26-5015-2022

Eini, M. R., Ziveh, A. R., Salmani, H., Mujahid, S., Ghezelayagh, P., & Piniewski, M. (2023). Detecting drought events over a region in Central Europe using a regional and two satellite-based precipitation datasets. *Agricultural and Forest Meteorology*, *342*, 109733. https://doi.org/10.1016/j.agrformet.2023.109733

Graf, R., & Wrzesiński, D. (2020). Detecting patterns of changes in river water temperature in Poland. *Water*, *12*(5), 1327. https://doi.org/10.3390/w12051327

Joint Research Centre [JRC]. (2020). Fact sheet: Oder River basin. https://water.jrc.ec.europa.eu/pdf/oder-fs.pdf

Kolada, A. (ed.) (2022). *Report of the team for the situation arising on the Oder River. The basis for further research – Odra.* Institute of Environmental Protection – National Research Institute. https://ios.edu.pl/projekt/prezentacja-wnioskow-ze-wstepnego-raportu-zespolu-ds-sytuacji-na-rzece-odrze/

Kreienkamp, F., Philip, S. Y., Tradowsky, J. S., Kew, S. F., Lorenz, P., Arrighi, J., Belleflamme, A., Bettmann, T., Caluwaerts, S., Chan, S. C., Ciavarella, A., De Cruz, L., Vries, H. de, Demuth, N., Ferrone, A., Fischer, M., Fowler, H. J., Goergen, K., Heinrich, D., …, & Wanders, N. (2021). Rapid attribution of heavy rainfall events leading to severe flooding in Western Europe during July 2021. *World Weather Attribution*. http://hdl.handle.net/1854/LU-8732135

Moravec, V., Markonis, Y., Rakovec, O., Svoboda, M., Trnka, M., Kumar, R., & Hanel, M. (2021). Europe under multi-year droughts: How severe was the 2014–2018 drought period? *Environmental Research Letters*, *16*(3), 034062. https://doi.org/10.1088/1748-9326/abe828

Parry, S., Hannaford, J., Lloyd-Hughes, B., & Prudhomme, C. (2012). Multi-year droughts in Europe: Analysis of development and causes. *Hydrology Research*, *43*(5), 689–706. https://doi.org/10.2166/nh.2012.024

Piniewski, M., Eini, M. R., Chattopadhyay, S., Okruszko, T., & Kundzewicz, Z. W. (2022). Is there a coherence in observed and projected changes in riverine low flow indices across Central Europe? *Earth-Science Reviews*, *233*, 104187. https://doi.org/10.1016/j.earscirev.2022.104187

Przybylak, R., Oliński, P., Koprowski, M., Filipiak, J., Pospieszyńska, A., Chorążyczewski, W., Puchałka, R., & Dąbrowski, H. P. (2020). Droughts in the area of Poland in recent centuries in the light of multi-proxy data. *Climate of the Past*, *16*(2), 627–661. https://doi.org/10.5194/cp-16-627-2020

Raczyński, K., & Dyer, J. (2024). Changes in streamflow drought and flood distribution over Poland using trend decomposition. *Acta Geophysica*, *72*(4), 2773–2794. https://doi.org/10.1007/s11600-023-01188-0

Sayegh, M., & Żabnieńska, A. (2019). Characteristics of Oder river water temperature for heat pump. *E3S Web of Conferences*, *116*, 00071. https://doi.org/10.1051/e3sconf/201911600071

Shah, S. A., & Kiran, M. (2021). Mann-Kendall test: trend analysis of temperature, rainfall and discharge of Ghotki feeder canal in district Ghotki, Sindh, Pakistan. *Environment & Ecosystem Science*, *5*(2), 137–142. https://doi.org/10.26480/ees.02.2021.137.142

Sługocki, Ł., & Czerniawski, R. (2023). Water quality of the Odra (Oder) River before and during the ecological disaster in 2022: a warning to water management. *Sustainability*, *15*(11), 8594. https://doi.org/10.3390/su15118594

Sperna Weiland, F. C., Visser, R. D., Greve, P., Bisselink, B., Brunner, L., & Weerts, A. H. (2021). Estimating regionalized hydrological impacts of climate change over Europe by performance-based weighting of CORDEX projections. *Frontiers in Water*, *3*, 713537. https://doi.org/10.3389/frwa.2021.713537

Stubbington, R., England, J., Sarremejane, R., Watts, G., & Wood, P. J. (2024). The effects of drought on biodiversity in UK river ecosystems: Drying rivers in a wet country. *WIREs Water*, *11*(5), e1745. https://doi.org/10.1002/wat2.1745

Sutanto, S. J., Weert, M. van der, Wanders, N., Blauhut, V., & Lanen, H. A. J. van (2019). Moving from drought hazard to impact forecasts. *Nature Communications*, *10*(1), 4945. https://doi.org/10.1038/s41467-019-12840-z

Szlauer-Łukaszewska, A., Ławicki, Ł., Engel, J., Drewniak, E., Ciężak, K., & Marchowski, D. (2024). Quantifying a mass mortality event in freshwater wildlife within the Lower Odra River: Insights from a large European river. *Science of The Total Environment*, *907*, 167898. https://doi.org/10.1016/j.scitotenv.2023.167898

Tallaksen, L. M., & Lanen, H. A. J. van (2023). *Hydrological drought: processes and estimation methods for streamflow and groundwater.* Elsevier.

United Nations Convention to Combat Desertification (2022, May 11). *World "at a crossroads" in drought management, up 29% in a generation and worsening, says UN*. UNCCD. United Nations Convention to Combat Desertification. https://www.unccd.int/news-stories/press-releases/world-crossroads-drought-management-29-generation-and-worsening-says-un

Van Loon, A. F. (2015). Hydrological drought explained. *WIREs Water*, *2*(4), 359–392. https://doi.org/10.1002/wat2.1085

Wrzesiński, D. (2021). Flow regime patterns and their changes. In M. Zeleňáková, K. Kubiak-Wójcicka & A. M. Negm (Eds), *Management of water resources in Poland* (pp. 163–180). Springer International Publishing. https://doi.org/10.1007/978-3-030-61965-7_9

Zhou, Z., Shi, H., Fu, Q., Li, T., Gan, T. Y., & Liu, S. (2020). Assessing spatiotemporal characteristics of drought and its effects on climate-induced yield of maize in Northeast China. *Journal of Hydrology*, *588*, 125097. https://doi.org/10.1016/j.jhydrol.2020.125097

Summary

Hydrological analysis of the Oder droughts for the period 1950–2022 in the context of the 2022 river disaster. The study aims to analyze the droughts of the Oder from 1950 to 2022 at three water gauge profiles located in the upper (Chałupki), middle (Połęcko), and lower (Gozdowice) reaches of the Oder. The subject of the analysis was the temporal variability of the lowest annual and monthly flows of the Oder, the durations of lows characterized by a flow lower than the adopted threshold criterion (average annual minimum flow, SNQ), and the trends of their changes in the analyzed period. We identified decreasing trends of the lowest annual river flows in the middle and lower reaches of the Oder. The lowest monthly flows of the Oder exhibit statistically significant trends in the months of April–September (Połęcko) and May–September (Gozdowice). The summer drought of 2022 was exceptionally long and severe (the discharge deficit amounted to more than 1.8 Mm³ in the Gozdowice profile) and is unlikely to be reduced to the SNQ level through any existing or planned reservoir. Changes in the drought indicators occur as a result of the course of hydrological processes taking place in the Polish part of the Oder basin.

Scientific Review Engineering and Environmental Sciences (2025), 34 (4), 417–435

Sci. Rev. Eng. Env. Sci. (2025), 34 (4) https://srees.sggw.edu.pl

ISSN 1732-9353 (suspended) eISSN 2543-7496 DOI 10.22630/srees.10786

Received: 04.09.2025
Accepted: 17.11.2025

Amar MEZIDI

Salem MERABTI✉

University of Khemis-Miliana, Faculty of Science and Technology, Acoustics and Civil Engineering Laboratory, Algeria

Comparative assessment of the physico-mechanical properties of crumb rubber concretes developed with natural and dune sands

Keywords: crumb rubber, dune sand concrete, ordinary concrete, physical property, mechanical property

Introduction

Environmental constraints and the limited availability of natural resources are increasingly directing research toward the valorization of waste into construction materials (Merabti et al., 2021; Mezidi et al., 2023; Serikma et al., 2024). In this context, end-of-life tires, which represent a major source of pollution, have been identified as a priority waste stream for reuse in the present study. Literature findings indicate that concrete incorporating rubber can maintain satisfactory durability under both static and dynamic loading, provided that the substitution rates remain limited (Abdelaleem et al., 2024).

Investigations of specific rubberized concrete formulations highlight the decisive role of mix composition in tailoring mechanical performance

✉s.merabti@univ-dbkm.dz

to the intended application (El-Nemr & Shaaban, 2024). Furthermore, recent advances in self-healing concrete combining bacteria and rubber particles confirm the potential of this approach to enhance durability and control crack propagation (Eisa et al., 2025).

From a mechanical and structural perspective, studies consistently report reductions in compressive and tensile strengths, counterbalanced by improvements in ductility and energy absorption capacity (Elbialy et al., 2024). Experimental investigations, coupled with SEM observations, have refined the understanding of the rubber-cementitious matrix interface (Sofi et al., 2024). Moreover, analyses of the durability and mechanical performance of crumb rubber concretes underscore the need for surface treatments to mitigate strength losses (Liu et al., 2016).

Recent reviews clearly emphasize both the strengths and limitations of rubberized concrete for structural applications (Elshazly et al., 2020). For non--structural uses, the durability of lightweight rubberized concretes, particularly in relation to water absorption and freeze–thaw resistance, has been well documented (Pham et al., 2019). In parallel, reviews of high-strength rubberized concretes describe promising structural potential, contingent on controlled mix design (Li et al., 2016).

Characterization of high-performance rubberized concretes demonstrates that particle size and dosage strongly influence the strength–ductility trade-off (Ge et al., 2024). Reviews dedicated to crumb rubber-based concretes consistently highlight the key properties and the importance of optimized mix design (Azunna et al., 2024). Material characterization and mechanical behavior studies contribute to elucidating the specific deformation and failure mechanisms of these composites (Hernández et al., 2021).

Abrasion resistance remains a critical factor for road and industrial applications (Noor et al., 2016). Dynamic performance and damping capacity, highly desirable for structures subjected to vibration or impact, are among the distinctive benefits of these composites (Eltayeb et al., 2016). The influence of pretreatment and rubber particle size distribution on overall concrete performance has been explored as a means of optimization (Agrawal et al., 2025).

Appropriate surface treatments of crumb rubber can enhance both mechanical and durability properties while maintaining the economic viability of these solutions (Assaggaf et al., 2019). The combination of rubber with glass powder has shown promise for pavement structures, particularly in white-topping systems (Grinys et al., 2021). Nevertheless, abrasion resistance remains a central issue for long-term durability (Noor et al., 2016).

Review papers provide an overview of applications and properties of rubberized concretes (Elshazly et al., 2020). The combined effect of particle size and content on static and dynamic responses confirms the importance of these formulation parameters (Du et al., 2024). Partial replacement of sand with rubber has been examined in detail, revealing improved workability at the expense of progressive reductions in mechanical strength (Siringi et al., 2013; Mezidi et al., 2025).

Microstructural analyses confirm the decisive role of the rubber–cement interface in overall performance (Kevin et al., 2025). Flexural tests on structural elements highlight promising behaviors for targeted applications (Naito et al., 2014). More broadly, cementitious composites incorporating rubber waste exhibit variable responses depending on the selected formulation (Bulut & Kandil, 2024).

Applications in residential slabs have demonstrated both industrial feasibility and economic relevance (Youssf et al., 2021). Enhancing durability through partial substitution with rubber particles aligns with sustainable construction objectives (Singaravel et al., 2024). Additionally, the development of highly workable rubberized mixtures for grouting applications opens new perspectives (Lu et al., 2022). High-temperature performance also reveals specific advantages for specialized applications (Han et al., 2023). Finally, the most recent reviews call for further optimization of mix design, long-term durability assessments, and comprehensive environmental impact analyses to ensure the safety and acceptability of large-scale deployment of rubberized concrete (Assaggaf et al., 2022).

Although numerous studies have explored rubberized concrete, comparative investigations addressing the combined influence of rubber incorporation and sand type are scarce, especially regarding the replacement of natural sand with locally available dune sand under realistic mix designs. This research gap is particularly relevant in regions where dune sand constitutes a major aggregate source, yet its interaction with rubber particles in both structural and non-structural applications remains insufficiently understood.

The present study aims to conduct a detailed assessment of the effects of incorporating crumb rubber (CR) at replacement ratios between 1% and 5% of the sand mass on the behavior of ordinary concrete (OCCR) and dune sand concrete (SCCR). The research focuses on a comparative evaluation of their physical and mechanical properties. Moreover, it intends to develop practical guidelines for the use of these innovative materials by considering normative standards, technical limitations, and the environmental advantages of rubber waste recycling, thereby supporting the advancement of sustainable and context-adapted construction practices.

Mezidi, A., Merabti, S. (2025). Comparative assessment of the physico-mechanical properties of crumb rubber concretes developed with natural and dune sands. *Sci. Rev. Eng. Env. Sci.*, *34* (4), 417–435. DOI 10.22630/srees.10786

Methodology

Material characterization

A single type of cement was used in this study: CPJ-CEM II 42.5. The compressive strength, determined according to standard NA 442 (Algerian Institute of Standardization [IANOR], 2013), reached 40 MPa after 28 days of curing. The specific surface area, measured using the Blaine apparatus, was 3,700 $cm^2 \cdot g^{-1}$, while the absolute density of the cement was 3.16 $g \cdot cm^{-3}$. The detailed chemical composition of the cement is presented in Table 1.

TABLE 1. Chemical composition of cement

Constituent	CaO	SiO_2	Al_2O_3	Fe_2O_3	SO_3	K_2O	Na_2O	MgO	CaO free
%	65	20.71	4	7	2.72	0.41	0.13	1	1.20

Source: own work.

Ordinary concrete was produced using natural sand (NS) and gravel, whereas dune sand concrete was prepared exclusively with dune sand (DS). The main physical properties of these three materials – natural sand, dune sand, and gravel – are summarized in Table 2, providing a clear comparison of their essential characteristics for concrete mix design.

TABLE 2. Physical characteristics of natural sand (NS) and dune sand (DS)

Physical characteristics	NS	DS	Gravel (3/8)	Gravel (8/15)
Fineness modulus	3.08	1.04	–	–
Visual sand equivalent [%]	89.49	91.52	–	–
Methylene blue value [$g \cdot l^{-1}$]	0.63	0.50	–	–
Friability [%]	39.20	21.00	–	–
Apparent density [$g \cdot cm^{-3}$]	1,452.00	1,870.00	1.31	1.42
Absolute density [$g \cdot cm^{-3}$]	2.50	2.56	2.50	2.50
Porosity [%]	43.37	27.07	47.60	43.36
Compactness [%]	56.63	72.93	52.40	56.64
Los-Angeles degradation of wear [%]	–	–	34.89	21.73
Micro-Deval coefficient [%]	–	–	38.40	18.20
Flattening coefficient [%]	–	–	26.00	8.58

Source: own work.

Both concretes were modified by incorporating blackish crumb rubber into the formulations. The Fourier transform infrared (FTIR) spectrum of the crumb rubber reveals several absorption bands characteristic of the polymer. A pronounced peak observed at 2,237 cm^{-1} corresponds to the stretching vibration of the nitrile group (C≡N), a typical signature of acrylonitrile-butadiene rubber (NBR). Additional bands located at 2,918 cm^{-1} and 2,848 cm^{-1} are attributed to the stretching vibrations of C–H bonds in methylene and methyl groups. The region between 1,450 cm^{-1} and 1,375 cm^{-1} exhibits absorptions associated with the deformation modes of CH_2 and CH_3 groups, while a peak at 966 cm^{-1} corresponds to the out-of-plane deformation of the C=C–H bond in the butadiene unit (Fig. 1). These results are consistent with the literature, confirming the identification of the analyzed polymer as NBR (Nuzaimah et al., 2017; Kevin et al., 2025). The results of the physical properties of CR are summarized in Table 3.

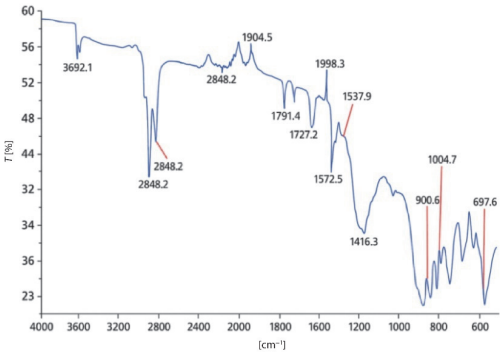

FIGURE 1. FTIR spectrum of crumb rubber
Source: own work.

TABLE 3. Physical properties of crumb rubber

Property	Value
Methylene blue value [$g \cdot l^{-1}$]	0.67
Relative compaction [%]	68.81
Porosity [%]	31.19
Absolute density [$g \cdot cm^{-3}$]	0.533
Apparent density [$g \cdot cm^{-3}$]	0.367

Source: own work.

Mezidi, A., Merabti, S. (2025). Comparative assessment of the physico-mechanical properties of crumb rubber concretes developed with natural and dune sands. *Sci. Rev. Eng. Env. Sci.*, *34* (4), 417–435. DOI 10.22630/srees.10786

The crumb rubber size ranges from 0.08 mm to 1.25 mm. These residues exhibit a relative density of 1.22 and an estimated purity of approximately 45%. Figure 2 illustrates the particle size distribution curves of all the materials used: natural sand, dune sand, gravel, and rubber particles.

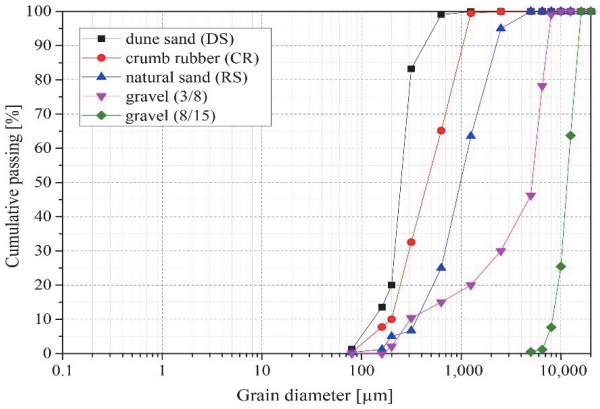

FIGURE 2. Grading curves of the materials used in the study
Source: own work.

Mixtures

The mixed formulations are summarized in Tables 4 and 5. Crumb rubber was incorporated by partially replacing sand at levels ranging from 0% to 5%. All concrete mixes contained Medaflow SR20 at 1.5% of the cement mass. The batch volume and admixture dosage were kept constant for both series of concretes; however, dune sand concrete required a higher mixing water content. Consequently, a greater absolute amount of CR was introduced into the dune sand concrete, which included dune sand as the sole fine aggregate. The water-to-cement ratio (W/C) was maintained at 0.52 for the OCCR and 0.69 for the SCCR. These proportions were chosen to achieve similar workability levels and to ensure satisfactory mechanical characteristics in both mixtures. This ratio was maintained constant for each concrete mix throughout the experimental program. Prisms measuring 70 × 70 × 280 mm^3 for flexural tensile strength and cubes measuring 100 × 100 × 100 mm^3 for compressive strength were prepared, with n = 3 specimens per mix. In total, 42 cubes and 18 prisms were tested for the first series. The tests were carried out at 7 days, 28 days, and 90 days. The mix design was

established using Faury's method. The specimens were stored by immersion until the testing age, in accordance with EN 12390-2 (European Committee for Standardization [CEN], 2019). The compactness and apparent density were measured, and the flexural tensile and compressive strengths were determined in accordance with EN 196-1 (CEN, 2016).

TABLE 4. Composition of ordinary concrete with crumb rubber (OCCR) [kg·m^{-3}]

Composition	Concrete variant					
	OCCR 0%	OCCR 1%	OCCR 2%	OCCR 3%	OCCR 4%	OCCR 5%
Cement	350.00	350.00	350.00	350.00	350.00	350.00
Medaflow SR20	5.25	5.25	5.25	5.25	5.25	5.25
Natural sand	535.04	529.69	524.34	518.98	513.64	508.29
Crumb rubber	0	5.35	10.70	16.05	21.40	26.75
Gravel (3/8)	164.00	164.00	164.00	164.00	164.00	164.00
Gravel (8/15)	1,086.50	1,086.50	1,086.50	1,086.50	1,086.50	1,086.50
Water	180.45	180.45	180.45	180.45	180.45	180.45

Source: own work.

TABLE 5. Composition of dune sand concrete with crumb rubber (SCCR) [kg·m^{-3}]

Composition	Concrete variant					
	SCCR 0%	SCCR 1%	SCC 2%	SCCR 3%	SCCR 4%	SCCR 5%
Cement	350.00	350.00	350.00	350.00	350.00	350.00
Medaflow SR20	5.25	5.25	5.25	5.25	5.25	5.25
Dune sand	1,541.70	1,526.28	1,510.86	1,495.44	1,480.02	1,464.60
Crumb rubber	0	15.42	30.84	46.26	61.68	77.01
Water	241.50	241.50	241.50	241.50	241.50	241.50

Source: own work

The elastic modulus was determined on cubic specimens (15 × 15 × 15 cm^3) instrumented with bonded electrical strain gauges oriented in both longitudinal and transverse directions. Each specimen, centered between the press plates, was subjected to incremental loading in steps of 20 kN, applied at an average rate of 15 kN·s^{-1}, with simultaneous recording of load and microstrain in both directions at each step. Preparation included surface cleaning, strain gauge bonding, and verification of connection continuity (Fig. 3a), while data acquisition was performed using a system that directly measured strains (Fig. 3b).

Mezidi, A., Merabti, S. (2025). Comparative assessment of the physico-mechanical properties of crumb rubber concretes developed with natural and dune sands. *Sci. Rev. Eng. Env. Sci.*, *34* (4), 417–435. DOI 10.22630/srees.10786

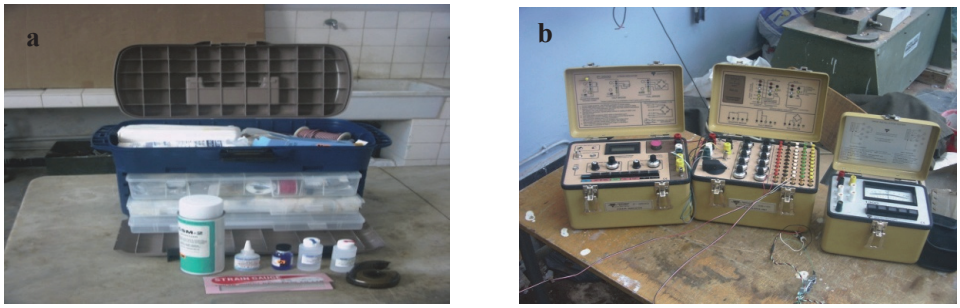

FIGURE 3. Apparatus used for modulus of elasticity testing: a – cleaning reagents, b – a strain-gauge bridge (extensometer)

Source: own work.

The longitudinal stress–strain curve was then plotted up to failure, and the elastic modulus was evaluated within the quasi-linear domain according to Hooke's law, $E = \Delta\sigma/\Delta\varepsilon$ (see Eq. 1). The determination of the secant modulus in compression was carried out in accordance with EN 12390-13 (CEN, 2021):

$$\sigma = E\varepsilon \tag{1}$$

where: σ is a compressive stress, E is an elastic modulus, and ε is a longitudinal strain.

Results and discussion

Apparent density

After 28 days of curing, the apparent density of OCCR remained consistent with that of conventional concretes, ranging from 2,453 kg·m^{-3} to 2,419 kg·m^{-3} (−1.4%), which is in line with the limited reductions typically reported for low levels of rubber substitution (Elshazly et al., 2020; Azunna et al., 2024). In contrast, the density of SCCR decreased from 2,190 kg·m^{-3} to 1,180 kg·m^{-3}, corresponding to a substantial reduction of −46.2%, indicative of a pronounced lightweighting effect. This is close to the higher values reported for mixes with elevated rubber content and/or the absence of coarse aggregates (Elshazly et al., 2020).

At the same CR content, the relative density gap between SCCR and OCCR increased from 10.7% to 51.22% when the CR content rose from 0% to 5%, highlighting the strong sensitivity of apparent density to CR substitution in matrices without coarse aggregates (Hisbani et al., 2025).

These results are consistent with recent reviews, which report density reductions ranging from a few percent up to approximately 30–45%, depending on the rubber volume fraction, particle size distribution, and possible surface treatments (Azunna et al., 2024). Finally, the relative position of SCCR with respect to OCCR falls within the well-established envelope of concrete formulated with dune sand, where density values may remain close to conventional levels at low replacement rates but decrease markedly as substitution increases (Azunna et al., 2024; Hisbani et al., 2025).

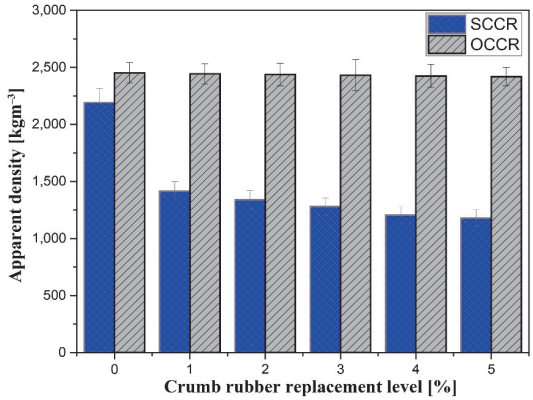

FIGURE 4. Apparent density versus crumb rubber content for dune sand concrete with crumb rubber (SCCR) and concrete with crumb rubber (OCCR)

Source: own work.

Compactness

The results presented in Figure 5 show a steady increase in compactness with increasing CR content for both materials. For SCCR, compactness increases from 92.0% to 96.8% between CR = 0% and CR = 5%, corresponding to a relative gain of about 5.2%. Similarly, OCCR increases from 93.13% to 97.02%, i.e., a relative gain of about 4.2%, reflecting a gradual densification of granular packing as the CR content increases (Bulut et al., 2024).

At identical CR levels, the compactness gap between SCCR and OCCR decreases markedly, from approximately 1.21% down to 0.23% (relative to OCCR), indicating a convergence of compactness degrees at the higher end of the studied CR range (Bulut et al., 2024; Singaravel et al., 2024). This trend is consistent with the literature, which highlights that optimized particle size distribution

Mezidi, A., Merabti, S. (2025). Comparative assessment of the physico-mechanical properties of crumb rubber concretes developed with natural and dune sands. *Sci. Rev. Eng. Env. Sci.*, *34* (4), 417–435. DOI 10.22630/srees.10786

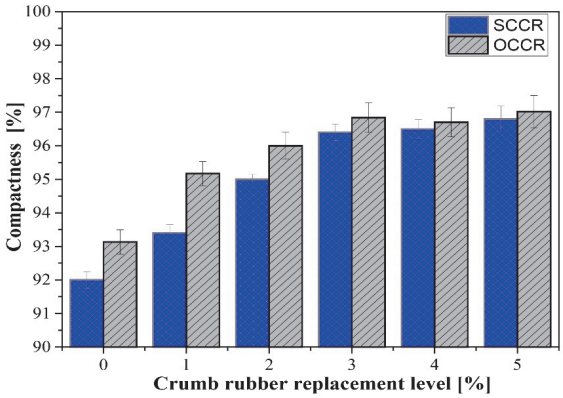

FIGURE 5. Compactness versus crumb rubber content for dune sand concrete with crumb rubber (SCCR) and concrete with crumb rubber (OCCR)

Source: own work.

and controlled rheology – depending on the size and treatment of the rubber particles – can lead to a filler effect within fine voids and an overall improvement in compactness (Singaravel et al., 2024). Overall, for CR levels between 4% and 5%, the compactness values of SCCR are very close to those of OCCR, suggesting that, within this range, the influence of the matrix type on compactness is secondary compared to the volumetric effect of rubber (Youssf et al., 2021).

Compressive strength

The results show that the incorporation of CR penalizes SCCR more severely than OCCR, mainly due to the fineness of dune sand, the smooth/rounded morphology of its grains, and its poor particle size distribution, which collectively increase water demand, porosity, and the weakness of the interfacial transition zone (ITZ). The reduction in compressive strength becomes more pronounced with the curing time, while the strength gain between 28 days and 90 days remains limited, and intergranular cohesion becomes critical at a CR content of 5%.

At 28 days, the SCCR control (0% CR) exhibited an approximate 46.82% reduction in compressive strength relative to its designated reference. The compressive strength reached 15.8 MPa for OCCR, compared with 7.65 MPa for SCCR containing CR, a decrease of approximately 51.58% for 5% crumb rubber content. In the long term, the relative gap in compressive strength between the two concretes decreases to reach 46.29%, whereas at an early age (7 days), the opposite trend is observed. Compared to the control mix without CR, a 5%

content of CR leads to a reduction of about 63% in compressive strength for OCCR and about 66% for SCCR.

These trends are consistent with previous studies highlighting the need for particle size correction to valorize dune sand (Moulay-Ali et al., 2021), the mechanical performance losses and rheological peculiarities associated with dune sand (Al-Harthy et al., 2007; Park et al., 2007), and the additional weakening induced by CR through a more fragile ITZ and higher porosity, despite potential gains in ductility for non-structural applications (Hisbani et al., 2025). Compression tests beyond 90 days of curing will be conducted to quantify late-age strength gains and to identify CR content thresholds beyond which strength loss becomes critical, with particular emphasis on self-compacting mixes.

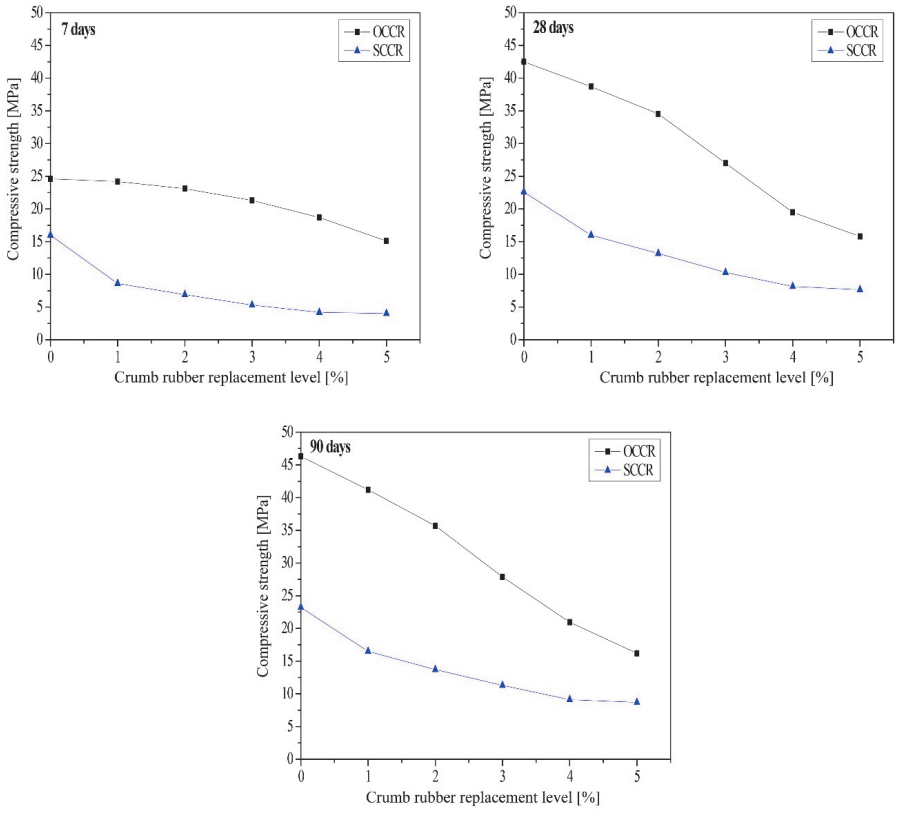

FIGURE 6. Compressive strength versus curing time for concrete with crumb rubber (OCCR) and dune sand concrete with crumb rubber (SCCR)

Source: own work.

Mezidi, A., Merabti, S. (2025). Comparative assessment of the physico-mechanical properties of crumb rubber concretes developed with natural and dune sands. *Sci. Rev. Eng. Env. Sci.*, *34* (4), 417–435. DOI 10.22630/srees.10786

Flexural tensile strength

The evaluation of flexural tensile strength at 28 days for concretes modified with crumb rubber highlights differentiated behaviors depending on both the concrete type and the incorporated rubber content (Elbialy et al., 2024; Sofi et al., 2024; Fig. 7). At a 1% crumb rubber dosage, OCCR exhibits relatively higher strength retention, reaching 84.91%, compared to 71.15% for SCCR (Azunna et al., 2024). However, between 2% and 3% rubber, this trend reverses: dune sand concrete maintains a higher strength ratio, with values ranging from 64.10% to 58.97%, whereas ordinary concrete drops to levels between 68.01% and 59.97%.

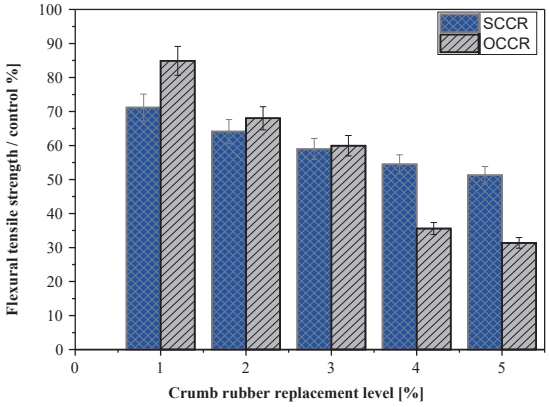

FIGUR E 7. Flexural tensile strength ratio relative to the control versus crumb rubber content for dune sand concrete with crumb rubber (SCCR) and concrete with crumb rubber (OCCR)

Source: own work.

At higher dosages – 4% and 5% – the gap becomes more pronounced, as SCCR sustains strengths of 54.48% and 51.28% of the control, while OCCR drops sharply to 35.61% and 31.39%, respectively. Thus, in the 3–5% range, dune sand concrete demonstrates greater stability in terms of flexural strength, whereas ordinary concrete performs better at lower dosages (Grinys et al., 2021; Sofi et al., 2024). Nevertheless, in terms of absolute flexural tensile strength, modified ordinary concrete maintains a clear superiority. For instance, at 5% crumb rubber, ordinary concrete records a flexural tensile strength of 1.56 MPa, compared to only 0.8 MPa for dune sand concrete, underscoring a more favorable mechanical performance for OCCR despite the relative strength losses observed. Overall, these findings indicate that OCCR retains adequate flexural capacity for applications subjected to bending.

Flexural testing will be expanded to delineate the 3–5% CR stability window and the crossover in relative retention between SCCR and OCCR. Microstructural verification and tightly controlled rheology will map how particle size, surface modification, and packing govern both flexural strengths.

Modulus of elasticity

The stress–strain curves of the reference concrete and a dune-sand concrete containing 3% crumb rubber were analyzed only within the elastic regime, with three points selected for OCCR concrete and five points for SCCR concrete. Non-proportional segments were excluded to avoid bias in the stiffness estimation (Mohammed & Azmi, 2011; Haridharan et al., 2017; Fig. 8). Young's modulus E was determined as the slope of the proportional region by linear regression of the model $\sigma = E\varepsilon + b$, and, when no offset was observed, by a constrained fit through the origin ($\sigma = E\varepsilon$, Eq. 1), in accordance with Hooke's law and standard practices in mechanics of materials (Aghamohammadi et al., 2023).

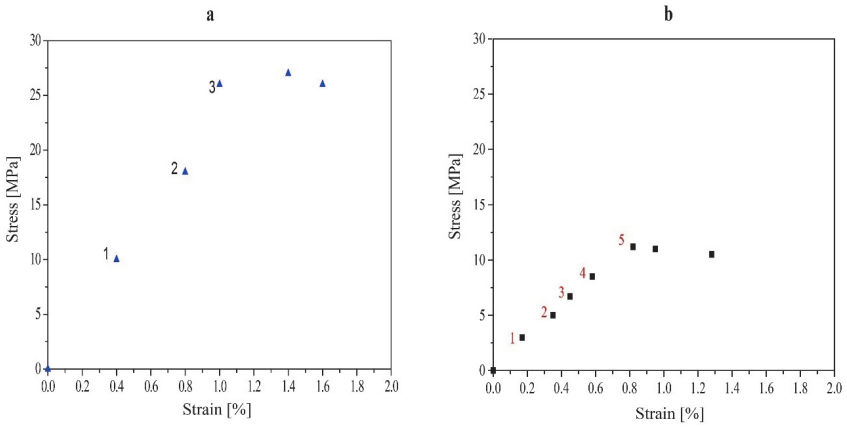

FIGURE 8. Concrete stress–strain curve: a – ordinary concrete with crumb rubber (OCCR), b – dune sand concrete with crumb rubber (SCCR)

Source: own work.

For OCCR concrete, the estimates gave E = 24.7 GPa with the regression constrained to the origin (R^2 = 0.987), and E = 25.7 GPa with a free intercept (R^2 = 0.964). For SCCR concrete, the values were E = 13.60 GPa with a free intercept (R^2 = 0.994) and E = 14.23 GPa with a regression constrained to the origin (R^2 = 0.991), confirming the strong linearity over the analyzed range.

In comparison, the Young's modulus of OCCR concrete, close to 25 GPa, exceeds that of SCCR concrete (13.6–14.2 GPa) by approximately 75–85%, indicating the higher stiffness of OCCR concrete relative to SCCR concrete, consistent with findings reported in the literature on the influence of recycled rubber in concrete (Haridharan et al., 2017; Aghamohammadi et al., 2023).

To situate these results within the complete mechanical response, the proportional-limit strain and stress are additionally reported for each mix, together with initial tangent and mid-range secant moduli for comparison. Where partial unload–reload segments were recorded, unloading–reloading slopes and residual strains are indicated to reveal hysteresis, and the applied strain-rate and confinement conditions are specified to ensure reproducibility.

Table 6 presents the main results obtained from the experimental program, enabling a direct comparison. At equal crumb rubber levels, OCCR is denser and stronger than SCCR. OCCR's density drops slightly from 2,453 kg·m^{-3} to 2,419 kg·m^{-3}, and SCCR's density drops sharply from 2,190 kg·m^{-3} to 1,180 kg·m^{-3}. In compression, OCCR decreases from 42.5 MPa to 15.8 MPa, and SCCR decreases from 22.60 MPa to 7.65 MPa. At comparable contents, SCCR is about half of OCCR. In flexure, OCCR decreases from 4.97 MPa to 1.56 MPa, and SCCR decreases from 1.56 MPa to 0.80 MPa. The gap narrows at higher rubber, but OCCR remains higher. Overall, OCCR handles rubber addition better, suggesting a stronger paste–rubber interface and lower porosity penalties.

TABLE 6. Comparison between the different parameters studied

CR	Apparent density [kg·m^{-3}]		Compressive strength [MPa]		Flexural strength [MPa]	
	OCCR	SCCR	OCCR	SCCR	OCCR	SCCR
0	2,453	2,190	42.50	22.60	4.97	1.56
1	2,443	1,415	38.70	16.00	4.22	1.11
2	2,438	1,340	34.54	13.20	3.38	1.00
3	2,432	1,280	27.00	10.00	2.98	0.92
4	2,425	1,205	19.50	8.15	1.77	0.85
5	2,419	1,180	15.80	7.65	1.56	0.80

CR – crumb rubber, OCCR – ordinary concrete with crumb rubber, SCCR – dune sand concrete with crumb rubber.

Source: own work.

Conclusions

This research aimed to analyze the influence of incorporating recycled rubber aggregates on the physical and mechanical properties of two types of concrete: ordinary concrete and dune sand concrete. The results highlight significant differences between these two formulations, particularly in terms of density, stiffness, and mechanical strength.

– Ordinary concrete maintains a density comparable to that of standard mixtures; at 5% crumb rubber content, an apparent density of 2,419 $kg \cdot m^{-3}$ is obtained for OCCR, while the relative difference with SCCR reaches 51.22%.
– The incorporation of 5% crumb rubber resulted in marked compressive strength losses of about 63% for OCCR and 66% for SCCR, while OCCR retained a clear advantage over time despite partial convergence.
– These outcomes indicate that a 5% CR dosage is close to a practical upper bound for strength-critical uses, with SCCR showing greater sensitivity than OCCR due to its matrix characteristics.
– The flexural behavior of crumb rubber-modified concretes is governed by both mix design and rubber dosage. OCCR shows higher absolute flexural strengths, declining from 4.97 MPa to 1.56 MPa as CR increases from 0% to 5%, whereas SCCR decreases from 4.22 MPa to 0.80 MPa over the same range. Despite a slightly better relative retention in SCCR with higher CR content, OCCR remains superior overall.
– The stress–strain response demonstrates a clear stiffness hierarchy between mixes: OCCR shows an elastic modulus near 25 GPa, whereas SCCR remains around 13.6–14.2 GPa. This 75–85% differential points to a more rigid elastic skeleton in OCCR, while the softer SCCR response is consistent with higher porosity and a more compliant interfacial zone introduced by dune sand and crumb rubber.

The most promising applications concern road infrastructure, safety devices, and constructions designed to reduce noise and vibrations, where the energy absorption capacity represents a key advantage. The study recommends further research on the particle size distribution and surface treatments of rubber to enhance the durability and overall performance of rubber-modified concretes.

References

Abdelaleem, A., Moawad, M., El-Emam, H., Salim, H., & Sallam, H. E. M. (2024). Long term behavior of rubberized concrete under static and dynamic loads. *Case Studies in Construction Materials*, *20*, e03087. https://doi.org/10.1016/j.cscm.2024.e03087

Aghamohammadi, O., Mostofinejad, D., Mostafaei, H., & Abtahi, M. (2023). Mechanical properties and impact resistance of concrete pavement containing crumb rubber, *International Journal of Geomechanics*, *24*(1), 04023211. https://doi.org/10.1061/IJGNAI.GMENG-7620

Agrawal, D., Ansari, K., Waghe, U., Goel, M., Raut, S. P., Warade, H., Althaqafi, E., Islam, S. & Al-Sareji, O. J. (2025). Exploring the impact of pretreatment and particle size variation on properties of rubberized concrete. *Scientific Reports*, *15*(1), 11394. https://doi.org/10.1038/s41598-025-96402-y

Algerian Institute of Standardization [IANOR], (2013). Composition, specifications and criteria for common cements (NA 442).

Al-Harthy, A. S., Halim, M. A., Taha, R., & Al-Jabri, K. S. (2007). The properties of concrete made with fine dune sand. *Construction and Building Materials*, *21*(8), 1803–1808. https://doi.org/10.1016/j.conbuildmat.2006.05.053

Assaggaf, R., Maslehuddin, M., Al-Osta, M. A., Al-Dulaijan, S. U., & Ahmad, S. (2022). Properties and sustainability of treated crumb rubber concrete. *Journal of Building Engineering*, *51*, 104250. https://doi.org/10.1016/j.jobe.2022.104250

Azunna, S. U., Aziz, F. N., Rashid, R. S., & Bakar, N. B. (2024). Review on the characteristic properties of crumb rubber concrete. *Cleaner Materials*, *12*, 100237. https://doi.org/10.1016/j.clema.2024.100237

Bulut, H. A., & Kandil, U. (2024). Mechanical properties of cement-based composites incorporating eco-friendly aggregate of waste rubber. *Revista de la Construcción*, *23*(2), 246–270. http://dx.doi.org/10.7764/rdlc.23.2.246

Du, T., Yang, Y., Cao, H., Si, N., Kordestani, H., Sktani, Z. D. I., Arab, A. & Zhang, C. (2024). Rubberized concrete: effect of the rubber size and content on static and dynamic behavior. *Buildings*, *14*(6), 1541. https://doi.org/10.3390/buildings14061541

Eisa, A. M., Tahwia, A. M., Osman, Y. A., & Elemam, W. E. (2025). Characteristics of bacteria based self healing rubberized concrete for sustainable and durable construction. *Scientific Reports*, *15*(1), 1–16. https://doi.org/10.1038/s41598-025-97174-1

Elbialy, S., Ibrahim, W., Mahmoud, S., Mamdouh, H., Ayash, N. M., & El-Kassas, A. (2024). Mechanical characteristics and structural performance of rubberized concrete: Experimental and analytical analysis. *Case Studies in Construction Materials*, *21*, e03727. https://doi.org/10.1016/j.cscm.2024.e03727

El-Nemr, A., & Shaaban, I. G. (2024). Assessment of special rubberized concrete types utilizing portable non-destructive tests. *NDT*, *2*(3), 160–189. https://doi.org/10.3390/ndt2030010

Elshazly, F. A., Mustafa, S. A., & Fawzy, H. M. (2020). Rubberized concrete properties and its structural engineering applications – An overview. *The Egyptian International Journal of Engineering Sciences and Technology*, *30*, 1–11. https://doi.org/10.21608/eijest.2020.35823.1000

Eltayeb, E., Ma, X., Zhuge, Y., Xiao, J., & Youssf, O. (2021). Dynamic performance of rubberised concrete and its structural applications – An overview. *Engineering Structures*, *234*, 111990. https://doi.org/10.1016/j.engstruct.2021.111990

European Committee for Standardization [CEN]. (2016). *Methods of testing cement. Part 1: Determination of strength* (EN 196-1:2016).

European Committee for Standardization [CEN]. (2019). *Testing hardened concrete. Part 2: Making and curing specimens for strength tests* (EN 12390-2:2019-07).

European Committee for Standardization [CEN]. (2021). *Testing hardened concrete. Part 13: Determination of secant modulus of elasticity in compression* (EN 12390-13:2021).

Ge, J., Mubiana, G., Gao, X., Xiao, Y., & Du, S. (2024). Research on static mechanical properties of high-performance rubber concrete. *Frontiers in Materials*, *11*, 1426979. https://doi.org/10.3389/fmats.2024.1426979

Grinys, A., Balamurugan, M., Augonis, A., & Ivanauskas, E. (2021). Mechanical properties and durability of rubberized and glass powder modified rubberized concrete for whitetopping structures. *Materials*, *14*(9), 2321. https://doi.org/10.3390/ma14092321

Han, Y., Lv, Z., Bai, Y., Han, G., & Li, D. (2023). Experimental study on the mechanical properties of crumb rubber concrete after elevated temperature. *Polymers*, *15*(14), 3102. https://doi.org/10.3390/polym15143102

Haridharan, M. K., Murugan, R. B., Natarajan, C., & Muthukannan, M. (2017). Influence of waste tyre crumb rubber on compressive strength, static modulus of elasticity and flexural strength of concrete. *IOP Conference Series: Earth and Environmental Science*, *80*(1), 012014. https://doi.org/10.1088/1755-1315/80/1/012014

Hernández, E., Liu, R., Palermo, A., Chiaro, G., & Scott, A. (2021, October 14–16). *Rubberised concrete: material characterisation and mechanical behaviour*. NZ Concrete Conference, Rotorua, New Zealand.

Hisbani, N., Shafiq, N., Shams, M. A., Farhan, S. A., & Zahid, M. (2025). Properties of concrete containing crumb rubber as partial replacement of fine aggregate – a review. *Hybrid Advances*, *10*, 100481. https://doi.org/10.1016/j.hybadv.2025.100481

Kevin, B., Sarker, P. K., & Madhavan, M. K. (2025). Performance assessment and microstructural characterization of combined surface, chemical and polymer treated crumb rubber concrete. *Scientific Reports*, *15*(1), 15853. https://doi.org/10.1038/s41598-025-97189-8

Li, D., Mills, J. E., Benn, T., Ma, X., Gravina, R., & Zhuge, Y. (2016). Review of the performance of high-strength rubberized concrete and its potential structural applications. *Advances in Civil Engineering Materials*, *5*(1), 149–166. https://doi.org/10.1520/ACEM20150026

Liu, H., Wang, X., Jiao, Y., & Sha, T. (2016). Experimental investigation of the mechanical and durability properties of crumb rubber concrete. *Materials*, *9*(3), 172. https://doi.org/10.3390/ma9030172

Lu, Y., Li, C., Zhang, X., Huang, X., & Zhao, Z. (2022). A workability characterization of innovative rubber concrete as a grouting material. *Materials*, *15*(15), 5319. https://doi.org/10.3390/ma15155319

Merabti, S., Kenai, S., Belarbi, R., & Khatib, J. (2021). Thermo-mechanical and physical properties of waste granular cork composite with slag cement. *Construction and Building Materials*, *272*, 121923. https://doi.org/10.1016/j.conbuildmat.2020.121923

Mezidi, A., Merabti, S., Benyamina, S., & Sadouki, M. (2023). Effect of substituting white cement with ceramic waste powders (CWP) on the performance of a mortar based on crushed sand. *Advances in Materials Science*, *23*(4), 123–133. https://doi.org/10.2478/adms-2023-0026

Mezidi, A., Merabti, S., Guelmine, L., & Meziani, B. (2025). Effect of crumb rubber on the fresh and hardened properties of dune sand concrete. *Advances in Materials Science*, *25*(2), 5–16. https://doi.org/10.2478/adms-2025-0008

Mohammed, B., & Azmi, N. J. (2011). Failure mode and modulus elasticity of concrete containing recycled tire rubber. *The Journal of Solid Waste Technology and Management*, *37*(1), 16–24. https://doi.org/10.5276/JSWTM.2011.16

Moulay-Ali, A., Abdeldjalil, M., & Khelafi, H. (2021). An experimental study on the optimal compositions of ordinary concrete based on corrected dune sand – Case of granular range of 25 mm. *Case Studies in Construction Materials*, *14*, e00521. https://doi.org/10.1016/j.cscm.2021.e00521

Naito, C., States, J., Jackson, C., & Bewick, B. (2014). Assessment of crumb rubber concrete for flexural structural members. *Journal of Materials in Civil Engineering*, *26*(10), 04014075. https://doi.org/10.1061/(ASCE)MT.1943-5533.0000986

Noor, N. M., Yamamoto, D., Hamada, H., & Sagawa, Y. (2016). Rubberized concrete durability against abrasion. *MATEC Web of Conferences*, *47*, 01006. https://doi.org/10.1051/matecconf/20164701006

Nuzaimah, M., Sapuan, S. M., Nadlene, R., & Jawaid, M. (2018). Recycling of waste rubber as fillers: A review. *IOP Conference Series: Materials Science and Engineering*, *368*, 012016. https://doi.org/10.1088/1757-899X/368/1/012016

Park, S., Lee, E., Ko, J., Yoo, J., & Kim, Y. (2018). Rheological properties of concrete using dune sand. *Construction and Building Materials*, *172*, 685–695. https://doi.org/10.1016/j.conbuildmat.2018.03.192

Pham, T. M., Elchalakani, M., Hao, H., Lai, J., Ameduri, S., & Tran, T. M. (2019). Durability characteristics of lightweight rubberized concrete. *Construction and Building Materials*, *224*, 584–599. https://doi.org/10.1016/j.conbuildmat.2019.07.048

Serikma, M., Benahmed, B., Kennouche, S., Mohd Hashim, M. H., & Merabti, S. (2024). Valorization of glass powder as filler in self-compacting concrete. *Scientific Review Engineering and Environmental Sciences*, *33*(3), 261–277. https://doi.org/10.22630/srees.9810

Singaravel, D. A., Veerapandian, P., Rajendran, S., & Dhairiyasamy, R. (2024). Enhancing high-performance concrete sustainability: integration of waste tire rubber for innovation. *Scientific Reports*, *14*(1), 4635. https://doi.org/10.1038/s41598-024-55485-9

Siringi, G. M., Abolmaali, A., & Aswath, P. B. (2013). Properties of concrete with crumb rubber replacing fine aggregates (sand). *Advances in Civil Engineering Materials*, *2*(1), 218–232. https://doi.org/10.1520/ACEM20120044

Sofi, F. A., Joo, M. R., & Rajak, S. (2024). *Experimental study on crumb-rubberized concrete: Mechanical properties and SEM analysis*. EasyChair Preprint. https://easychair.org/publications/preprint/j2Rf/open

Youssf, O., Mills, J. E., Ellis, M., Benn, T., Zhuge, Y., Ma, X., & Gravina, R. J. (2022). Practical application of crumb rubber concrete in residential slabs. *Structures*, *36*, 837–853. https://doi.org/10.1016/j.istruc.2021.12.062

Summary

Comparative assessment of the physico-mechanical properties of crumb rubber concretes developed with natural and dune sands. This paper investigates the incorporation of crumb rubber from recycled tires into ordinary concrete (OCCR) and dune sand concrete (SCCR), analyzing the effect of incorporation rates ranging from 1% to 5% relative to the sand mass. A comparative study was conducted focusing mainly on apparent density, compactness, mechanical strengths, and the elastic modulus in the linear regime. The results show that the addition of crumb rubber in concrete leads to a reduction in both compressive strength and flexural tensile strength. For an incorporation rate of 3%, Young's modulus decreases significantly in SCCR compared to OCCR. Specifically, the elastic modulus is E = 24.7 GPa for OCCR and E = 14.23 GPa for SCCR, representing a reduction of approximately 42%.

Instruction for Authors

The journal publishes in English languages, peer-reviewed original research, critical reviews and short communications, which have not been and will not be published elsewhere in substantially the same form. Author of an article is required to transfer the copyright to the journal publisher, however authors retain significant rights to use and share their own published papers. The published papers are available under the terms of the principles of Open Access Creative Commons CC BY-NC license. The submitting author must agree to pay the publication charge (see Charges).

The author of submitted materials (e.g. text, figures, tables etc.) is obligated to restricts the publishing rights. All contributors who do not meet the criteria for authorship should be listed in an Acknowledgements section of the manuscript. Authors should, therefore, add a statement on the type of assistance, if any, received from the sponsor or the sponsor's representative and include the names of any person who provided technical help, writing assistance, editorial support or any type of participation in writing the manuscript.

Uniform requirements for manuscripts

The manuscript should be submitted by the Open Journal System (OJS) at https://srees.sggw.edu.pl/about/submissions. All figures and tables should be placed near their reference in the main text and additionally sent in a form of data files (e.g. Excel, Visio, Adobe Illustrator, Adobe Photoshop, CorelDRAW). Figures are printed in black and white on paper version of the journal (color printing is combined with an additional fee calculated on a case-by-case basis), while on the website are published in color.

The size of the manuscript should be limited up to 10 pages including overview, summary, references and figures (the manuscript more than 13 pages is unacceptable); Please set the text format in single column with paragraphs (A4 paper format), all margins to 25 mm, use the font Times New Roman, typeface 12 points and line spacing one and half.

The submitted manuscript should include the following parts:

- name and SURNAME of the author(s) – up to 5 authors
- affiliation of the author(s), ORCID Id (optional)
- title of the work
- key words
- abstract (about 500 characters)
- text of the paper divided into: Introduction, Material and Methods, Results and Discussion, Conclusions, References and Summary
- references in APA style are listed fully in alphabetical order according to the last name of the first author and not numbered; please find the details below
- post and mailing address of the corresponding author:

  Author's address:
  Name, SURNAME
  Affiliation
  Street, number, postal code, City
  Country
  e-mail: adress@domain

- Plagiarism statement (https://srees.sggw.edu.pl/copyright)

Reference formatting

In the Scientific Review Engineering and Environmental Sciences the APA 7th edition style is used.

Detailed information

More information can be found: https://srees.sggw.edu.pl